INTERNET BASED SEISMIC VULNERABILITY ASSESSMENT

SOFTWARE DEVELOPMENT FOR R/C BUILDINGS

A THESIS SUBMITTED TO
THE GRADUATE SCHOOL OF NATURAL AND APPLIED SCIENCES
OF
MIDDLE EAST TECHNICAL UNIVERSITY

BY
BARIŞ YALIM

IN PARTIAL FULFILLMENT OF THE REQUIREMENTS FOR THE DEGREE OF
MASTER OF SCIENCE
IN
CIVIL ENGINEERING

DECEMBER 2004

Approval of the Graduate School of Natural and Applied Sciences

Prof. Dr. Canan Özgen

Director

I certify that this thesis satisfies all the requirements as a thesis for the degree of Master of Science.

Prof. Dr. Erdal Çokca

Head of Department

This is to certify that we have read this thesis and that in our opinion it is fully adequate, in scope and quality, as a thesis for the degree of Master of Science.

Asst. Prof. Dr. Ahmet Türer

Supervisor

Examining Committee Members

Prof. Dr. Polat Gülkan   (METU,CE)

Asst. Prof. Dr. Ahmet Türer   (METU,CE)

Asst. Prof. Dr. Ahmet Yakut   (METU,CE)

Asst. Prof. Dr. Uğurhan Akyüz   (METU,CE)

M.S. Volkan Aydoğan   (PROYA YAZILIM)

I hereby declare that all information in this document has been obtained and presented in accordance with academic rules and ethical conduct. I also declare that, as required by these rules and conduct, I have fully cited and referenced all material and results that are not original to this work.

Name, Last Name :

Signature   :

ABSTRACT

INTERNET BASED SEISMIC VULNERABILITY ASSESSMENT SOFTWARE DEVELOPMENT FOR R/C BUILDINGS

YALIM, Barış

M.Sc., Department of Civil Engineering

Thesis Supervisor: Assoc. Prof. Dr. Ahmet Türer

December 2004, 162 pages

Structural evaluation and seismic vulnerability assessment of Reinforced Concrete (R/C) buildings have especially become the focus of many researches in Turkey and abroad especially after the August 17, 1999 earthquake causing major life and property losses. A devastating earthquake being expected in Istanbul-Marmara region raises many questions on how well the existing buildings are constructed and whether they can stand a major earthquake. Evaluation of existing buildings for seismic vulnerability requires time consuming input preparation (pre-processing), modelling, and post processing of analysis results. The objective of the study is to perform automated seismic vulnerability assessment of existing R/C buildings automatically over the internet by asking internet users to enter their building related data, and streamlining the modelling-analysis-reporting phases by intelligent programming. The internet based assessment tool is prepared for two levels of complexity: (a) the detailed level targets to carry out seismic evaluation of the buildings using a linear structural analysis software developed for this study; (b) the simplified level produces seismic evaluation index for buildings, based on simple and easy to enter general building information which can be entered by any person capable of using an internet browser. Detailed level evaluation program includes a user friendly interface between the internet user and analysis software, which will enable data entry, database management, and online evaluation/reporting of R/C

buildings. Building data entered by numerous users over the internet will also enable formation of an extensive database of buildings located all around Turkey.

36 buildings from Düzce damage database, generated by the cooperation of Scientific and Research Council of Turkey (TÜBİTAK) and Structural Engineering Research Unit (SERU) after the 17 August 1999 Kocaeli and the 12 November 1999 Düzce earthquakes, are used in the analyses to identify relationship between calculated indices and observed damage levels of buildings, which will enable prediction of building damage levels for future earthquakes. The research is funded by Science Research Program (BAP 2003-03-03-03), NATO-SfP 977231, and TUBITAK ICTAG-I574 projects.

The contribution of the research is composed of a) online building index - performance analysis/evaluation software which might be used by any average internet user, b) an ever-growing R/C building database entered by various internet users.

Keywords: Earthquake, seismic vulnerability, internet-based, software development, Düzce earthquake

ÖZ

BETONARME YAPILARI SİSMİK AÇIDAN İNTERNET TABANLI DEĞERLENDİRME PROGRAMI

YALIM, Barış

Yüksek Lisans, İnşaat Mühendisliği Bölümü

Tez Danışmanı: Yard. Doc. Dr. Ahmet Türer

Aralık 2004, 162 sayfa

Betonarme binaların yapısal ve sismik açıdan zayıflık değerlendirmesi, birçok yaşam ve mülk kaybına yol açan 17 Ağustos 1999 depreminden sonra Türkiye'de ve yurtdışında birçok araştırmacı tarafından ilgi odağı haline gelmiştir. İstanbul-Marmara bölgesinde yıkıcı bir deprem beklentisi, varolan binaların inşaat kalitesi ve böyle bir depreme karşı dayanımları konusunda birçok soruyu gündeme getirmektedir. Hali hazırdaki binaların sismik hasargörebilirlik değerlendirmesi, girdi hazırlanma, modelleme ve analiz sonuçlarının işlenmesi açısından zaman harcanması gereken bir konudur. Bu çalışmanın amacı, internet kullanıcılarının kendi binalarıyla ilgili bilgilere dayanarak, modelleme-analiz-raporlama aşamalarından oluşan akıllı programlama sayesinde varolan betonarme binaların internet üzerinden otomatik olarak sismik hasargörebilirlik değerlendirmesini yapmaktır. İnternet tabanlı değerlendirme programı iki zorluk derecesinde hazırlanmıştır: (a) detaylı aşama, bu çalışma kapsamında geliştirilen lineer yapısal analiz programını kullanarak binaların sismik açıdan değerlendirilmesini hedeflemektedir; (b) basitleştirilmiş aşamanın amacı ise internet kullanabilen bir kişinin kolayca cevaplayabileceği, genel bina bilgilerine dayanan bina sismik değerlendirme indeksi üretmektir. Detaylı değerlendirme programı internet kullanıcısı ile program arasında kullanımı kolay, bilgi girdisini, veritabanı işletmesini ve betonarme binaların internet üzerinden değerlendirilmesini sağlayacak bir arayüz içermektedir. Türkiye'nin heryerinden

birçok internet kullanıcısı tarafından girilen bina bilgileri geniş çaplı bina veritabanı oluşmasını da imkan verecektir.

17 Ağustos 1999 Kocaeli ve 12 Kasım 1999 Düzce depremleri sonrası Türkiye Bilimsel ve Teknik Araştırma Kurumu (TÜBİTAK) ve Yapı Mekaniği Araştırma Ünitesi (YMAÜ) ortak çalışmaları sonucunda elde edilen Düzce hasar verileri arasından seçilen 36 bina analiz edilerek, hesaplanan indekslerden binaların gelecek depremlerdeki hasar seviyeleri belirlenmeye çalışılmıştır. Bu araştırma Bilimsel Araştırma Programı (BAP 2003-03-03-03), NATO-SfP 977231 ve TÜBİTAK İÇTAG-I574 projeleri tarafından desteklenmektedir.

Araştırmanın sağlayacağı katkılar şunlardır: a) herhangi bir ortalama internet kullanıcısının faydalanabileceği internet üzerinden bina analiz/değerlendirme programı, b) çeşitli internet kullanıcıları tarafından girilen betonarme yapı veri bankasının oluşturulması.

Anahtar Kelimeler: Deprem, sismik hasar görebilirlik, internet tabanlı program geliştirme, Düzce depremi

Dedicated to my family

ACKNOWLEDGEMENTS

I would like to express my grateful thanks to my supervisor Asst. Prof. Dr. Ahmet Türer for his support and encouragement during this study.

I also would like to thank Prof. Dr. Güney Özcebe and Prof. Dr. Tanvir Wasti for their invaluable suggestions and moral support since the very first day of the study. I would like to extend my thanks to Asst. Prof. Dr. Ahmet Yakut for his efficient final suggestions.

Special thanks go to my friend Elif İnce for her great motivation throughout the study.

I would like to extend my thanks to Melih Süsoy, İbrahim Erdem, Hakan Erdoğan, Sezgin Küçükçoban and Ufuk Yazgan for their priceless support and friendship during the entire study.

I would like to offer sincere thanks to Mr. Bahadır Alkaç who has provided invaluable contribution to this study during programming stage.

Finally, I would like to present my deepest thanks to my family for their endless love, support and encouragement throughout all my life.

TABLE OF CONTENTS

xi

LIST OF TABLES

LIST OF FIGURES

xiv

xvi

CHAPTER 1

INTRODUCTION

1.1   GENERAL

Turkey is one of the most unfortunate countries in terms of its seismic activities. Earthquake prone regions cover approximately 95% of both area and population in Turkey. Although 130 major earthquakes occurred in Turkey since the beginning of this century [5], the ones occurred in the last decade, which caused building collapses and killed about 18000 people, have significantly drawn public attention. Thus, estimation of the potential damage of the structures is inevitably essential in order to minimize economic and human live losses during any future earthquakes.

Amount of time and financing to perform seismic assessment of existing buildings is directly proportional with the number of buildings which are under seismic risk. Seismic assessment of buildings is usually conducted in two or more phases. Quick (walk down survey) assessment is usually the first step to identify possible defective buildings. Comprehensive evaluation methods are then used on a smaller number of buildings. Existing comprehensive methods on seismic evaluation are generally based on performance analyses of the computer model carried out by a qualified engineer. The time range varies between several days and couple of weeks. Quick evaluation techniques, on the other hand, are relatively economical but generally lack accuracy and reliability. Current approaches in rapid seismic vulnerability methods basically rely on analysis of

1

observations by past experiences. The goal of such methods is to detect the buildings that need immediate investigation. The time needed for a fast evaluation of a particular building is about an hour for an average engineer. However, based on DIE 2000 data, there are close to 4 million reinforced concrete existing buildings in Turkey, and evaluation of such large quantities requires a vast number of qualified technical personnel, funding, and time. This study aims to develop an easy-to-use, internet based seismic evaluation tool to distribute the data collection work load to the households of each building.

1.2 OBJECTIVE AND SCOPE

The primary objective of this study is to develop a web-based computer program for seismic assessment of existing reinforced concrete buildings. The web-based computer program is prepared in two levels of complexity. The simplistic approach collects general building data (such as in the case of a walk down, quick survey) and calculates an evaluation index for the seismic assessment of the building. The second level (complicated) approach consists of entrance of detailed building information (column, beam sizes, reinforcement, etc.) using a user-friendly graphical interface through internet and a detailed linear analysis of the building automatically carried out at METU server. An analysis report is automatically prepared and sent back to the user through the internet.

The secondary objective of the study is to generate a detailed comprehensive database of existing buildings entered by a large number of users in Turkey. Although the collected data's correctness and accuracy is in the mercy of the user, the information gathered through internet users is still expected to be valuable.

The final objective of this study is to serve to the needs of the public (quick-detailed seismic assessment of buildings) and also educate and raise awareness about earthquake and building resistance through detailed reports.

Two existing buildings (K7 building at METU-Ankara and Isbank Kabatas-Istanbul branch building) are evaluated using the developed programs for basic

and complicated levels. The programs are tested and opened to public use on November 01, 2004 at "www.idp.metu.edu.tr" internet site address. The building data entries are mostly expected to be received from populated large cities with high seismic risk and where internet use is customary in houses and internet cafes.

In chapter 1, general information about the study is briefly given. Objectives and scope of the study are explained. In chapter 2, previous relevant studies on seismic vulnerability assessment of existing buildings are summarized in addition to seismic evaluation techniques in United States and Japan. Chapter 3 involves the theoretical background of the software developed for seismic evaluation of existing reinforced concrete buildings. Building modeling and analysis method are introduced in detail. In chapter 4, results produced by the software are interpreted. Analysis reliability of the software is tested on the example buildings. Proposed methods (in two levels of complexity) for seismic vulnerability assessment of the buildings are described in detail. Then, application of the proposed methods are performed on 36 buildings from Düzce damage database in order to provide a link between building damage score and the expected damage level of a building. Furthermore, validity of the cut-off values for damage states is checked by using 9 buildings (one is from Bingöl database) from the same database. Finally, summary and main conclusions of the study together with possible recommendations for the future are included in Chapter 5.

CHAPTER 2

REVIEW OF PAST STUDIES

2.1 INTRODUCTION

Although numerous studies have been carried out in the field of "existing building vulnerability assessment" and some utility programs are developed, an internet (web) based analysis/assessment program is a new concept which was not widely practiced before. Nevertheless, review of past studies would greatly enhance the theoretical background of the used assessment procedure which is similar to past studies in theory. In the following sections, key features of internet-based computer programming will be discussed. After that, the most common seismic evaluation techniques applied in other countries will be summarized. Next, several methods on earthquake vulnerability evaluation proposed by different researchers from Turkey will be discussed.

2.2 WEB-BASED PROGRAMMING AND TRAINING

Technologies, such as advancement of web-based software can offer tremendous advantages if used in proper context. It is important to note that computers are excellent tools for helping people to learn through an active and interactive process rather than a passive one. Consequently, more web based tools should be developed for the benefit/well-being of public.

Major advantages of web based tools/programs may be as follows;

- low cost, easy to reach
- can be used for teaching/education/training

2.3   EXAMPLE TOOL

One and good example of a web-based computer program is called "OpenSees" [17] developed at Pacific Earthquake Engineering Research Center at University of California Berkeley. It is an object-oriented software framework for applications in earthquake engineering using finite element methods. It is a framework for building models of structural and geotechnical systems, performing nonlinear analysis with the model, and processing the response results. As its name implies, the software is open to public and may be downloaded from the website: www.opensees.berkeley.edu. Similar to this program developed in this study, working principle of OpenSees [17] is composed of a number of modules to perform creation of finite element model, selection of analysis procedures and output of results. Users conduct a simulation with a scripting language named as "Tcl". Definition of model is done through Tcl environment using special commands. Software is capable of performing nonlinear analysis.

2.4   SEISMIC EVALUATION TECHNIQUES

In this section, seismic vulnerability evaluation methods used in United States and Japan, which are also earthquake prone countries, are briefly examined.

2.4.1   Methodology in United States [1, 2, 3]

Applied Technology Council (ATC) suggests stepwise seismic evaluation approach which is composed of three stages. In the first stage, called as "rapid visual screening", buildings posing risk of death, injury, or severe curtailment in case of an earthquake are quickly identified. The methodology can be used by trained personnel to identify potentially hazardous buildings on the basis of a 15

to 30 minute exterior inspection, using a data collection form. These forms may be different from region to region depending on the expected ground motion.

Initial structural score is calculated for the building if it is one of the structural types specified in FEMA-154 [3]. Twelve basic structural parameters are inspected, leading to a numerical basic structural score by means of visual inspection. These parameters include poor condition of the structure, soft story, floor torsion, short column, and irregularities in plan and elevation and soil type etc. Then, basic score is reduced to a final structural score based on several deficiencies associated by each parameter. A low score implies that further evaluation is needed, whereas a high score indicates the sufficiency of the building's seismic performance.

If the structure is detected as inadequate, the second stage of the evaluation process, called as "evaluation in detail" is carried out by an engineer. This stage identifies building deficiencies and search for any vulnerable locations on the structure or component that present unacceptable risks in the case of an earthquake. Lateral load carrying capacity is assessed in terms of shear stress and drift checks. Shear stress check is performed by quick estimation of average shear stress in columns and shear walls. Drift check basically covers the story drift judgment which relies on relative rigidity of frame elements. Building is then subjected to several questions to find out the possible weaknesses. These questions differ for each of the structural categories given in FEMA-178 [1]. No further evaluation is required provided that the structure fulfill all statements with true responses. On the other hand, false responses are the indication of more detailed study for that structure.

Below areas are suggested by FEMA-178 [1] for evaluation statements of frame type reinforced concrete structures;

- Building system: weak story, soft story, geometry, mass, vertical irregularities, torsion, reinforced concrete deterioration, corrosion, etc.

- Moment frames: Shear stress check, drift check, strong column-weak beam, redundancy, joint eccentricity, stirrup and tie hooks, stirrup spacing, column and beam-bar splices etc.
- Diaphragms: Plan irregularity, diaphragm continuity, spans etc.
- Connections: Connection of columns to foundation, pile caps etc.

In the case of structural deficiency from previous stages, final evaluation stage, called as "engineering evaluation" is performed by an experienced structural engineer. In this detailed investigation stage nonlinear static and dynamic analyses are carried out based on current design code. Structure is evaluated under the guidance of FEMA-273 [2]. As far as the final decision about the structure is concerned, this stage may be treated as the most trusted and in-depth of them all.

2.4.2 Methodology in Japan [15]

The Japanese seismic evaluation standard, named as "Standard and Commentary for Evaluation of Seismic Capacity of Existing Reinforced Concrete Buildings" [15] suggests three levels of evaluation procedures with different phases. These procedures are applicable for low-rise reinforced concrete buildings less than six stories with or without shear walls. Similar to the methodology in the United States, screening stages are in order from the simplest to the most complicated.

To diagnose the seismic performances of reinforced concrete buildings, first, the lateral load carrying capacity and deformation capacity of the building are evaluated from the strength and deformation capacity of its structural elements. Then, the structural seismic index, I_s, is calculated from the shape and aging related deterioration of the building. The seismic performance of the building is evaluated by comparing the structural seismic index, I_s, with the structural seismic judgment index, I_{so}, which is based on the estimation of equivalent static earthquake forces. If structural index is greater than the seismic performance index, building is identified as seismically adequate and no additional evaluation is needed. On the other hand, lower value of structural index requires further evaluation analysis.

7

2.5   RELEVANT PAST STUDIES

In this section, past researches on seismic vulnerability estimation of existing reinforced concrete buildings are briefly summarized.

2.5.1   Hassan & Sozen Method [14]

Hassan and Sozen [14] presented a simplified method for seismic vulnerability assessment of low-rise buildings. Procedure requires only the column and wall dimensions of a structure. Authors defined "wall index" and "column index" to be plotted on two-dimensional graph. These indices are given below.

$$Wall\ Index\ (WI)\ = \frac{A_{cw} + \dfrac{A_{mw}}{10}}{A_{ft}} * 100 \tag{2.1}$$

where A_{cw} is the total cross-sectional area of reinforced concrete walls in one horizontal direction at the base level, A_{mw} is cross-sectional area of masonry walls in one horizontal direction at the base level, and A_{ft} is total floor area above the base.

$$Column\ Index\ (CI)\ = \frac{A_{ce}}{A_{ft}} * 100 \tag{2.2}$$

where A_{ce} is the effective cross-sectional area of columns at the base ($A_{col}/2$); A_{col} is total cross-sectional area of columns above the base. A building is represented by a point defined by WI and CI. A "priority index (PI)" is defined as the summation of WI and CI, which shows high vulnerability when PI value is relatively low.

Authors underlined the fact that proposed method includes too few variables but it provides general idea to identify the most vulnerable buildings. They also tested the procedure with post-earthquake data from 1992 Erzincan earthquake and observed that results proved to be quite satisfactory.

8

2.5.2 Gulkan & Sozen Method [12]

Gulkan and Sozen [12] proposed a procedure for seismic vulnerability of reinforced concrete frame type buildings consisting of masonry infills. Method is simply based on cross-sectional dimensions of columns and masonry infill walls. Ranking is performed in line with the graphical representation of column and wall ratios. Column ratio is defined as the ratio of total cross-sectional area of columns at the base to total floor area above the base. Similarly, wall ratio is defined as the ratio of the sum of infill wall area at the base to total floor area. Both fractions are calculated for each direction and critical one is considered. Authors also proposed a vulnerability formulation based on ground story drift. They indicated that the ground story drift is directly proportional with the seismic vulnerability of a structure. Study is conducted on the database collected after 1992 Erzincan earthquake. Authors concluded that the proposed ranking procedure provides good conformity with the damage database.

2.5.3 Ersoy & Tankut Method [10]

Ersoy and Tankut [10] proposed another seismic assessment technique for reinforced concrete buildings with less than seven stories. Authors stated that detailed evaluation is not needed if structure satisfies below conditions;

- minimum requirements for the dimensions of structural elements and the reinforcement ratios given in the "Specifications for Structures to be Built in Disaster Areas" [16]

- $(k\sum A_c + \sum A_w) \geq 0.003 \sum A_p$ **(2.3)**

- $\sum A_w \geq 0.002 \sum A_p \geq 0.01 A_{pb}$ **(2.4)**

where

$\sum A_c$: total column area in a given direction at the base level of structure

$\sum A_w$: total shear wall area in a given direction at the base level of structure

9

$\sum A_p$: total floor area above base level of structure

A_{pb} : floor area at the base level of the structure

k : 1/2 (square and circular columns)

      1/3 (rectangular columns in their shorter directions)

      2/3 (rectangular columns in their longer directions)

A form of damage identifier is defined as the ratio of column and shear wall areas of an existing structure to the "required area" based on above states. If the ratio is greater than one then no severe damage is expected during an earthquake. Conversely, severe damage is possible for the structure if the ratio is less than one. Authors tested the soundness of the proposed method with damage data for 1992 Erzincan earthquake and concluded that results show acceptable correlations with the observed damage states.

2.5.4   Peter Fajfar's (N2) Method [11]

Fajfar [11] proposed a simple nonlinear method, called as N2 method, for expected seismic damage evaluation. The method uses an analytical method producing acceptable results for the structures vibrating in their first fundamental modes, rather than curve fitting to available post-earthquake data. Most vulnerable portions of a structure can also be determined using N2 method. Even though method includes great uncertainty due to the assumptions made for the properties of expected ground motion, author believes that proposed method (which is mainly based on pushover analysis) is a practical tool for building seismic performance evaluation. Author also verifies the reliability of the method by analyzing a four story reinforced concrete frame building example.

2.5.5   Rodriguez's (I_D) Method [19]

A coefficient I_D for seismic damage prediction is proposed by researchers Rodriguez & Aristazabal [19].

$$I_D = \frac{\gamma^2 E_H}{2\pi\lambda h D_{rd}}$$ (2.5)

where λ is equal to n/T, n being the number of storeys, T is fundamental period of the structure; $\gamma = \delta_m / (\mu_m u_y)$, δ_m is the maximum roof drift ratio, μ_m is ductility ratio, u_y is yield displacement.

Proposed parameters neither include the characteristics of the ground motion nor also structural properties of the structure. I_D coefficient considers total energy dissipated by a SDOF system (E_H), and maximum roof drift ratio (D_{rd}) which is equal to 0.01. λ value in the equation is selected as 10 for typical reinforced concrete frames and h is the story height. Authors tested the I_D parameter using data from 11 different earthquakes and concluded that it provides an approximate measure of structural response and can be used for quick evaluation of existing regular RC buildings. Another conclusion drawn from the study is that controlling roof and inter-story drift ratios plays important role in minimizing seismic damage. The I_D method should be carefully used for irregular buildings due to inconsistencies with the assumed and actual deflected shapes.

2.5.6 Wasti & Sucuoglu & Utku's Approach [24]

Authors carried out a rehabilitation research project about moderately damaged reinforced concrete buildings after 1 October 1995 Dinar-Turkey earthquake. The structural damage index values for buildings are defined by assigning individual damage appraisal values to the structural members. A member type damage grade (D_m) was calculated first for beams, columns, shear walls, infill walls, and connections separately using the relation [13]:

$$D_m = \frac{\alpha_m (1L + 2M + 4S)}{N_m}$$ (2.6)

where L, M, and S letters stand for the number of light, medium, and severely damaged members, N_m is the total number of members, and α_m is the member

11

importance factor which takes values of 1, 2, 6, 1, and 0.5 for beams, columns, shear walls, connections, and infill walls, respectively. The summation of all D_m values for all structural members gives the Total Member Damage Grade, (TMDG). Then, the Structural Damage Grade (SDG) is calculated as:

$$SDG = \frac{TMDG * 100}{4\delta_b + 8\delta_c + 24\delta_{sw} + 4\delta_j + 2\delta_i}$$

(2.7)

where δ is either 0 or 1, depending on the existence of that member type in the system. According to these scores, a structural damage rating was performed as below;

    0-5   : No structural damage

    6-14   : Light structural damage

    15-43   : Moderate structural damage

 Above 43   : Heavy structural damage

Although the study does not target to define a seismic vulnerability assessment method, it provides valuable information on how to link member type damage to the overall building performance evaluation.

2.5.7 Pay's Approach [18]

Pay [18] proposed a method based on statistical background called as discriminant analysis for rapid evaluation of buildings. Database was formed after 1999 Kocaeli and Düzce earthquakes and involves 152 R/C type buildings up to 6 stories high with and without shear walls. Five structural parameters (number of stories, square root of sum of squared moment of inertias (SRSSI), soft story, overhang ratio, and redundancy) are used to evaluate seismic vulnerability of a building. Soft story and overhang ratio were detected as statistically insignificant and removed from the analysis. Four different damage state levels ("immediate occupancy", "life safety", "severe damage", and "collapse") are defined. The overall correct classification rate for the indicated four levels is found to be

49.3%, whereas success rate has increased to about 72% when light and heavy damage states are processed separately.

2.5.8 Aydogan's Method [4]

Aydogan [4] developed another statistical model for the preliminary seismic vulnerability assessment of low-to mid rise existing reinforced concrete structures. Method is based on discriminant analysis of 484 buildings compiled after 1999 Marmara earthquakes using the following basic estimation parameters: number of stories, minimum normalized lateral stiffness index, minimum normalized lateral strength index, redundancy score, soft story index, and overhang ratio. The first group of analysis was performed for two damage state levels namely "immediate occupancy performace level (IOPL)" and "life safety performance level (LSPL)". Correct classification rates of 69.0% in LSPL and 72.5% in IOPL are achieved. The second group of analysis for three damage state levels produced 54.1% correct classification rate. On the other hand, optimal classification methodology was developed for the two damage state groupings. In this case, severely damaged and collapsed buildings are identified with 80.3% success rate. The number of stories was found to be the most effective parameter in all groups of classifications.

CHAPTER 3

DESCRIPTION OF SOFTWARE

3.1 INTRODUCTION

In this chapter, theoretical background of the software called "EQMASTER" is explained in detail. Brief description is given on graphical user interface of the software. Working scheme of the software on the internet platform is introduced. Program code and capabilities of EQMASTER are theoretically discussed.

3.2 LAYOUT

Software is basically formed by two main parts. The first one is the graphical user interface (GUI). GUI provides strong visual interaction with the user resulting in very user friendly environment (see Figure 3.1). Recent trends in almost all computer programs have progressed in that manner and effectiveness is greatly increased. Design of GUI is completed by the cooperation of the author and Komer Ltd. Co. approximately in eight months.

It is very difficult to create 3D GUI since it requires considerable amount of time and financing. Yet, 2D graphical interface which is used in this study can also be efficiently applied to 3D structures if properly designed. EQMASTER uses a 2D interface. Each floor is represented in separate layers. In addition, fast modeling is provided by means of several facilitative properties including object templates, quick insertion of objects and story replication. Lack of 3D modeling is tried to be compensated as much as possible with such properties.

14

The second part of the software involves the core program developed by the author. Code development has been carried out in MATLAB 6.5 [21] which is available in civil engineering department server.
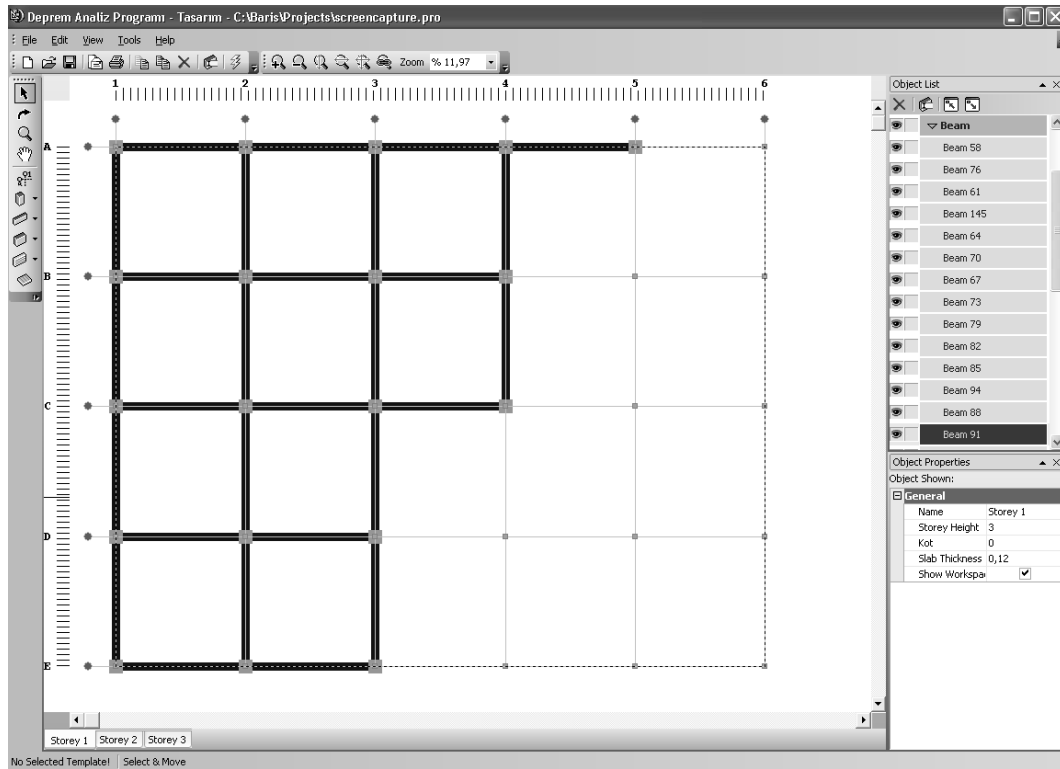
Figure 3.1 - Graphical User Interface

Software has been designed as a web-based application that all operations are performed on the internet platform. Figure 3.2 represents the software's execution logic.
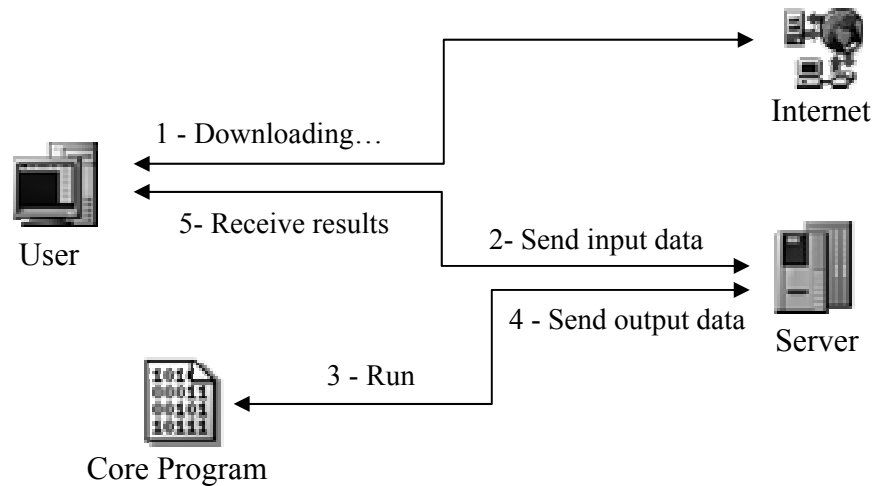
Figure 3.2 - Working Scheme

As can it be inferred from the Figure 3.2, process is started by downloading the free software from the internet. Next, the user creates his model using GUI. As soon as the modeling is completed, GUI prepares a data file representing what has been modeled. That file is then transferred into the server by means of internet. After that server at METU receives the data, the core program is executed and all necessary analyses are carried out based on the incoming data. Subsequently, an output file is constructed and saved to the server by the core program. Finally, all results are automatically organized in a report format and sent to the user in a suitable format.

Unlike other typical software packages, EQMASTER has particular advantages due to its web-based environment. Some valuable properties are listed below.

- Available to all users by downloading
- Free of charge
- Reachable 7 days 24 hours
- Forms well-organized and comprehensive database

There are several minor standards that should be followed in writing a computer program. In particular, software should be as simple as possible to employ if large

numbers of user groups are targeted. For instance, a developed program should be accessed by average computer user in Turkey which is one of the most important criteria when designing a graphical user interface. On the other hand, it should produce adequate and reliable results. All of them should also be presented to user in a well prepared report involving visual aids such as graphics, animations. Besides, the report should be small in terms of download size since the report will be transferred via internet. Other important point is that program should be able to run without errors in all versions of windows based computers. Moreover, program code should be updated easily. These criteria are met as much as possible in this study.

3.3 EXPLANATION OF THE CODE
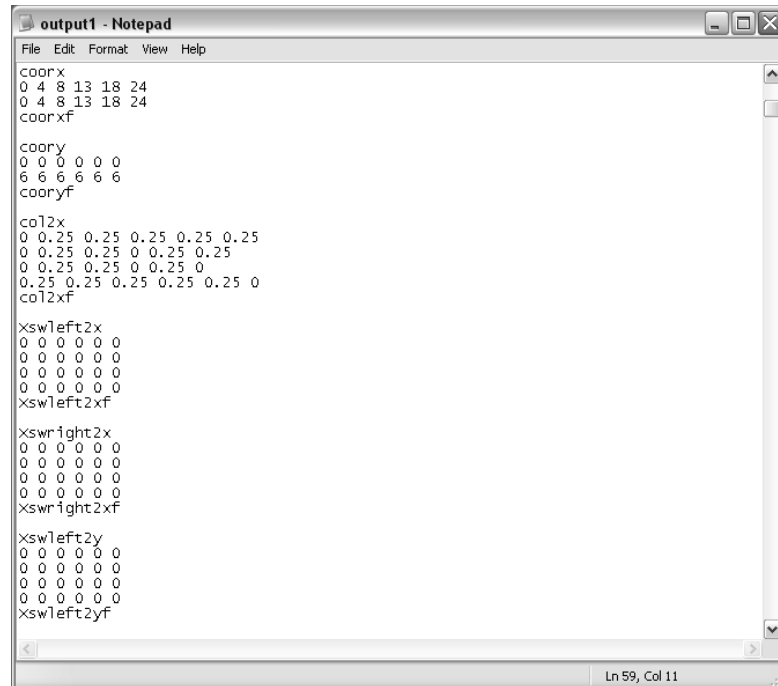
In this section, the code algorithms and logic behind them will be discussed. Total program code includes eleven subroutines. Each subroutine is identified by a function containing hundreds of lines. First subroutine is the engine which executes other functions. At the end, each subroutine's new variables are stored in a global data matrix to be used in other parts of the program.

3.3.1 Input Data

Graphical user interface provides visual connection between user and software. Although the user sees and interacts with a simplified graphical user interface, the collection, storage and processing of information involves complicated and lengthy code. Each object defined in GUI is represented by a number which then sent to a text file. Therefore input data is formed interactively as soon as the modeling is completed in GUI. Part of the sample input data sent by GUI is shown in Figure 3.3.

Data shown in Figure 3.3 is read and assigned to variables for further operations. Explanation of each input variable is given in Appendix D. MATLAB [21] is very powerful tool in terms of matrix manipulations. MATLAB [21] is the abbreviation of "Matrix Laboratory". Thus, each variable is stored as matrix regardless of its

17

size. If the object is defined for each story such as columns, beams etc., necessary data for each story are combined in a single variable. This is achieved by using three dimensional matrices. Consequently, very organized input data becomes available before starting computations.

```
output1 - Notepad
File  Edit  Format  View  Help
coorx
0 4 8 13 18 24
0 4 8 13 18 24
coorxf

coory
0 0 0 0 0 0
6 6 6 6 6 6
cooryf

col2x
0 0.25 0.25 0.25 0.25 0.25
0 0.25 0.25 0 0.25 0.25
0 0.25 0.25 0 0.25 0
0.25 0.25 0.25 0.25 0.25 0
col2xf

Xswleft2x
0 0 0 0 0 0
0 0 0 0 0 0
0 0 0 0 0 0
0 0 0 0 0 0
Xswleft2xf

Xswright2x
0 0 0 0 0 0
0 0 0 0 0 0
0 0 0 0 0 0
0 0 0 0 0 0
Xswright2xf

Xswleft2y
0 0 0 0 0 0
0 0 0 0 0 0
0 0 0 0 0 0
0 0 0 0 0 0
Xswleft2yf
                                              Ln 59, Col 11
```

Figure 3.3 - Example of Input Data

Up to now, all essential data in order to analyze a structure is obtained. Next step is the identification of model required for engineering evaluations.

3.3.2   Representation of Model

Definition of model is one of the most important parts of the analysis. All solution methods and consequences are based on how the model is identified. In this study, multistory buildings with symmetric and unsymmetrical plans are considered. Such buildings, when subjected to ground motion in a given direction, would undergo lateral motion in two horizontal directions and torsion about the vertical direction simultaneously. Representative lumped-mass model is shown in Figure 3.4.
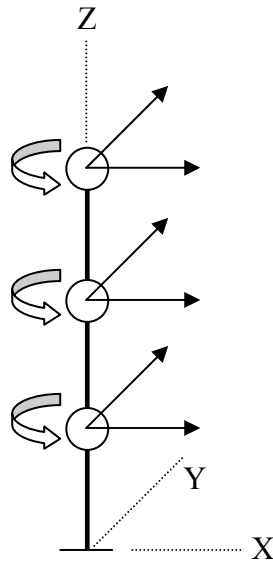
Figure 3.4 - Model Designation

There are three degree of freedoms (DOFs) defined at each floor. Two of them is translational assigned in X and Y directions. Other one is defined in Z-direction showing torsional motion. Each floor mass is lumped at the center of mass of that floor.

After the model is constructed, two fundamental dynamic properties, namely, stiffness matrix and mass matrix of the system can be developed. Theory of formulations together with the applications in the software is given in the next sections.

3.3.3 Formation of Frame Lateral Stiffness Matrix

The first step in determination of lateral stiffness matrix of a frame is the assignment of dofs to joints. Figure 3.5 demonstrates dofs considered for each frame. Note that diaphragm action is considered for each floor. Thus, two perpendicular translational dofs and one rotational dof (+z-direction) are defined for all the joints at a given floor. On the other hand, such an assumption can not be made when the rotation of slab is considered (rotation in x&y directions) since floor is flexible in bending. So, different rotational dofs are assigned at each joint.

19

However, the axial deformations in structural elements are neglected due to diaphragm action.
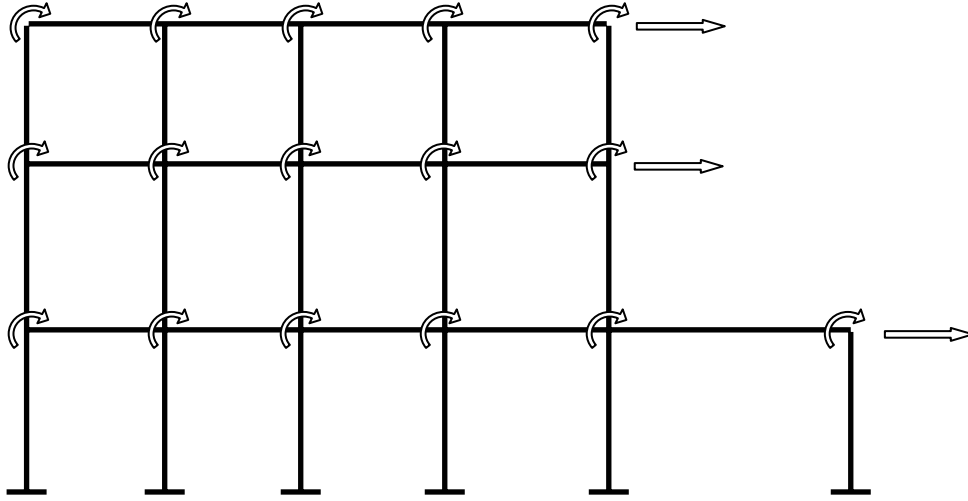
Figure 3.5 - Frame Degree of Freedoms

Assembly of frame lateral stiffness matrix is a rather simple procedure. Assigned dofs for each member are identified and properly mapped into the global matrix. Element stiffness matrix, k_e, for an axially rigid element having one translational and one rotational dof at each node is shown in Figure 3.6.

$$k_e = \frac{EI}{L} \begin{bmatrix} \dfrac{12}{L^2} & \dfrac{6}{L} & -\dfrac{12}{L^2} & \dfrac{6}{L} \\ \dfrac{6}{L} & 4 & -\dfrac{6}{L} & 2 \\ -\dfrac{12}{L^2} & -\dfrac{6}{L} & \dfrac{12}{L^2} & -\dfrac{6}{L} \\ \dfrac{6}{L} & 2 & -\dfrac{6}{L} & 4 \end{bmatrix}$$

Figure 3.6 - Element Stiffness Matrix

Program code recognizes each frame by using the assembly of structural elements defined on grid lines in the graphical user interface (GUI). Joints are automatically formed at the intersection points of GUI grids. In this way, frames including vertical irregularities such as non-existing beams or columns etc. can also be

modeled. Down side of such idealization is the need for automatic assignment of degree of freedoms at each grid intersection even if no structural elements are connected to that joint. This leads to diagonal zero terms in the stiffness matrix. In order to prevent such singularity, the global stiffness matrix is controlled and modified by removing both rows and columns that involve only zero values including their diagonal.

Another obstacle in grid idealization of the frames comes from long span beams. Many grids in both X and Y directions are defined especially for irregular frame configurations in plan. Therefore, there is great possibility of these "grid" lines dividing beams into several segments (Figure 3.7-a). Connection points of these segments provide, indeed, vertical restraints to the beam since no movement is allowed in that direction. This causes errors in deformed shape and global stiffness matrix (Figure 3.7-b&c). Such situations are managed in the software by introducing special joints at restrained locations and stiffness contributions of beams are corrected accordingly.

Joints are formed without columns, which causes false vertical restraints.

(a)

"imaginary" grid line

(b)

without "imaginary" grid line

(c)
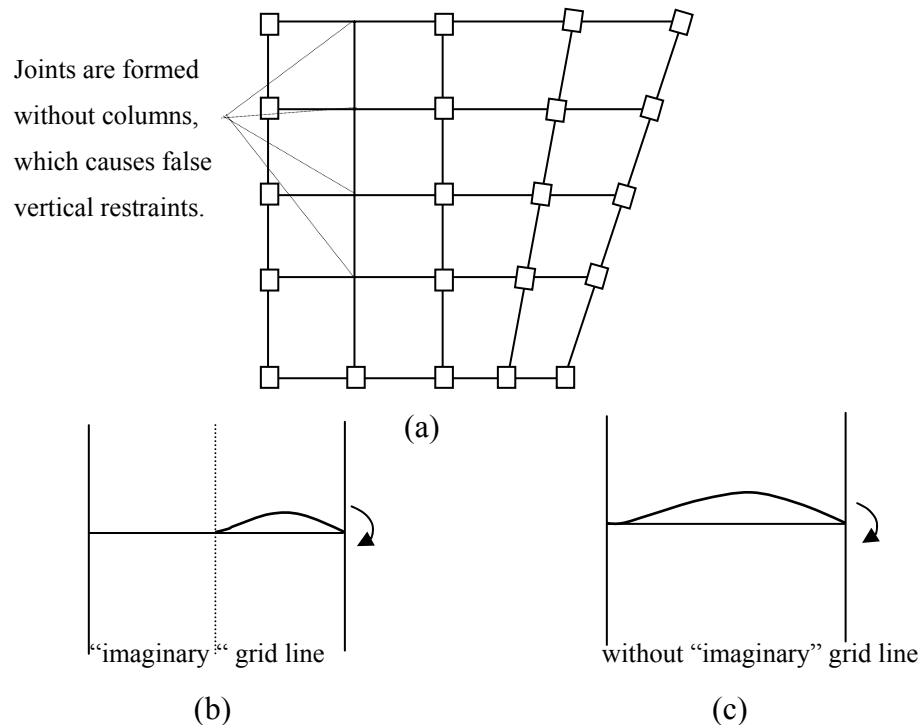
Figure 3.7 – Formation of Joints by Imaginary Grid Lines

21

One of the properties implemented in the software is the definition of non-parallel axis systems. Frames can sometimes be placed in skewed, non-parallel geometry which may usually be seen at a corner building (See Figure 3.8).

Angular arrangement of the frames oriented in the x-direction is represented by angles between the x-axis and the frame itself. Similarly, angles defined between the vertical direction frames and y-axis direction defines the orientation of these frames. Angles are positive in clockwise direction for both directions. Contribution of angular frames into stiffness matrix is determined by multiplying all stiffness terms by the cosine of frame skew angle. Note that stiffness of parallel frames is not affected since cosine of zero is equal to unity.
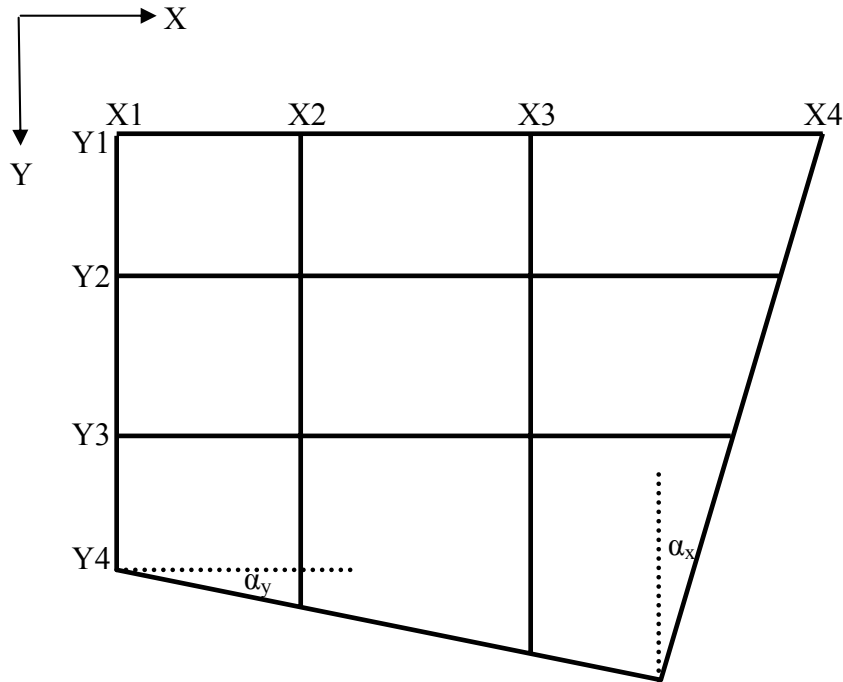
Figure 3.8 - Non-Parallel Axis System

Additional measures are taken in the program for base column stiffness adjustment. First story columns are considered as fixed at the ground level. However, such an assumption can be slightly modified including the effects of soil stiffness. Figure 3.9 illustrates the two extreme cases of support conditions. Theoretically, "4EI/L" and "3EI/L" are used as stiffness influence coefficients for

fixed and pinned supports respectively. However, the actual value is expected to be between these values and can be best estimated as a function of soil type. Note that adjustment of the assumption can also be made considering building foundation type. However, foundation is not taken into account in the developed program.
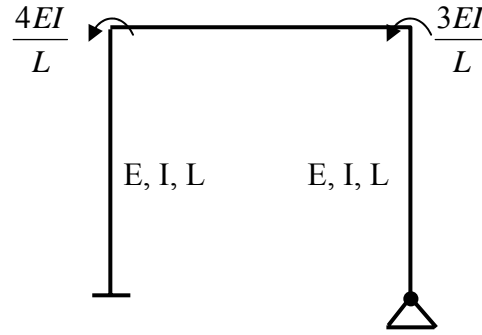
Figure 3.9 - Stiffness Influence Coefficients Based on Support Condition

The assumed EI/L coefficients implemented into stiffness generation algorithm as a function of soil type is given in Table 3.1.

Table 3.1 - Coefficient of EI/L Based on Soil Type

Soil Type (specified in the TEC[*])	Coefficient of EI/L
Z1	4
Z2	3.8
Z3	3.6
Z4	3.4

*Turkish Earthquake Code [16]

Next step in formation of frame lateral stiffness matrix is conversion of frame dofs into global directions (Figure 3.4). For this purpose, static condensation method is used to eliminate rotational dofs in elevation leaving only translational dofs at frame level. As it is mentioned in section 3.3.2, floor masses are idealized as concentrated lumped masses at the center of masses of each floor. Therefore,

diagonal elements of mass matrix corresponding to rotational dofs contain zero terms. These terms can be eliminated from the dynamic analysis of the structure provided that the dynamic excitation does not include any external forces in the rotational dofs, as in the case of earthquake excitation.

Considering set of equations given in Equation 3.1, eliminated dofs are rotational whereas translational dofs are kept.

$$\begin{bmatrix} k_{tt} & | & k_{tr} \\ \hline k_{rt} & | & k_{rr} \end{bmatrix} \begin{Bmatrix} u_t \\ u_r \end{Bmatrix} = \begin{Bmatrix} P_t \\ 0 \end{Bmatrix} \tag{3.1}$$

where

k_{tt} : Stiffness terms for translation-translation interaction

k_{tr} : Stiffness terms for translation-rotation interaction

k_{rt} : Stiffness terms for rotation-translation interaction

k_{rr} : Stiffness terms for rotation-rotation interaction

u_t : Dofs with force assigned (translational)

u_r : Dofs with zero force assigned (rotational)

P_t : Lateral force due to ground motion

Expanding upper and lower partition of Equation 3.1 gives;

$$k_{tt}u_t + k_{tr}u_r = P_t \tag{3.2.a}$$

$$k_{rt}u_t + k_{rr}u_r = 0 \tag{3.2.b}$$

Solving for u_r in Equation 3.2.b;

$$u_r = -k_{rr}^{-1}k_{rt}u_t \tag{3.3}$$

It is important that condensed dofs are not discarded. They are expressed as functions of remaining dofs as shown in Equation 3.3. Substituting Equation 3.3 into Equation 3.2.a;

$$k_{tt}u_t - k_{tr}k_{rr}^{-1}k_{rt}u_t = P_t \tag{3.4}$$

After arranging terms;

$$\left(k_{tt} - k_{tr}k_{rr}^{-1}k_{rt}\right)u_t = P_t \tag{3.5}$$

As it can be seen, Equation 3.1 condenses to the form;

$$\hat{k}_{tt}u_t = P_t \tag{3.6}$$

where condensed stiffness matrix is given by

$$\hat{k}_{tt} = \left(k_{tt} - k_{tr}k_{rr}^{-1}k_{rt}\right) \tag{3.7}$$

Condensation procedure is applied to all frames in each direction. Uncondensed forms of the matrices are also stored for determination of eliminated rotational displacements using Equation 3.3.
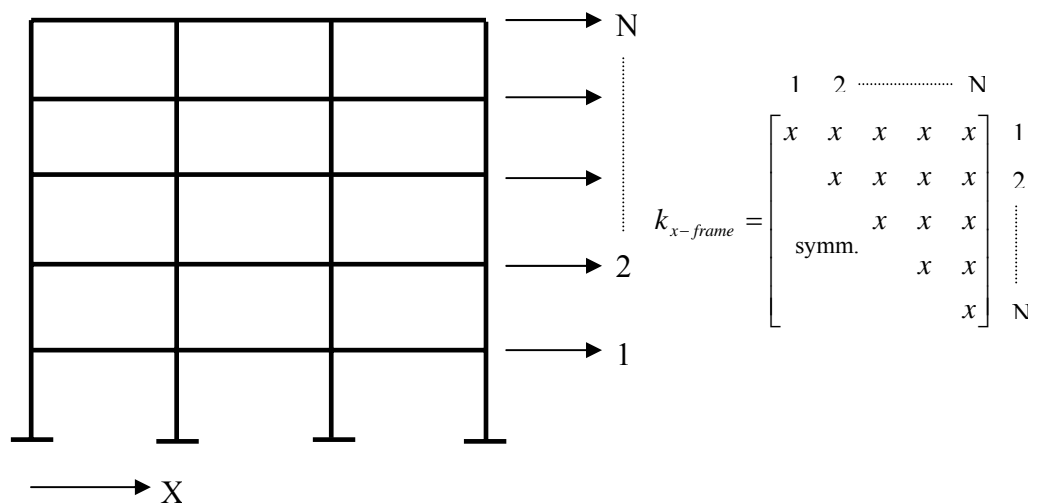
Figure 3.10 - Condensed Form of Frame Lateral Stiffness Matrix

25

After all rotational dofs are statically condensed, NxN symmetric lateral stiffness matrix is obtained for each frame oriented in X and Y directions separately (Figure 3.10). N represents the number of story for a frame. It was pointed out earlier that two translational and one torsional dof is assigned at each floor. Subsequent stage of the program flow is to construct the global structural stiffness matrix referring to directions of dofs defined in global sense (Figure 3.4). Details on global stiffness matrix generation are given in the section 3.3.6 in further detail.

3.3.4   Infill Walls

In addition to load carrying members, non-structural elements such as infill walls provide significant contribution to initial lateral stiffness of frame systems. Seismic response of frame type structures may basically change leading to considerable deviations in distribution of internal forces due to existence of infill walls. Moreover, increase in stiffness may intensify the base shear during earthquakes. Therefore, infill wall effects on system stiffness and mass needs to be taken into consideration.

Although there are a number of on-going studies, effect of masonry walls on the system stiffness is not theoretically well defined. Great percentage of these uncertainties comes from the complicated interaction between frame-wall systems and nonlinear behaviour during earthquakes.
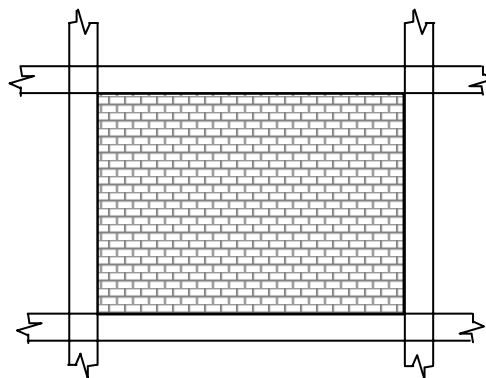
Figure 3.11 - Frame with Infill Wall

Considering a representative wall given in Figure 3.11, one of the simplest assumptions that can be made on overall stiffness is summing the contributions of the frame and wall. Direct summation may be correct if the wall is considered as independent from enclosing beams and columns. However, combined system stiffness is larger if there is any interaction between them. Interaction between wall and surrounding frame depends basically on contact area and degree of bond at the interface. Such factors produce additional unclear points. As far as the approximate nature of the software is concerned, it may be acceptable to formulate wall stiffness based on separate contributions.

Proposed method considers both shear and bending stiffness contributions in order to determine lateral wall stiffness. First, these contributions are estimated and then summed up based on simultaneous shear and bending behaviour of the wall. Figure 3.12 shows deformed shape of a typical wall subjected to unit displacement in its strong direction. Shear strain in x-y plane is symbolized by γ_{xy} expressed in radians. Note that the deformation is purely shear without any rotation.
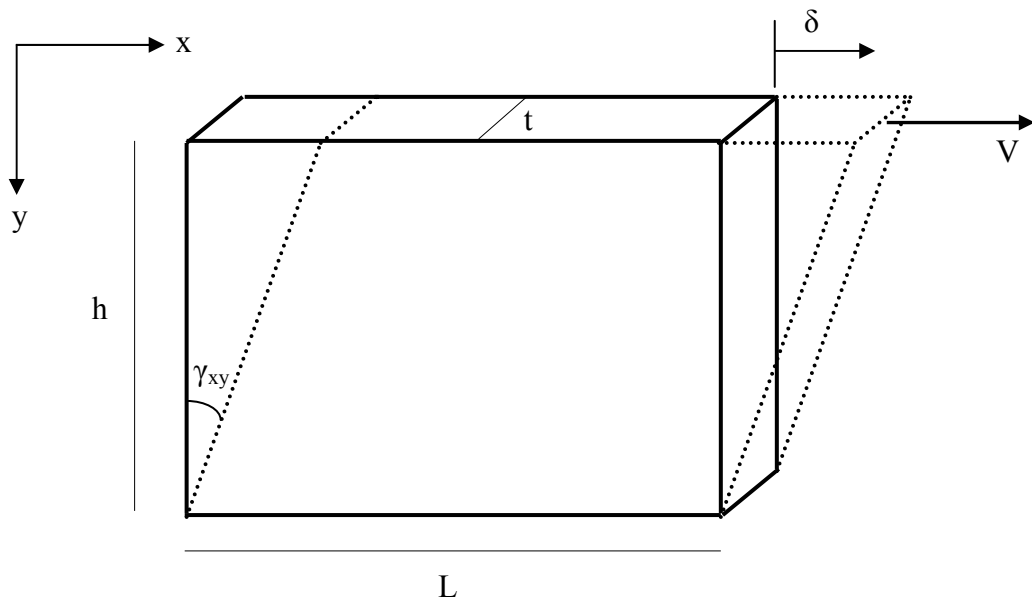
Figure 3.12 - Deformed Shape of the Infill Wall

Referring to Figure 3.12,

$$\tan \gamma = \frac{\delta}{h} \tag{3.8}$$

Since γ_{xy} is very small, Equation 3.8 leads to;

$$\gamma = \frac{\delta}{h} \tag{3.9}$$

Corresponding shear stress is found by Hooke's law for shear stress-strain relation;

$$\tau_{xy} = \gamma_{xy} G \tag{3.10}$$

where

G : Shear modulus of wall $\approx 0.4 E_w$

τ_{xy} : Shear stress in x-y plane

After necessary substitutions shear force becomes;

$$V = \tau_{xy} A = \gamma_{xy} GtL = \frac{\delta}{h} GtL \tag{3.11}$$

Finally, shear based lateral stiffness of the wall is determined by equating δ to unity;

$$k_{w-shear} = \frac{G}{h} tL \tag{3.12}$$

Based on elementary structural analysis, bending stiffness of wall shown in Figure 3.12 can be defined by Equation 3.13;

$$k_{w-bending} = \frac{12 E_w I}{h^3} \tag{3.13}$$

in which

E_w : Elastic modulus of the infill wall

I : Moment of inertia of wall, $= tL^3/12$

h : Height of wall

Modulus of elasticity for infill wall is computed using the following relation given in FEMA 273 [2];

$$E_w \cong 550 f_w \tag{3.14}$$

Default value for compressive strength of infill, f_w, in fair condition is taken as 600 psi ($\approx$ 4.1 MPa) as stated in FEMA 273 [2]. Accordingly, elastic modulus of infill wall becomes 2.255×10^6 kN/m^2.

Finally, shear and bending stiffness are combined to calculate total wall stiffness. Combination is done in such a way that both shear and bending behaviour effect overall stiffness like in serial spring analogy. Hence, formulation turns out to be;

$$k_{total} = \frac{1}{\dfrac{1}{12E_wI/h^3} + \dfrac{1}{GLt/1.2h}} \tag{3.15}$$

One observation from Equation 3.15 becomes shear dominant as the length of wall increases. If two contributions are directly summed up then total stiffness diverges from shear value which builds up above formulation. Shear stress mainly develops on middle region of the wall surface. On the edges, it approaches to zero. Therefore shear stiffness of the wall is slightly modified by the factor of 1.2 which is shown in Equation 3.15.

3.3.5 Shear Walls

Reinforced concrete shear walls provide significant earthquake resistance to buildings. They also contribute to the ductility of the system considerably. Collapse may be avoided due to existence of such walls even if other structural elements have exceeded their capacity. In general, shear walls fundamentally alter the seismic performance and behaviour of a building by resisting relatively much greater amount of external forces due to its relatively high resistance and strength. Consideration of these strong walls gains much importance due to their critical role in the overall seismic resistance.

Handling of shear walls in the software may be different than that of columns. Although shear walls are usually placed in between adjacent axes, they may also be placed independently at axes intersections. In the second case, shear wall is considered as a single column with the given cross sectional dimensions. On the other hand, if it is placed between two axes, as usual in practice, it is divided into two equivalent columns such that total stiffness of the equivalent columns is same as the shear wall. In other words, stiffness is equally divided and lumped into adjacent joints. Stiffness of a typical shear wall with length L and height H is given by Equation 3.15.

Half of the stiffness given in Equation 3.15 is equated to column stiffness. Then, it is written as;

$$\frac{12EI_e}{H^3} = \frac{0.5}{\dfrac{1}{12EI/H^3} + \dfrac{1}{GLt/1.2H}} \qquad (3.16)$$

where $G \approx 0.4E$ and equivalent column inertia, I_e, is defined as;

$$I_e = \frac{tL_e^3}{12} \qquad (3.17)$$

After some arrangements and simplifications, equivalent column length (or width) L_e turns out to be;

$$L_e = L \sqrt[3]{\frac{0.5}{1 + \frac{13}{5}\frac{L^2}{H^2}}}$$

(3.18)

As the H/L ratio approaches to infinity, equation comes close to the form in which equivalent column length is approximately %79 of shear wall length (L/1.26). This percentage also corresponds to equivalent inertia requirement which is derived as below.
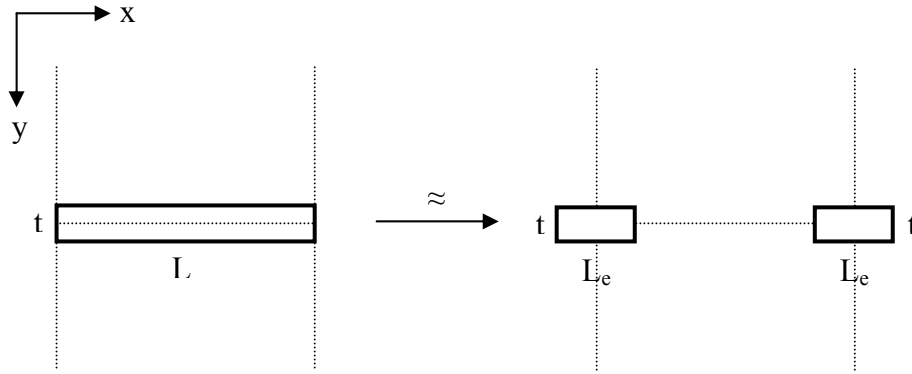
Figure 3.13 – Top View of Equivalent Column Designation for Single Shear Walls

Note that equivalent column thickness remains unchanged. Referring to Figure 3.13, moment of inertia of shear wall with respect to y-y direction;

$$I_{sw-y} = \frac{1}{12}tL^3$$

(3.19)

I_{sw-y} should be equal to total moment of inertia of columns with respect to y-y direction. Then,

$$\frac{1}{12}tL^3 = \frac{1}{6}t(L_e)^3$$

(3.20)

31

After simplifications, equivalent column width becomes,

$$L_e = \frac{L}{1.26}$$

(3.21)

The Equation 3.21 is valid for cases when H/L ratio converges to infinity. When it is relatively larger than L, the shear wall converges to a column and shear contribution in Equation 3.16 becomes negligible. Therefore, the Equation 3.21 turns out to be correct for a column in bending.

Another frequently faced situation in practice is the existence of shear walls designed for more than one span. It may even surround whole perimeter of the building. In such cases, inertia contributions from both sides of an axis are taken into account so that an identical column is formed at the joint (Figure 3.14). Thickness and length of adjacent shear walls may be different.
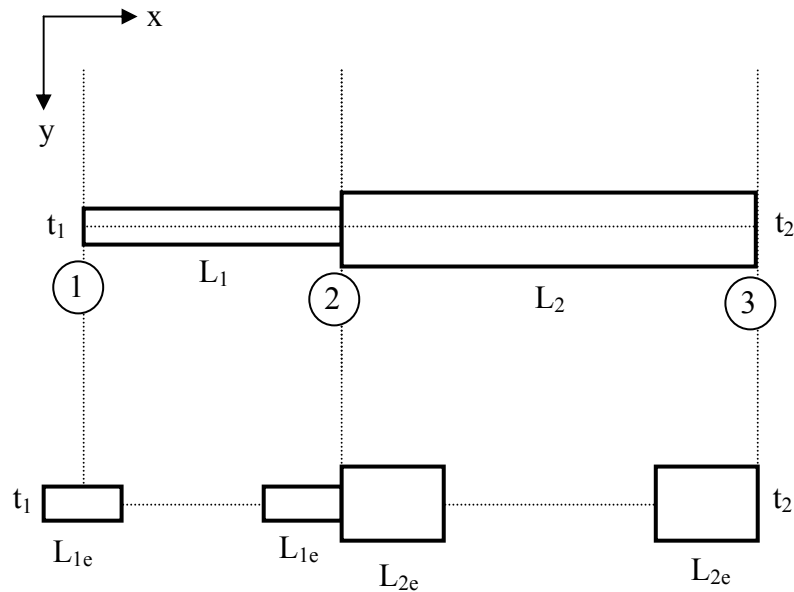
Figure 3.14 - Equivalent Column Designation for Adjacent Shear Walls

Equation 3.18 is simply applied to shear walls 1-2 and 2-3 (L_1 and L_2) separately, but, further arrangement is necessary for joint 2. Average thickness of columns located at joint 2 is selected to represent equivalent thickness. Such estimation

does not bring major error to total inertia in that direction since wall thickness is negligibly small compared to wall length. Thus, average thickness, t^* is given by,

$$t^* = \frac{t_1 + t_2}{2} \qquad (3.22)$$

From Equation 3.17, the equivalent column stiffness derived from the shear wall stiffness can be written in the following form;

$$I_{et} = I_{e1} + I_{e2}$$
$$\frac{t^* \left(L^* \right)^3}{12} = \frac{t^* \left(L_{e1} \right)^3}{12} + \frac{t^* \left(L_{e2} \right)^3}{12} \qquad (3.23)$$

Replacing both column thickness by t^* and equating total moment of inertia in Y-direction leads to equivalent length of newly formed column;

$$L^* = \left(L_{1e}{}^3 + L_{2e}{}^3 \right)^{1/3} \qquad (3.24)$$

Exactly similar calculations are also valid for shear walls defined in other perpendicular direction.

3.3.6 Formation of Global Stiffness Matrix

Stiffness matrix of overall structure is generated by using direct stiffness method [7]. Multistory buildings with symmetric and unsymmetrical plans may be defined by the user and program should be capable of handling extremes. Many buildings have poor structural system configuration resulting in undesirable responses to strong ground motion. Hence, a general formulation is developed considering two-way unsymmetrical floor plans. Such systems generally have mass and rigidity centers away from each other resulting in eccentricities which generate torsional deformations in addition to translational ones. Figure 3.15 shows an arbitrary system consisting of several frames oriented in X and Y directions. Note that framing plan is unsymmetrical about both directions.

(a) Multistory System

(b) a-a frame in y-direction   **(c)** b-b frame in x-direction
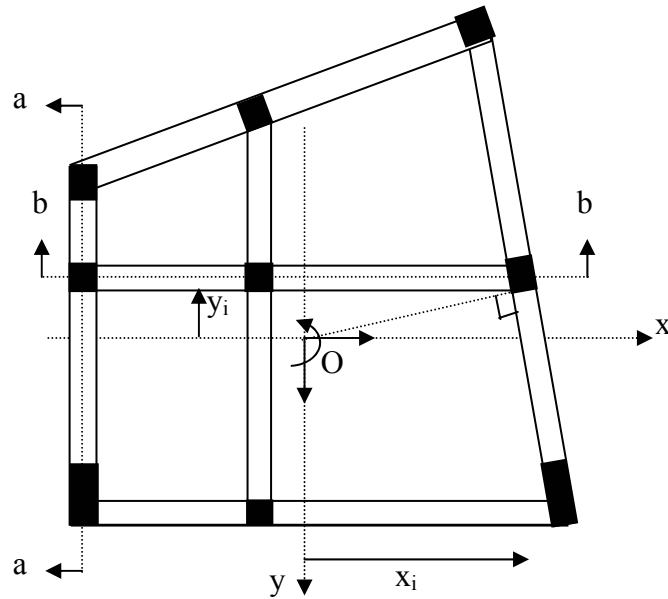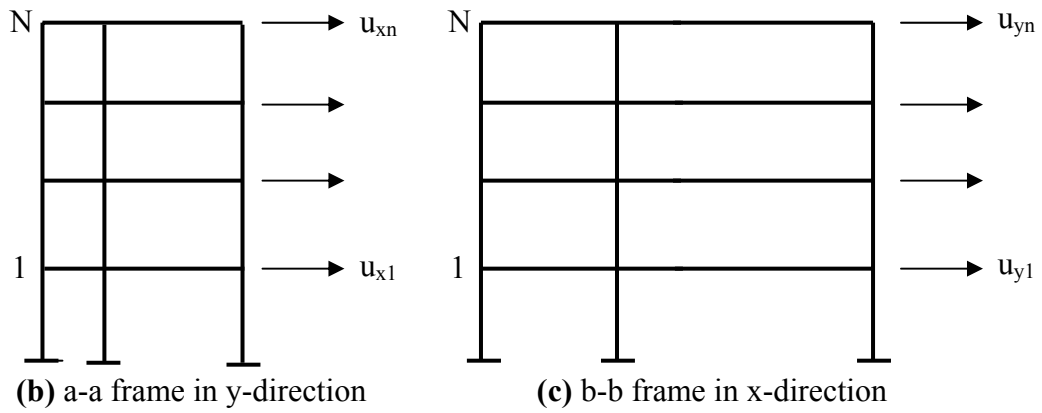
Figure 3.15 - Two-way Unsymmetrical Floor Plan

Center of mass (point O) of all floor diaphragms may not lie on the same vertical axis due to differences in mass properties of the frames and possible openings in the slab. Therefore, single mass center is determined for entire system using the weighted average relation given in Equation 3.25 and Equation 3.26.

$$MC_x = \frac{\sum_i M_i mc_{xi}}{\sum_i M_i} \tag{3.25}$$

$$MC_y = \frac{\sum_i M_i mc_{yi}}{\sum_i M_i} \tag{3.26}$$

where,

(x_i, y_i) : Distance of each frame to mass center (point O)

M_i : Total mass of ith floor

mc_{xi} : Mass center of ith floor in x-direction

mc_{yi} : Mass center of ith floor in y-direction

MC_x : Mass center of entire system in x-direction

MC_y : Mass center of entire system in y-direction

Remark: Calculation of floor mass center and total floor mass is given in the section 3.3.7.

In order to relate dofs for the frame to global dofs for the building, displacement transformation matrices are used. In the case of multistory buildings with arbitrary plan with no axis of symmetry, Nx3N (N being the number of stories) matrix is generated. Each of the 3N modes generally contains coupled X-lateral, Y-lateral and torsional motion and is excited by ground motion in the X or Y directions. These transformation matrices are given in Equation 3.27 and Equation 3.28. Verification of transformation matrices is given in Appendix E.

$$\underline{a}_{xi} = \begin{bmatrix} \underline{I} & \underline{0} & -y_i \underline{I} \end{bmatrix} \tag{3.27}$$

$$\underline{a}_{yi} = \begin{bmatrix} \underline{0} & \underline{I} & x_i \underline{I} \end{bmatrix} \tag{3.28}$$

In Equations 3.27 and 3.28, x_i and y_i represents the location of ith frame oriented in the Y and X directions, respectively (Figure 3.15). If the frame is skewed components of the perpendicular distance between that frame and the mass center are considered. $\underline{I}$ is an identity matrix of order N and $\underline{0}$ is a square matrix of order N with all elements equal to zero.

Finally, contribution of each frame to the global stiffness matrix is determined using the following transformation.

$$\underline{k}_i = \underline{a}_{xi}{}^T \underline{k}_{xi} \underline{a}_{xi} \tag{3.29}$$

$$\underline{k}_i = \underline{a}_{yi}{}^T \underline{k}_{yi} \underline{a}_{yi} \tag{3.30}$$

where;

$\underline{a}_{xi}, \underline{a}_{yi}$: transformation matrices as shown in Equation 3.27 and 3.28

k_{xi} : lateral stiffness matrix of the ith frame oriented in x-direction

k_{yi} : lateral stiffness matrix of the ith frame oriented in y-direction

k_i : contribution of the ith frame to global stiffness matrix

Then, stiffness matrices of all frames are added to obtain global stiffness matrix.

$$\underline{k}_{global} = \sum_i \underline{k}_i \tag{3.31}$$

Three global dofs at each story results in a final global stiffness matrix size of 3Nx3N. Arrangement of stiffness terms in this matrix depends on the orientation of global dofs. Insertion of frame lateral stiffness matrices of a three-story building into global stiffness matrix is illustrated in Figure 3.16.

It can be seen from Figure 3.16 that the first NxN set of stiffness terms belongs to frames oriented in X-direction. The second NxN set corresponds to frames oriented in Y-direction. Finally, torsional stiffness of floors is represented by last

NxN stiffness matrix shown in Figure 3.16-b. Existence of coupled terms shown with letter *c* in the matrix depends on frame location pattern. Coupled terms would be equal to zero if the frames are symmetrically placed in x and y directions.

(a) 3-Story Model   **(b)** Global Stiffness Matrix
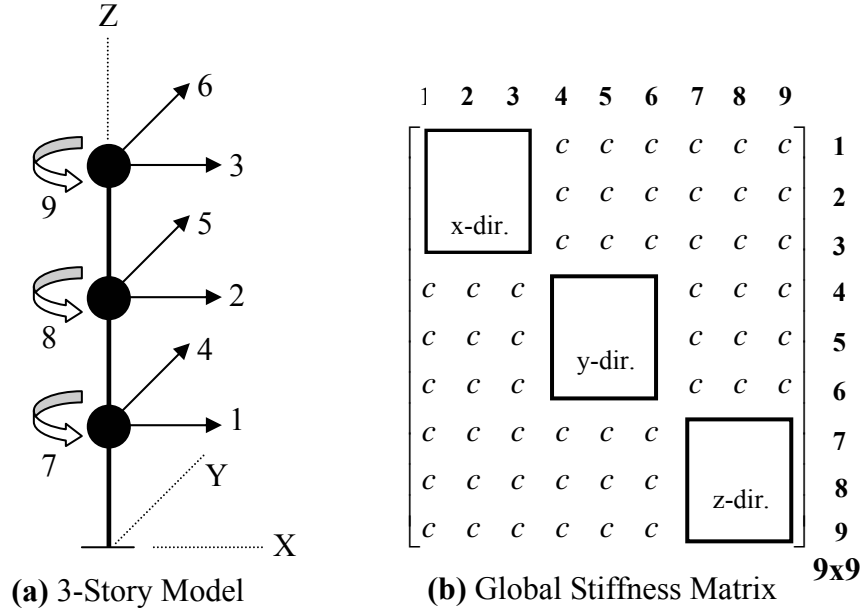
Figure 3.16 - Assembly of Global Stiffness Matrix

A condensed mathematical designation of global stiffness matrix may be given by substituting Equation 3.27 (or 3.28) into Equation 3.29 (or 3.30) and latter into Equation 3.31;

$$\underline{k}_{global} = \begin{bmatrix} \underline{k}_{xx} & \underline{k}_{xy} & \underline{k}_{x\theta} \\ \underline{k}_{yx} & \underline{k}_{yy} & \underline{k}_{y\theta} \\ \underline{k}_{\theta x} & \underline{k}_{\theta y} & \underline{k}_{\theta\theta} \end{bmatrix} \tag{3.32}$$

where

$$\underline{k}_{xx} = \sum_i \underline{k}_{xi} \quad \underline{k}_{xy} = \underline{k}_{yx}{}^T = 0 \quad \underline{k}_{x\theta} = \underline{k}_{\theta x}{}^T = \sum_i y_i \underline{k}_{xi} \tag{3.33}$$

$$\underline{k}_{yy} = \sum_i \underline{k}_{yi} \quad \underline{k}_{y\theta} = \underline{k}_{\theta y}{}^T = \sum_i x_i \underline{k}_{yi} \quad \underline{k}_{\theta\theta} = \sum_i x_i{}^2 \underline{k}_{yi} + y_i{}^2 \underline{k}_{xi} \tag{3.34}$$

37

At this stage of the program code, frame stiffness matrices formation and assembly of the global stiffness matrix is completed. Note that all stiffness formulations include the contribution of infill walls and shear walls based on the theory and related major considerations as discussed in sections 3.3.4 and 3.3.5, respectively.

3.3.7   Generation of Mass Matrix

Mass matrix is one of the most important dynamic properties of a structural system. In the preceding sections, it was pointed out that lumped mass idealization is utilized. For the frames, mass may be considered as lumped at each node. Each structural element is represented by point masses at its nodes. The amount of lumped mass at each node is the sum of mass contributions of all structural elements connected to that node (Figure 3.17).
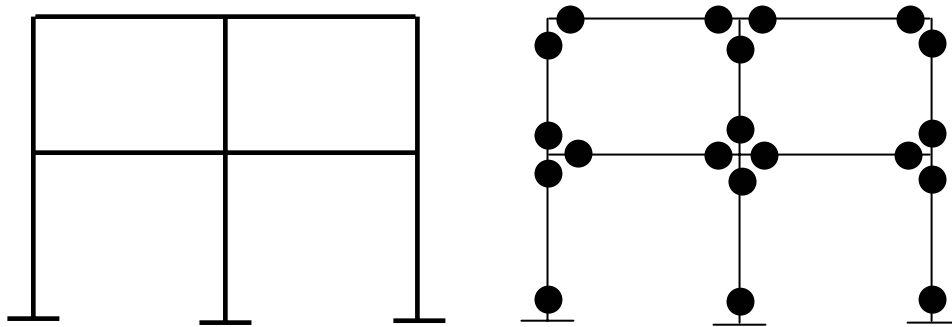
Figure 3.17 - Lumped Mass Idealization for Frames

Arrangement of mass may further be simplified for multistory buildings because of the constraining effects of the floor slabs. As it was mentioned previously, each floor diaphragm is assumed to be infinitively rigid in its own plane. However, slab is capable of rigid body rotation in the vertical direction (torsion) and translation in two horizontal directions. Introducing this assumption results in degree of freedoms of all joints at a floor are functions of three global dofs of the floor diaphragm (see Figure 3.4). Hence, single rotational mass in the direction of rotational dof and two translational equal masses in the directions of horizontal

dofs are assigned for each floor level. Implementation of mass matrix in the program code depends on these idealizations.

Translational mass of each floor is the sum of contributions from all structural and non-structural components including beams, columns, walls and slab at that floor (Equation 3.35).

$$TM_i = (M_i)_{slab} + \sum (M_i)_{wall} + \sum (M_i)_{column} + \sum (M_i)_{beam} \qquad (3.35)$$

where

TM_i : Total translational mass at i^{th} floor

$(M_i)_{slab}$: Mass due to slab at i^{th} floor

$(M_i)_{wall}$: Mass due to a wall at i^{th} floor

$(M_i)_{column}$: Mass due to a column at i^{th} floor

$(M_i)_{beam}$: Mass due to a beam at i^{th} floor

Concrete density is selected as 25 kN/m^3 in calculating beam, column and slab mass. Infill walls are considered as made up of brick. Dimensions and weight of a sample was determined to calculate brick density. Table 3.2 shows the geometric and mass properties taken from laboratory measurements.

Table 3.2 - Laboratory Measurements for Brick Sample

Thickness	66 mm
Width	82 mm
Height	95 mm
Volume	514140 mm^3
Mass	420 gr
Density	$\approx$ **8.2 kN/m^3**

Great portion of the mass at a floor comes from the slab as expected. However, little more effort is needed to find out the slab mass in particularly for the buildings with non-rectangular plan. Such situation is common in practice due to

holes or discontinuities in the slab for architectural requirements. In order to handle this, slab is divided into pieces separated by axes lines. Contribution of each slab piece are calculated and added up accordingly. Note that each piece may not necessarily be in rectangular shape depending on the angular position of the axis. In such cases, corresponding area is considered as two triangular regions for simplicity.

Mass defined in the direction of rotational dof includes the rotational moment of inertia of both structural and non-structural elements about vertical axis passing through the mass center of the building. Formulation of rotational inertia for an element is given in Equation 3.36.

$$RM_i = \left(RM_i\right)_{self} + M_i d_i^{\,2} \tag{3.36}$$

where

RM_i : Rotational mass inertia of ith member about "Center of Mass"

$(RM_i)_{self}$: Rotational mass inertia of ith member about its own axis

M_i : Mass of ith element

d_i : Distance of ith element to the center of mass

Equation 3.36 is applied to beams, columns, walls, and slab. Summation gives the total inertia of the floor corresponding to torsional motion. Relatively greater contribution to element rotational inertia comes from the second part of Equation 3.36 since distance to the mass center may be quite large. Similar to translational mass formulation, slab is divided into pieces and contributions from each piece are added up. Mass center of each floor is found from Equation 3.37.

$$mc_i = \frac{\sum \left(m_b d_b\right)_i + \sum \left(m_c d_c\right)_i + \sum \left(m_w d_w\right)_i + \sum \left(m_s d_s\right)_i}{\sum \left(m_b + m_c + m_w + m_s\right)_i} \tag{3.37}$$

In Equation 3.37, subscripts b, c, w, and s stand for beam, column, wall, and slab, respectively. Denominator is the total mass of these elements at ith floor. d is the

distance to a certain fixed point. Same calculation is carried out for both x and y directions.

Mapping of all mass terms are also important for the generation of final mass matrix. True locations of these terms are determined based on the direction of dofs. Assembly is performed in a fashion similar to formation of global stiffness matrix. Recall that translational dofs in both directions are first assigned to each story. Thus, the first 2N diagonal elements of the matrix belong to total translational mass of each floor. Remaining N diagonal elements correspond to total rotationals inertias of floors. Better visualization on a simple model is shown in Figure 3.18.

a) 3-Story Model　　　　b) 3Nx3N Mass Matrix
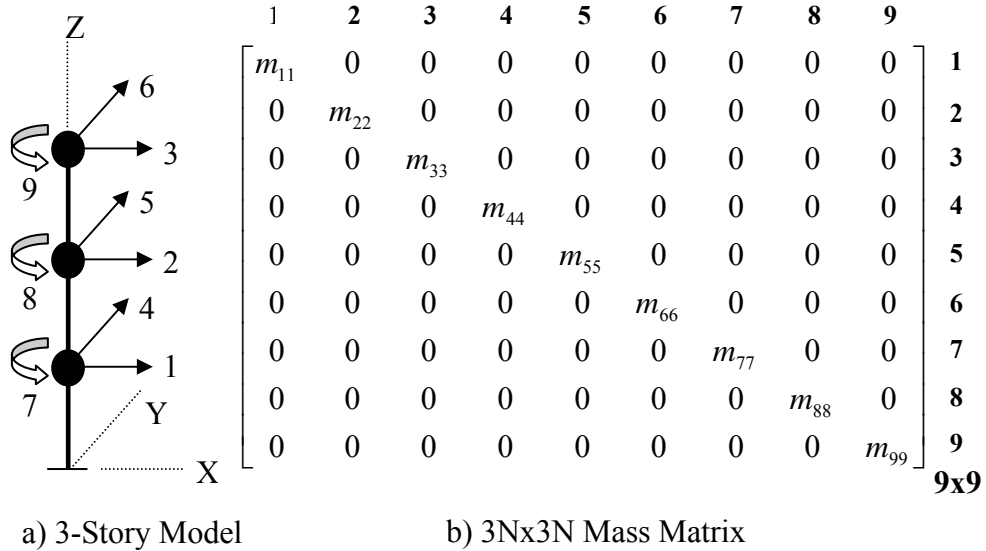
Figure 3.18 - Assembly of Mass Matrix

Observe that lumped mass at a floor is associated with two translational dofs (X and Y direction) and a torsional dof (Z direction) of that floor. Therefore, mass matrix is always diagonal for lumped-mass idealization as done in this study. Similar to the stiffness matrix, size of the mass matrix is also 3Nx3N.

3.3.8 Eigenvalue Analysis

The first step of a dynamic analysis is eigenvalue analysis where the periods and modes of a structure are determined based on its stiffness and mass properties. Various researches have been conducted to propose solution to eigenvalue problem. Several methods have been developed depending on the characteristics of engineering interests. Solution techniques include vector iteration methods (ex: Power method) and transformation methods based on orthogonality property of modes (ex: Jacobi's method). From theoretical viewpoint, discussion of these techniques is beyond the scope of this study. However, it is necessary to underline the major features of eigenvalue problem in structural engineering.

Finding the natural frequencies and modal shapes of a structure requires the solution of matrix eigenvalue problem which is represented in Equation 3.38.

$$\underline{k}\phi_n = w_n{}^2\,\underline{m}\phi_n \tag{3.38}$$

where

k : Global stiffness matrix of the system

m : Lumped diagonal mass matrix

w_n : Frequency for the nth mode

ϕ_n : Shape vector for the nth mode

w_n and Φ_n are only unknowns in Equation 3.38 which can be rewritten in the form of;

$$\left[\underline{k} - w_n{}^2\,\underline{m}\right]\phi_n = \underline{0} \tag{3.39}$$

Note that Equation 3.39 can always be satisfied if Φ_n is equal to zero. Yet, this leads to trivial solution meaning that structure does not vibrate. Nontrivial solution may be provided if;

$$\det\left[\underline{k} - w_n{}^2\,\underline{m}\right] = 0 \qquad\qquad\qquad\qquad\qquad \textbf{(3.40)}$$

Roots of the Equation 3.40 give the eigenvalues which are identical to square of frequencies. When a frequency of a mode is known, corresponding modal shape (Φ_n), which is also known as eigenvector for that mode is determined by Equation 3.39. In general, maximum number of vibration frequencies and modes is limited with the number of dof in the system. Since total number of dofs is proportional to the square of number of stories, 3N eigenpairs (w_n, Φ_n) are obtained for the structure. All of the modes and frequencies calculated from the eigenvalue analysis are used to earthquake load demands using CQC method (section 3.3.10).

Finding the roots of Equation 3.40 is an iterative process and requires much computational effort according to number of dofs. Choice of solution methods for this purpose depends on geometric properties of mass and global stiffness matrices. Size of the matrices, bandwidth of $\underline{k}_{global}$, required number of modes and diagonal condition of $\underline{m}$ all effect the iterative solution of the eigenvalue problem. In addition, diagonal mass matrix appears as a result of lumped mass idealization which intensifies the reliability in obtaining accurate solutions and provides efficient computations. Although such is the case in many structural engineering applications, quite complex eigenvalue problems can be easily solved by technical computing tool such as MATLAB [21] which has superior built-in functions for these purposes.

3.3.9 Response Spectrum Analysis

Most building codes require that a dynamic lateral force analysis procedure be used for buildings. Also depending on the seismicity of the area, height and the fundamental periods of the selected building, codes usually stipulate that only a theoretically sound dynamic analysis should be carried out. Response spectrum analysis (RSA) is the most common dynamic analysis procedure developed for structures subjected to earthquake excitation.

By definition, RSA involves the evaluation of the maximum value of structure responses such as displacements, member forces etc. for each mode of vibration using a spectrum of earthquake records. In other words, objective of such procedure is to combine the contribution of each mode and therefore to find a single "peak response" based on a spectrum defining the dynamic characteristics of the ground motion.

Considering the nonlinear behaviour of ground motion, variation in stiffness properties according to deformation level obviously provides better estimates. However, even if the structure experiences structural damage, peak displacements may be well predicted by linear model approximations. Consequently, application of RSA in this study results in linear peak response of a system. How well the computed response agrees with the actual response of structure during an earthquake depends primarily on the quality of structural idealization. It is declared earlier that multistory buildings with both symmetric and unsymmetrical plans are considered. RSA procedure for multi-degree of freedom systems (MDOF) lead to accurate results enough for design applications. In the following parts, theoretical explanations of RSA for such systems are discussed and are implemented in the software.

3.3.9.1. *Modal Expansion of Effective Earthquake Forces*

For n-story building, distribution of applied forces referring to idealized model (Figure 3.4) is formulated as;

$$\underline{S} = \sum_{i=1}^{3n} \Gamma_i \underline{m} \phi_i \tag{3.41}$$

where

$\underline{m}$: 3n x 3n building mass matrix

ϕ_i : Shape vector for i^{th} mode

In Equation 3.41, Γ_i is called as modal participation factor. It is a measure of the degree to which the ith mode participates in the response and given by;

$$\Gamma_i = \frac{L_i^h}{M_i} \tag{3.42}$$

where

$$L_i^h = \sum_{j=1}^{n} \left(m_{tj}\phi_{jxi} + m_{tj}\phi_{jyi} + m_{rj}\phi_{j\theta i} \right) \tag{3.43}$$

$$M_i = \sum_{j=1}^{n} \left(m_{tj}\phi_{jxi}^{\;2} + m_{tj}\phi_{jyi}^{\;2} + m_{rj}\phi_{j\theta i}^{\;2} \right) \tag{3.44}$$

In these equations, ϕ_{jxi}, ϕ_{jyi} and $\phi_{j\theta i}$ stand for x, y and z components of the ith mode shape at jth floor respectively. m_{tj} is total mass for jth floor and m_{rj} represents the mass due to rotational mass inertia of the jth floor about vertical axis. Using the orthogonality of the modes ith mode contribution to the distribution of effective earthquake force becomes;

$$\underline{S}_i = \left\{ \begin{array}{c} \underline{S}_{xi} \\ \underline{S}_{yi} \\ \underline{S}_{\theta i} \end{array} \right\} = \Gamma_i \left\{ \begin{array}{c} \underline{m}_t \phi_{xi} \\ \underline{m}_t \phi_{yi} \\ \underline{m}_r \phi_{\theta i} \end{array} \right\} \tag{3.45}$$

3.3.9.2. Modal Static Responses

Modal static response r^{st} is determined by static analysis of the structure subjected to external forces $\underline{S}_i$ given in Equation 3.45 The ith mode contribution to any response quantity is then given by;

$$r_i = r^{st} A_i \tag{3.46}$$

Direction of forces is controlled by the algebraic sign of modal shapes. They are all in the same direction for the fundamental mode but in reversed direction for the higher modes.

Modal static responses calculated in the program include shear, torque and moment on a story basis, base shear in both horizontal directions, base torque, overturning moment and floor displacements (lateral & torsional). Formulation of these response quantities based on Figure 3.19 is presented in Table 3.3.
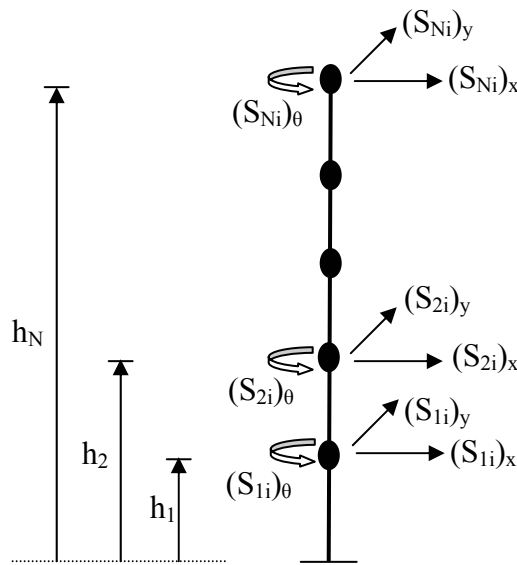
Figure 3.19 - Computation of Modal Static Forces

Table 3.3 - Summary of Modal Static Responses

Response	Modal Static Response
Story Shear (x & y)	$$\left(V_{ni}\right)_x^{st} = \sum_{j=n}^{N}\left(S_{ji}\right)_x$$ $$\left(V_{ni}\right)_y^{st} = \sum_{j=n}^{N}\left(S_{ji}\right)_y$$
Story Torque	$$\left(T_{ni}\right)^{st} = \sum_{j=n}^{N}\left(S_{ji}\right)_\theta$$

46

Table 3.3 (continued)	
Story Moment (x & y)	$$\left(M_{ni}\right)_x^{st} = \sum_{j=n}^{N}\left(h_j - h_{n-1}\right)\left(S_{ji}\right)_x$$ $$\left(M_{ni}\right)_y^{st} = \sum_{j=n}^{N}\left(h_j - h_{n-1}\right)\left(S_{ji}\right)_y$$
Base Shear (x & y)	$$\left(V_{bi}\right)_x^{st} = \sum_{j=1}^{N}\left(S_{ji}\right)_x$$ $$\left(V_{bi}\right)_y^{st} = \sum_{j=1}^{N}\left(S_{ji}\right)_y$$
Base Torque	$$\left(T_{bi}\right)_x^{st} = \sum_{j=1}^{N}\left(S_{ji}\right)_\theta$$
Overturning Moment (x & y)	$$\left(M_{bi}\right)_x^{st} = \sum_{j=1}^{N} h_j\left(S_{ji}\right)_x$$ $$\left(M_{bi}\right)_y^{st} = \sum_{j=1}^{N} h_j\left(S_{ji}\right)_y$$
Floor Displacements (lateral & torsional)	$$\left(\underline{u}_i\right)_x^{st} = \frac{\Gamma_i}{w_i^2}\underline{\phi}_{xi} \;,\; \left(\underline{u}_i\right)_y^{st} = \frac{\Gamma_i}{w_i^2}\underline{\phi}_{yi}$$ $$\left(\underline{u}_i\right)_\theta^{st} = \frac{\Gamma_i}{w_i^2}\underline{\phi}_{\theta i}$$
Story Drifts (x & y)	$$\left(\Delta_{ji}\right)_x^{st} = \frac{\Gamma_i\left(\underline{\phi}_{jxi} - \underline{\phi}_{j-1,xi}\right)}{w_i^2}$$ $$\left(\Delta_{ji}\right)_y^{st} = \frac{\Gamma_i\left(\underline{\phi}_{jyi} - \underline{\phi}_{j-1,yi}\right)}{w_i^2}$$

3.3.9.3. *Response and Design Spectrum Concepts*

Pseudo-acceleration response A_i of the system in Equation 3.46 is obtained from pseudo-acceleration response spectrum. That quantity is generally different from peak acceleration of the system. Therefore, prefix "pseudo" is used to avoid confusions. In general, plot of the peak value of a response quantity as a function of the fundamental vibration period (or frequency) of the system is called "response spectrum" for that quantity. In case of deformation response spectrum, peak value of deformation is determined from ground deformation history characterized by ground motion record. Other two spectra, namely, pseudo-velocity and pseudo-acceleration are derived from deformation response spectrum using following equations.

$$V = w_i D \quad \text{and} \quad A = w_i^2 D \tag{3.47}$$

in which

D : Peak deformation

w_i : Frequency of the system for i^{th} mode

A : calculated peak pseudo-acceleration

V : calculated peak pseudo-velocity

Similarly, pseudo-acceleration response spectrum is obtained by calculating pseudo-acceleration at each natural period (or frequency) of the system. Important observation here is that each response spectrum is the product of only one excitation. However, it is the "design spectrum" which should be used for seismic evaluation of existing structures to resist future earthquakes.

By definition, design spectrum is an average of a number of earthquake records modified for site specific conditions and then smoothed out for design purposes. Construction of design spectrum is based on statistical analysis of peak spectral values (D, V, A) obtained from a number of response spectra which are plotted

for set of ground motions. These values correspond to different vibration periods. Each ground motion is normalized so that all ground motions have the same peak ground acceleration. Statistical analysis provides the probability distribution for spectral values and their means at each period. All mean values are connected and shifted by amount of one standard deviation. Smooth elastic design spectrum is finally obtained after idealization of connected straight lines.

Design spectrum represents the ground motions at the sites under similar soil conditions. Some other factors affecting the prediction of design spectrum are the fault distance to the site, fault mechanism and earthquake magnitude.

According to Turkish Earthquake Code [16], pseudo-acceleration response corresponding to %5 damped elastic design spectrum normalized by the gravitational acceleration is given by;

$$A = A_0 I S(T) \tag{3.48}$$

In this equation, A_0 is the effective ground acceleration coefficient which takes values 0.4, 0.3, 0.2, 0.1 for seismic zone 1, 2, 3, and 4, respectively. Building importance factor I is taken as unity specified for residential and office buildings. Spectrum coefficient $S(T)$ is captured from Figure 3.20 depending on the local site conditions shown on Table 3.4.
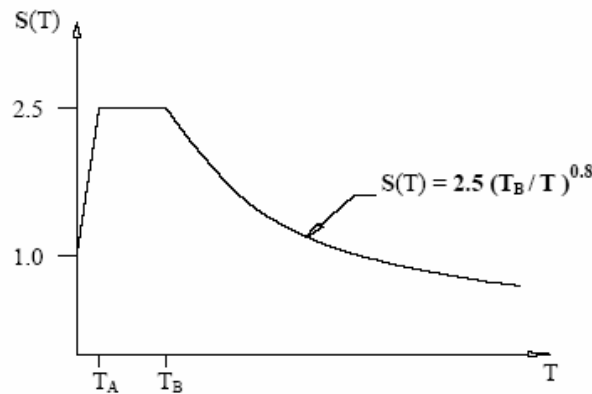
Figure 3.20 - Spectrum Coefficient vs. Period

49

Table 3.4 - Spectrum Characteristic Periods

Local Site Class	T_A (second)	T_B (second)
Z1	0.10	0.30
Z2	0.15	0.40
Z3	0.15	0.60
Z4	0.20	0.90

3.3.9.4. Element Forces

In addition to story forces for the building, it is desired to compute element forces such as bending moment, shear and axial load on beams and columns of each frame. For this purpose, transformation matrices, relating the frame degree of freedoms to global ones, for the building are required (Equations 3.27 & 3.28). For the sake of completeness, it is useful to repeat here;

$$\underline{u}_i = a_{xi}\underline{u} \qquad \text{and} \qquad \underline{u}_i = a_{yi}\underline{u} \tag{3.49}$$

where

$$a_{xi} = \begin{bmatrix} 1 & 0 & -y_i I \end{bmatrix} \qquad \text{and} \qquad a_{yi} = \begin{bmatrix} 0 & 1 & x_i I \end{bmatrix} \tag{3.50}$$

Contribution of nth mode to the global displacement $\underline{u}$ is given by;

$$\underline{u}_{xn} = \Gamma_n \phi_{xn} \frac{A_n}{w_n^2} \qquad \underline{u}_{yn} = \Gamma_n \phi_{yn} \frac{A_n}{w_n^2} \qquad \underline{u}_{\theta n} = \Gamma_n \phi_{\theta n} \frac{A_n}{w_n^2} \tag{3.51}$$

Substituting Equation 3.51 into Equation 3.49 leads to lateral displacements $\underline{u}_{in}$ of the ith frame;

$$\left(\underline{u}_{in}\right)_x = \Gamma_n \underline{a}_{xi} \underline{\phi}_n \frac{A_n}{w_n^2} \qquad \left(\underline{u}_{in}\right)_y = \Gamma_n \underline{a}_{yi} \underline{\phi}_n \frac{A_n}{w_n^2} \tag{3.52}$$

The first part of the Equation 3.52 is for frames oriented in x-direction and the second for frames in the y-direction. Note that these relations now represent dynamic response. The first step in calculation of element forces is to solve for displacements corresponding to condensed dofs. Equation 3.53 provides link between joint rotations and lateral floor displacements.

$$\underline{u}_r = -\underline{k}_{rr}^{-1}\underline{k}_{rt}\underline{u}_t \tag{3.53}$$

Once joint rotations are obtained, element forces can be computed using stiffness coefficients for a flexural element. Figure 3.21-a shows these coefficients for joint rotations of an element with length L, moment of inertia I and elastic modulus E. Coefficients for joint translation of same element is given in Figure 3.21-b. Considering the identical flexural element having two nodes at the ends (Figure 3.22), there are two translational and two rotational dofs defined at each node assuming that element is axially inextensible.
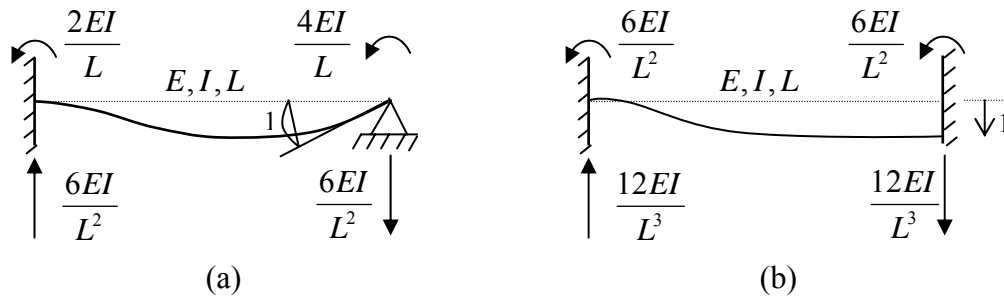
Figure 3.21 - Stiffness Coefficients for a Flexural Element
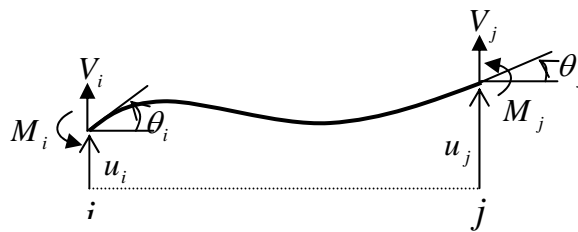
Figure 3.22 - Typical Flexural Element

51

Then, the bending moments at the nodes are;

$$M_i = \frac{4EI}{L}\theta_i + \frac{2EI}{L}\theta_j + \frac{6EI}{L^2}u_i - \frac{6EI}{L^2}u_j \qquad (3.54)$$

$$M_j = \frac{2EI}{L}\theta_i + \frac{4EI}{L}\theta_j + \frac{6EI}{L^2}u_i - \frac{6EI}{L^2}u_j \qquad (3.55)$$

Shear forces at the nodes are;

$$V_i = \frac{12EI}{L^3}u_i - \frac{12EI}{L^3}u_j + \frac{6EI}{L^2}\theta_i + \frac{6EI}{L^2}\theta_j \qquad (3.56)$$

$$V_j = -\frac{12EI}{L^3}u_i + \frac{12EI}{L^3}u_j - \frac{6EI}{L^2}\theta_i - \frac{6EI}{L^2}\theta_j \qquad (3.57)$$

These equations are free from fixed-end moments. As far as response spectrum analysis is concerned, it makes sense since there is no externally applied load on the element span. In case of static analysis, contribution of fixed-end moments coming from dead and live loads are added to Equation 3.54 and Equation 3.55 to find out total nodal moments. More details are given in the section 3.3.11. All formulation described above for element forces is repeated for every elements in each frame.

3.3.10 Modal Combination

There are several rules for the combination of peak modal responses. The most conservative method that is used to estimate a peak value of displacement or force, r_{peak}, within a structure is to use the sum of the absolute of the modal response values. This approach, also called as "Absolute Sum", assumes that the maximum modal values, for all modes, occur at the same time.

$$r_{peak} \le \sum_{i=1}^{3n} \left| \left(r_{peak} \right)_i \right| \qquad (3.58)$$

Notice that sign is ignored leading to an upper bound to the peak value of the total response. This method is not popular in structural design applications since it is too conservative.

Another very common approach is to use the "Square Root of the Sum of the Squares" (SRSS) on the maximum modal values. The SRSS method assumes that all of the maximum modal values are statistically independent. The peak response in each mode is squared and the squared modal peaks are summed. (Equation 3.59)

$$r_{peak} \cong \left(\sum_{i=1}^{3n} \left(r_{peak} \right)_i^2 \right)^{1/2}$$
(3.59)

The SRSS method of combining modal maximum responses has found wide acceptance among structural engineers. It is also used in almost all professional programs for dynamic analysis. However, this method may produce unacceptable results especially for asymmetrical building systems. In such systems, natural frequencies are closely spaced and mode shapes are complex. Mode shape can even include translational as well as torsional components. SRSS method may underestimate or overestimate exact results for this type of frequency distribution and coupled mode shapes.

The relatively new method of modal combination is the "Complete Quadratic Combination" (CQC) method which is the one used in the developed program. It has been developed by Der Kiureghian [25] in 1981 and incorporated as an option to SRSS methods in most modern computer programs for seismic analysis. The peak value of any response quantity can be estimated, from the maximum modal values, by the CQC method with the application of following double summation;

$$r_{peak} \cong \left(\sum_{i=1}^{3n} \sum_{j=1}^{3n} \rho_{ij} \left(r_{peak} \right)_i \left(r_{peak} \right)_j \right)^{1/2}$$
(3.60)

where $\left(r_{peak}\right)_i$ is the modal response associated with mode i. Cross terms $\left(r_{peak}\right)_i, \left(r_{peak}\right)_j$ may either be positive of negative depending on the corresponding modal static responses. Sign is lost for r_{peak} since Equation 3.60 is always positive. The equation for correlation coefficients, ρ_{ij}, is proposed by Der Kiureghian [25]. These coefficients for the CQC method with constant damping are determined by;

$$\rho_{ij} = \frac{8\xi^2\left(1+\beta_{ij}\right)\beta_{ij}^{3/2}}{\left(1-\beta_{ij}^{2}\right)^2 + 4\xi^2\beta_{ij}\left(1+\beta_{ij}\right)^2} \tag{3.61}$$

in which β_{ij} is the ratio of vibration frequencies for the ith and jth mode. It is remarkable that the correlation coefficient array is symmetric and all terms are positive. If the frequencies are well-separated, the off-diagonal terms approach zero and CQC method reduces to SRSS method.

In short, CQC modal combination rule provides very good estimate of the peak response. The error in the prediction is not more than several percent for typical structures. In addition to modal static responses summarized in Table 3.3, moment & shear at top and bottom of columns, moment & shear at beam ends together with axial load on columns are all combined for their corresponding peaks according to CQC rule in the developed program.

3.3.11 Static Analysis

Static analysis procedure is an easy task compared to response spectrum analysis. Static analysis is also performed in frame wise manner to be consistent with RSA. Main idea is to from load vector due to dead and live loads on structural elements. The load vector is then multiplied by the inverse of frame stiffness matrix.

$$\underline{k}^{-1}\underline{P} = \underline{d} \tag{3.62}$$

Frame displacements including floor translations and joint rotations are solved using Equation 3.62. Finally, member forces are computed in the similar fashion described for RSA. This procedure is repeated for all frames oriented in x and y directions. The most challenging part of the static analysis is the generation of frame load vector. Initial step for this purpose is to specify the loads on elements. Distributed dead load due to self weight of beams and infill walls is calculated using the relations below.

$$Q_{beam} = w_{beam} h_{beam} \rho_{conc} \quad \text{and} \quad Q_{wall} = w_{wall} h_{wall} \rho_{wall} \qquad \text{(3.63)}$$

in which $w_{beam}, h_{beam}, w_{wall}, h_{wall}$ are width and height of the beam and infill wall respectively. ρ_{conc} is the density of concrete (25 kN/m^3) and ρ_{wall} is the wall density (8.2 kN/m^3). 12 cm infill wall width is decided as typical value. Notice that dead load due to existence of infill wall is considered on the beam beneath it. Amount of live load is used as 0.2 t/m^2 as stated in the code [22] for residential buildings. Live load participation factor is chosen as 0.3 which is provided in Turkish Earthquake Code [16] for residential buildings. Loading also consists of slab contribution. Total load on each slab piece is transferred to the adjacent beams. Load sharing of each surrounding beam depends on the geometry of related slab piece. Beams on the longer edges take trapezoidal where as beams on the shorter edges are subjected to triangular loading distribution (Figure 3.23).
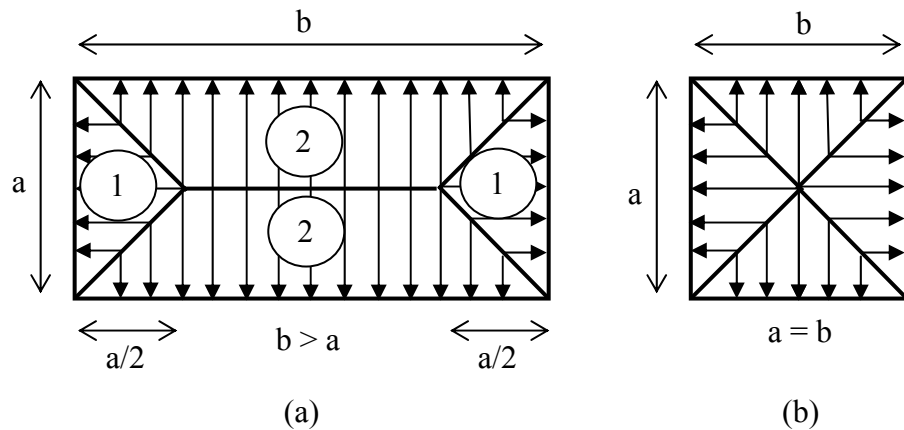
Figure 3.23 - Types of Load Transfer into Surrounding Beams

55

When one edge is longer than other, distributed load on beams is calculated by finding the total eccentric load coming from dependent area divided by the length of the beam. In Figure 3.23-(a), area of triangular region (region 1) is $a^2/4$ and area of trapezoidal region (region 2) is equal to $(ab - a^2/2)/2$. Thus, corresponding eccentric load TL_{ecc} on these regions become;

$$(TL_{ecc})_1 = TL_1 \frac{a^2}{4} \tag{3.64}$$

$$(TL_{ecc})_2 = TL_2 \frac{(ab - a^2/2)}{4} \tag{3.65}$$

where TL_1 and TL_2 is sum of dead and live load on region 1 and 2 respectively. Then, distributed load on beams at shorter and longer edges turns out to be;

$$DistLoad_{shorteredge} = \frac{TL_1 a^2/4}{a} = TL_1 \frac{a}{4} \tag{3.66}$$

$$DistLoad_{longeredge} = \frac{TL_2(ab - a^2/2)}{2b} = \frac{TL_2(a - a^2/2b)}{2} \tag{3.67}$$

If the slab piece is square as shown in Figure 3.23-(b), then total load is equally shared by surrounding beams. In this case, distribute load on each beam is given by;

$$DistLoad_{alledges} = TL\frac{a}{4} = TL\frac{b}{4} \tag{3.68}$$

Once all loading values are settled on, they are discretized to joints. Consider a beam with distributed load q shown in Figure 3.24.
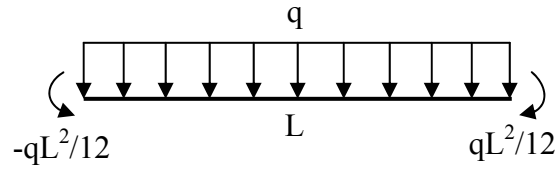
Figure 3.24 - Designation of Beam End Moments

Moment at either end of the beam is $qL^2/12$. This value is negative for the left hand side since direction of the force is opposite to rotational dof at joint. Recall that rotational dofs in a frame are assigned in counter-clockwise manner to be positive. Similarly, sign of the moment becomes positive considering the direction of dof at that joint. It is better to show representative load vector for a simple frame given in Figure 3.25.

$$\underline{P} = \begin{Bmatrix} 0 \\ 0 \\ -q_1 L_1^2/12 \\ q_1 L_1^2/12 - q_1 L_2^2/12 \\ q_1 L_2^2/12 \\ -q_2 L_1^2/12 \\ q_2 L_1^2/12 - q_2 L_2^2/12 \\ q_2 L_2^2/12 \end{Bmatrix} \begin{matrix} 1 \\ 2 \\ 3 \\ 4 \\ 5 \\ 6 \\ 7 \\ 8 \end{matrix}$$
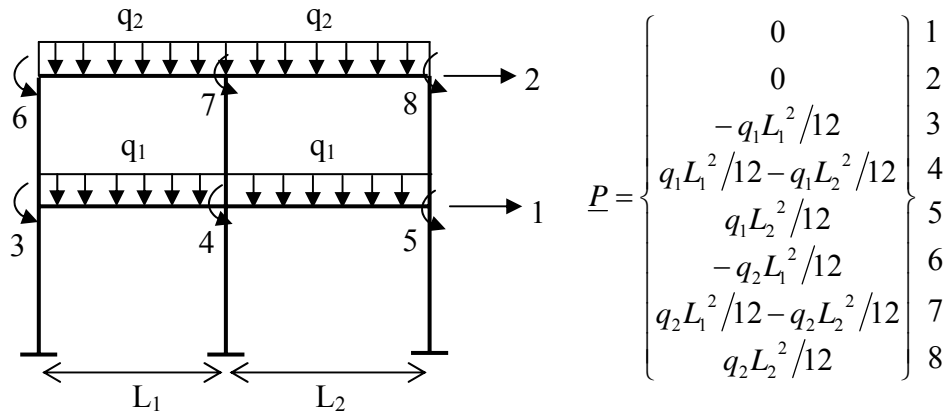
Figure 3.25 - Formation of Load Vector

Notice that zero terms appear corresponding to translational dofs since no force exist in that direction. As soon as the load vector is completed, joint displacements are obtained from Equation 3.62. Next step is the computation of member forces. Figure 3.26 shows a typical beam element taken out from a frame.
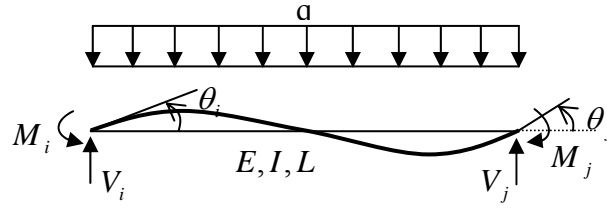
Figure 3.26 - Member Forces Designation

Connection between joint rotations and resulting moments are given in equations 3.54 and 3.55 $\left(u_i = u_j = 0\right)$. Unlike response spectrum analysis additional moments, also called as fixed-end moments (FEM), come out in static analysis due to existence of external loads. Hence, final end moments for a beam element in Figure 3.26 turn into;

$$M_{left} = \frac{4EI}{L}\theta_i + \frac{2EI}{L}\theta_j + FEM \tag{3.69}$$

$$M_{right} = \frac{4EI}{L}\theta_j + \frac{2EI}{L}\theta_i + FEM \tag{3.70}$$

where FEM is equal to $qL^2/12$. Different from load vector formation, algebraic sign of FEM is now positive for left end and negative for right end of the beam respectively. On the other hand, shear at the beam ends are determined from following equations which are derived from preliminary statics.

$$V_{left} = \frac{M_{left}}{L} + \frac{M_{right}}{L} + \frac{qL}{2} \tag{3.71}$$

$$V_{right} = -\frac{M_{left}}{L} - \frac{M_{right}}{L} + \frac{qL}{2} \tag{3.72}$$

The last terms in both equations are due to distributed load on beam. They are cancelled out in finding shear at column ends. Calculation of end forces (shear &

moment) for columns is exactly the same as carried out in response spectrum analysis (Equations 3.54 through 3.57). For both type of analysis, axial load on columns are derived from shear at beam ends. At a joint, shear coming from beams connected to that joint is transferred to the bottom column. This transfer process is also carried out in a story basis by adding i^{th} story column axial load to the column at $(i-1)^{th}$ story. Lateral displacements obtained from static analysis belong to separate frames. As global dofs require, they should be converted into a single displacement value defined for each floor. (see Figure 3.4). For this reason, actual displacement at i^{th} floor in x-direction is considered as the average of ith floor lateral displacements of all frames oriented in x-direction. This makes sense since the lateral displacements are negligibly small under vertical loading. Simplification is also valid for actual horizontal displacements in y-direction.

One final remark before closing this section is that algebraic sign of all member forces gain importance in static analysis. This is not the case for RSA since peak value of the response quantity is taken into account. In other words, sign is lost during modal combination.

3.3.12 Load Factors and Load Combinations

Structural safety problem comes from the uncertain nature of the forces acting on structures, of material strengths and of structural analysis procedures. Codes and standards provide the foundation of good engineering practice considering the safety in structural design. Hence, contribution of different type of analysis should be taken into account.

There are several ways of combining the effect of different analysis types. If structural model is linear the principle of superposition can be applied. Member forces for each load case are computed. Then, they are multiplied with a safety factor and added to each other. When the earthquake loading is considered, the following load combination for design forces is used as suggested in TS-500 [23];

$$F_d = 1G + 1Q + 1E \tag{3.73}$$

and for vertical loads only;

$$F_d = 1.4G + 1.6Q \qquad\qquad\qquad \textbf{(3.74)}$$

where

G : Dead load effect

Q : Live load effect

E : Earthquake loading

The coefficients represent the importance of corresponding loading type. In case of static analysis, live load coefficient is relatively greater since it includes larger uncertainties. They are all unity for earthquake analysis reflecting the rare occurrence of the earthquake. In program code, E symbolizes the forces due to application of RSA. G and Q stand for the forces coming from static analysis. Member forces resulting from two analyses are combined according to $1G + 1Q + 1E$ in the developed program.

There are four different response quantities for the beams computed by both analyses, namely, shear forces and moments at each end. As previously mentioned, all of these values are positive as far as RSA is concerned. All the forces defined for beams change their directions due to cyclic behavior of earthquake. This reveals that despite being independent from sign, earthquake forces will always be in the direction of static forces. Therefore, absolute value of the static forces should be directly added to ones found from RSA. Similarly, five response quantities are defined for columns involving shear and moment at the ends together with the axial load. These quantities are combined in the same way as described for beams. Combination of forces gives overall effect of vertical and lateral loading in member level. Maximum values of forces should then be computed for each member. Maximum forces for beams and columns are the ones which are the greatest of end forces (shear and moment). Note that only one value of axial load, which is already the highest, exists on columns

3.3.13 Member Capacity Computations

In this section, the philosophy and procedure for strength of reinforced concrete beams and columns is explained. All discussion is the mirror of what has been applied in the developed program code. Before starting detailed description of analysis it is convenient to summarize the behaviour of reinforced concrete members subjected to flexure. For this purpose, typical flexural beam having rectangular cross-section shown in Figure 3.27 is considered. Beam has small amount of reinforcement located in tension zone. Elasto-plastic stress-strain relation is used for steel. Model for concrete in compression and tension is parabolic (Figure 3.28-a,b,c).
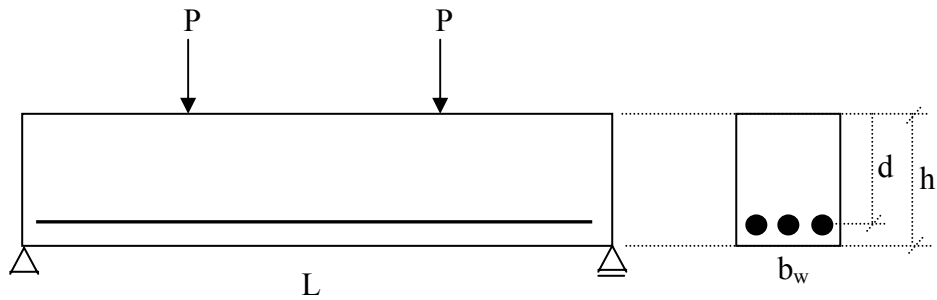
Figure 3.27 - Reinforced Concrete Beam
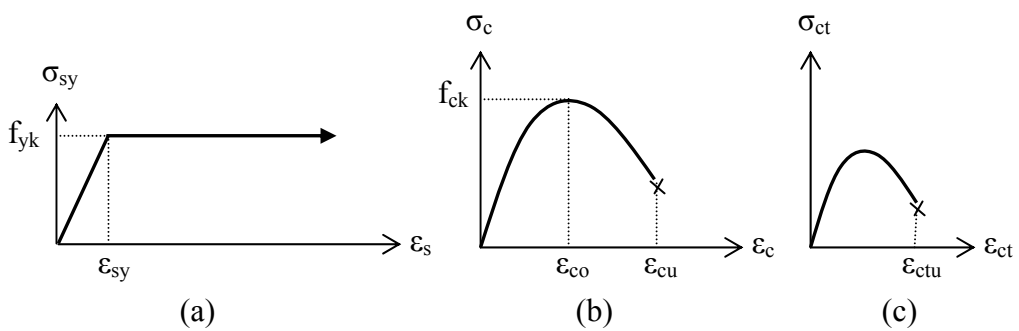
Figure 3.28 - Steel and Concrete Models

Stress-strain distribution on the section under very low loads is shown in Figure 3.29-a. Concrete in tension does not crack yet and contribution is still considered. On the next stage, tension concrete cracks as the tensile strain capacity of concrete in the extreme fiber, ε_{ctu} is reached. Hairline cracks perpendicular to beam axis develop and stress distribution in the compression zone is linear (Figure 3.29-b).

As the load increases stress block in compression zone resembles the shape of $\sigma - \varepsilon$ curve for concrete in compression and thus becomes nonlinear. Corresponding stress-strain distribution is shown in Figure 3.29-c Then, strain in the tension steel becomes ε_{sy} and yielding begins. But beam is able to carry more loads due to concrete in compression zone (Figure 3.29-d).
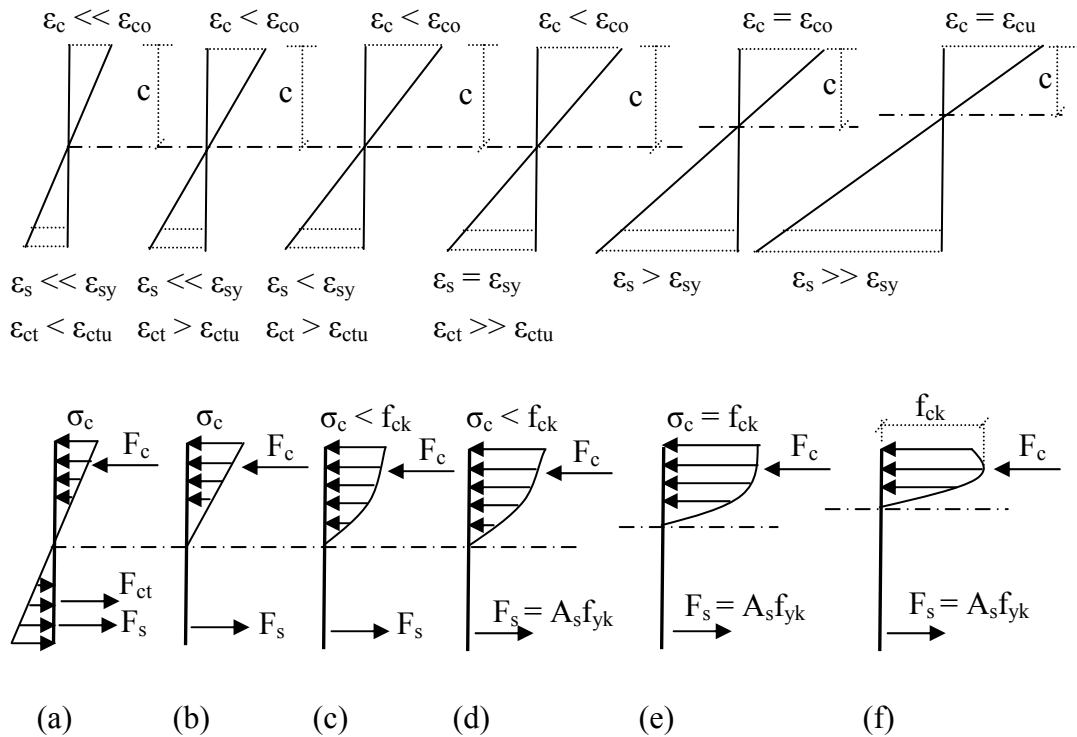
Figure 3.29 – Stress & Strain Distribution

Stress-strain distribution is shown in Figure 3.29-e when the strain in the concrete reaches to ε_{co}. Steel force is constant after yielding. However, stress in the concrete becomes larger which increases concrete force. In order to keep the

62

sectional equilibrium rise of neutral axis is inevitable. At the final stage, ultimate strain in extreme compression fiber, ε_{cu}, is reached and failure occurs. Stress-strain distribution now represents the full $\sigma - \varepsilon$ curve of concrete (Figure 3.29-f). Corresponding load is called as the ultimate strength of the member.

Strength of reinforced concrete members subjected to flexure falls into the "analysis problem" in which objective is to find resisting moment using known cross-sectional dimensions, steel area and design material strengths. Analysis of beams is exactly the same as that of columns except axial load existing in force equilibrium on the section.

Besides singly reinforced, beams may be in practice, double reinforced meaning that steel bars available in the compression zone. This kind of application is used either to increase ductility of the beam or to decrease section size for architectural requirement. Figure 3.30 shows the forces acting on the typical double reinforced beam section. Resulting moment is divided into two couples. The first couple consists of concrete force and tension steel force. The second one is composed of both tension and compression steel forces.
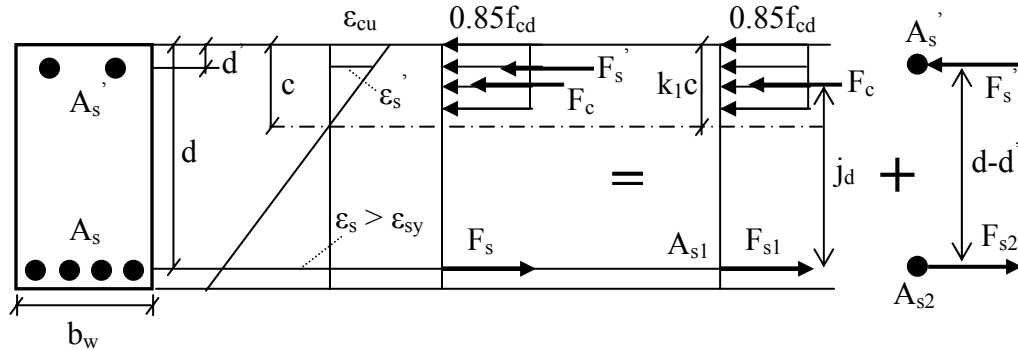
Figure 3.30 - Free Body Diagram for Double Reinforced Beam Section

In case of double reinforced beam analysis, known variables are $A_s, A_s', b_w, d, d', f_{cd}$ and f_{yd}. Unknown variables are $c, \sigma_s', \varepsilon_s'$ and M_r. Equation of the force equilibrium leads to;

$$f_{y_d} A_s - 0.85 f_{cd} b_w k_1 c - A_s' \sigma_s' = 0 \qquad \textbf{(3.75)}$$

Resisting moment is calculated by taking moment with respect to tension steel;

$$M_r = 0.85 f_{cd} b_w k_1 c \left(d - 0.5 k_1 c\right) + A_s' \sigma_s' \left(d - d'\right) \qquad \textbf{(3.76)}$$

Strain in the compression zone using compatibility relations is given by;

$$\varepsilon_s' = \varepsilon_{cu} \frac{c - d'}{c} \qquad \textbf{(3.77)}$$

Then, corresponding stress becomes;

$$\sigma_s' = \varepsilon_s' E_s \qquad \textbf{(3.78)}$$

There are now four equations (Equations 3.75, 3.76, 3.77 and 3.78) and four unknowns ($c, \varepsilon_s', \sigma_s', M_r$) to solve. Observe that two equilibrium equations are sufficient if compression steel also yields which is common in practice. In that case, σ_s' is replaced by f_{yd} and further simplifications in Equations 3.75 and 3.76 leads to;

$$k_1 c = \frac{\left(A_s - A_s'\right) f_{yd}}{0.85 f_{cd} b_w} \qquad \textbf{(3.79)}$$

$$M_r = 0.85 f_{cd} b_w k_1 c \left(d - 0.5 k_1 c\right) + A_s' f_{yd} \left(d - d'\right) \qquad \textbf{(3.80)}$$

In addition to double reinforced beams steel bars can be located at several layers on the section. In Figure 3.31, steel strains and sectional forces for beams with multi-layer steel are shown.
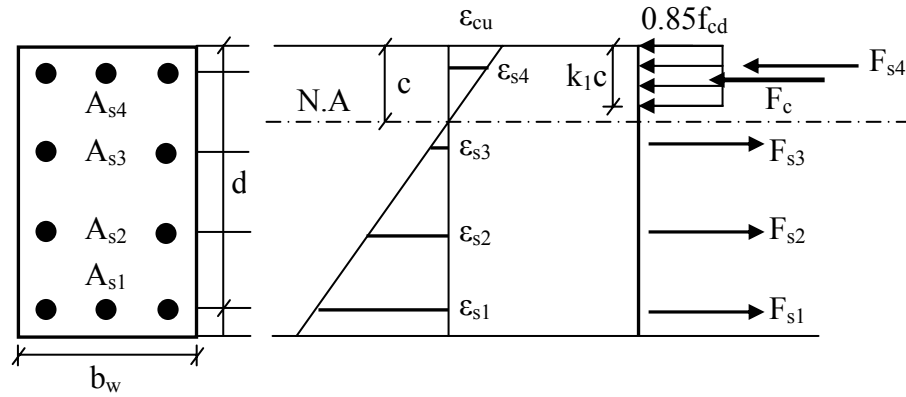
Figure 3.31 - Free Body Diagram for Beam with Multi-Layer Steel

In many professional structural engineering programs beams are characterized as double reinforced. This is basically because applied load is mostly shared by the top and bottom reinforcements. Nevertheless, intermediate steel layers have considerable contribution to moment capacity. Depending on the cross-sectional dimensions, %20 - %30 increase in the moment capacity is acquired. Even though solution of such beams requires more computational effort it is thus better to come up with more approximate results by simply applying certain procedure. Below steps are followed in the analysis of rectangular beams with multi-layer steel.

- Neutral axis depth, c, is assumed.
- Based on c, strains at each layer of steel is determined using compatibility relations (see Figure 3.31).
- Steel strains for each layer is calculated and compared with the yield stress, f_{yd}
- Corresponding steel forces are computed.
- Concrete force in the compression zone is determined using rectangular stress block.
- Force equilibrium on the section is checked.
- Above steps are repeated until each force equilibrium is satisfied.
- Moment capacity is calculated by taking moment about a convenient point.

65

Iterative procedure outlined above is followed in the developed program code. Accuracy criterion in the force equilibrium is selected as 1N which is absolutely sufficient. Convergence is usually achieved at most after ten iterations.

The only difference in capacity calculation of columns comes from the existence of axial load. Therefore, force equilibrium is established accordingly. Theoretically, effect of axial load on the moment capacity is represented by "interaction diagram" shown in Figure 3.32. For each assumed c value, (N,M) pair is computed using equilibrium and compatibility relations. Final curve obtained in this way consists of points defining the safety region. Any (N,M) combination falling outside of this region leads to failure.

Similar to flexural failure classifications in beams two types of failure are possible for columns, namely compression and tension failures. Point A in between these two cases corresponds to balanced failure. Region 1 in Figure 3.32 shows possible compression failure locations. In this region, tension steel does not yield where as concrete strain at the uppermost compression fiber reaches to crushing strain leading to brittle failure.
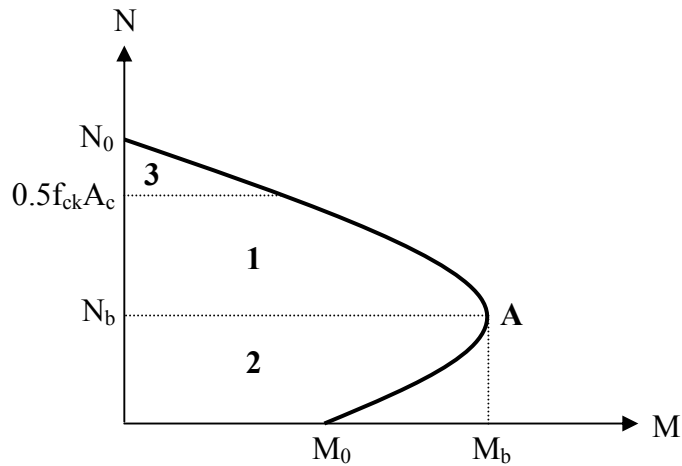
Figure 3.32 - Axial Load – Moment Interaction Diagram

On the other hand, tension failure is observed in region 2 in which tension steel yields before extreme fiber in compression reaches to crushing strain. It is mentioned earlier that this type of failure is desirable due to its ductile behaviour. For the balanced failure, concrete in extreme compression fiber crushes simultaneously with the yielding tension steel. As it can be inferred from Figure 3.32, high level of axial load results in sudden failure (region 3) and is not allowed by the code [16] according to the following limitation;

$$(N_d)_{max} \leq 0.5 f_{ck} A_c \tag{3.81}$$

While bending is most often the critical failure mechanism for reinforced concrete sections, shear should always be taken into account. Design shear is resisted by the contributions of both concrete and shear reinforcement as shown in Equation 3.82.

$$V_r = V_c + V_w \tag{3.82}$$

According to specifications in TS-500 [23] shear strength provided by concrete, V_c , is in general defined as %80 of diagonal cracking strength V_{cr} which is given in the following equation.

$$V_{cr} = 0.65 f_{ctd} b_w d \tag{3.83}$$

where f_{ctd} is design tensile strength of concrete and equal to $0.35\sqrt{f_{cd}}$. Contribution of shear reinforcement to shear strength is calculated by;

$$V_w = \frac{A_{sw}}{s} f_{ywd} d \tag{3.84}$$

in which A_{sw} is the total cross-sectional area of shear reinforcement and s is the stirrup spacing. After substitutions shear strength of reinforced concrete member is written in the form of;

$$V_r = 0.8\left(0.65 f_{ctd} b_w d + \frac{A_{sw}}{s} f_{ywd} d\right)$$ (3.85)

To prevent brittle failure, upper limit for design shear in TS-500 [23] is set to;

$$V_d \leq 0.22 f_{cd} b_w d$$ (3.86)

This limit is represented in the developed program code as a graphical format showing whether it is exceeded or not for each member.

Input data coming from user is essential as far as the reliability of analyses results are concerned. Geometrical properties such as cross-sectional dimensions for members, story heights, bay widths etc. may approximately estimated by visual inspection. However, it is very possible for the average user not knowing the reinforcement detailing for a given building. In order to eliminate such an obstacle, an option is provided to assign minimum reinforcement amounts which are given in Table 3.5 specified in Turkish Earthquake Code [16]. These values are also valid for equivalently formed columns representing shear wall between axes.

Table 3.5 - Minimum Reinforcement Quantities

Beam longitudinal reinf.	$\rho = \dfrac{A_s}{b_w d} > \dfrac{f_{ctd}}{f_{yd}}$ $\quad \phi = 12$
Column longitudinal reinf.	$\rho = \dfrac{A_{st}}{A_c} \geq 0.01$ or $6\phi 14$
Beam lateral reinf.	$\phi = 8$ $\newline$ spacing $= \min\left(\dfrac{h}{4}, 8\phi, 150\,\text{mm}\right)$
Column lateral reinf.	$\phi = 8$ spacing $= \begin{cases} > 50\,\text{mm} \\ < 100\,\text{mm} \\ < \dfrac{\text{shorter side}}{3} \end{cases}$

Another option is provided by three default reinforcement arrangements shown in Figure 3.33. These are the typical ones used in most of the buildings.
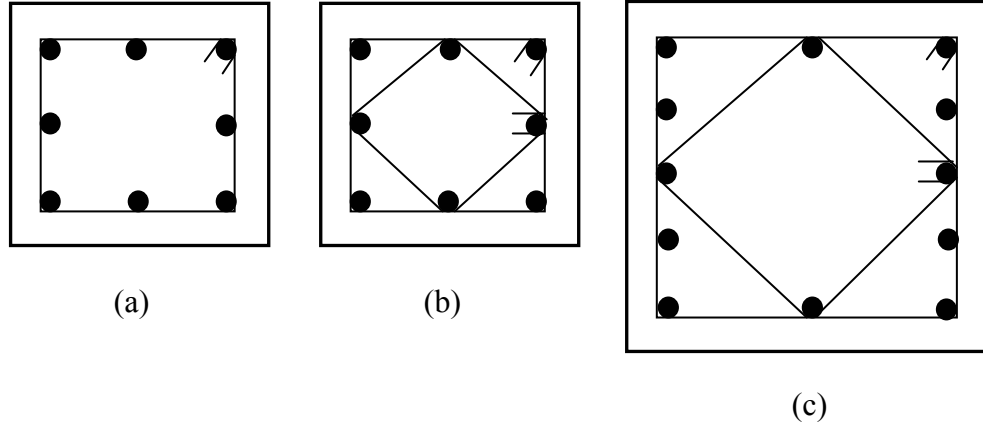
Figure 3.33 - Default Reinforcement Configurations

Additional stirrup connecting longitudinal reinforcement at the same level can be added in all types of configurations. Furthermore, number of layer for longitudinal reinforcement in both directions can be increased for the case in Figure 3.33-a.

Due to non-homogenous nature of concrete and unsymmetrically placed vertical loads, pure axial compression is not possible reinforced concrete. Yet, it is necessary to clarify the axial load capacity of columns subjected to uniaxial compression since it is the limiting case for combined flexure and axial load (see Figure 3.32). Thus, axial strength of columns subjected to uniaxial compression is determined by the sum of strengths of concrete and the longitudinal reinforcement;

$$N_0 = 0.85 f_{ck} A_c + A_{st} f_{yk} \tag{3.87}$$

Before closing this section, it is necessary to present all constant values used in the developed program code for ultimate strength calculations. (Table 3.6)

69

Table 3.6 - Constants Used in Member Capacity Calculations

Constant	Definition	Value
E_s	Elastic modulus of steel	2×10^5 MPa
k_1	Equivalent rectangular compression block depth factor	0.85
ε_{cu}	Strain at the extreme concrete fiber in compression	0.003

Value of ε_{cu} is selected based on the assumptions for ultimate strength theory (TS-500) [23]. It decreases under high axial load level since strain distribution turns to be rectangular. But this is not the case since axial load is limited in Turkish Earthquake Code.

3.3.14 Demand-Capacity Checks

In the preceding sections, computation of element forces through two types of analyses, namely "response spectrum analysis" and "static analysis", is discussed. CQC method is explained in detail for the peak value of each response quantity as far as the RSA is concerned. In the next stage, selection of load combination is notified to properly combine resulting forces. Then, determination of the maximum (design) value of these forces involving axial load, shear and moment is presented. Furthermore, shear and flexural behaviour of reinforced concrete beams and columns are briefly summarized in line with the theoretical formulations for their ultimate strength computations. It is now appropriate to look at the demand-capacity ratio from which linear safety of members is identified. For columns, interaction of shear with torsion is considered. Combined axial load and flexure behaviour is also taken into account for columns.

Many reinforced concrete members, in particularly columns are subjected to simultaneous effect of shear and torsion. Besides shear force itself, additional shear stresses appear on the member due to torsion. Such an interaction can not be ignored since shear stresses caused by these two actions are additive in one face of

the member. The interaction theory proposed by Ersoy and Ferguson [9] can be used to predict ultimate strength of columns;

$$\left(\frac{T_d}{T_{r0}}\right)^2 + \left(\frac{V_d}{V_{r0}}\right)^2 = 1 \qquad \textbf{(3.88)}$$

where

T_d : Applied torque

V_d : Applied shear

T_{r0} : Ultimate torsional capacity when $V_d = 0$

V_{r0} : Ultimate shear capacity when $T_d = 0$

Safety of column under combined shear and torsion can be decided using Equation 3.88. Note that both directions should be checked and the ones giving greater value should be considered. Graphical representation of Equation 3.88 is shown in Figure 3.34. Shear capacity is calculated from Equation 3.85. On the other hand, torsional capacity is determined from the following equation;

$$T_{r0} = \frac{A_{0t}}{s} 2 A_e f_{ywd} \qquad \textbf{(3.89)}$$
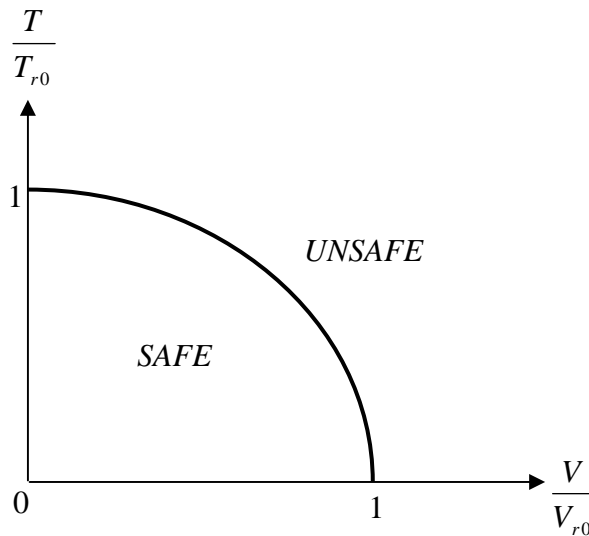
Figure 3.34 - Interaction Diagram for Combined Shear and Torsion

71

In Equation 3.89, s is the spacing of shear reinforcement. A_{0t} is the cross-sectional area of transverse steel required for torsion only. Confined area on the section is represented by A_e and f_{ywd} is the yield strength of steel. Besides the capacity, applied torque on the column is computed by multiplying torsional displacement of the floor with the torsional stiffness of the column at that floor;

$$T_{ij} = k_{T\,ij}\theta_j \tag{3.90}$$

in which

θ_j : Torsional displacement of the jth floor

$k_{T\,ij}$: Torsional stiffness of the ith column at the jth floor

T_{ij} : Torque on the ith column at the jth floor

Torsional stiffness of a member subjected to pure torsion is given by;

$$k_T = \frac{GJ}{L} \tag{3.91}$$

where

G : Shear modulus of concrete, $\cong 0.4E_c$

J : Polar moment of inertia with respect to centroid of the section, for a
section having width b and height h, $J = \dfrac{1}{12}bh(b^2 + h^2)$

L : Length of the member

Although columns are likely to carry vertical loads they are in practice designed as combined axial and flexure. Appreciable bending moment exists on columns mainly because of initial crookedness and unbalanced gravity loads. In addition, second order moments are present due to deflection of columns. For these reasons, most of the design codes specify minimum eccentricity on the column even if resulting moment is very small.

As it is stated previously, existence of axial load is also considered in capacity calculation of columns. Free body diagram shown in Figure 3.35 forms the basis for this purpose. Referring to Figure 3.35, necessary equilibrium and compatibility equations are written as described in the section 3.3.13 and moment capacity is determined accordingly. Despite being designed for uniaxial bending in many applications, great majority of the columns are subjected to biaxial bending in addition to axial loads. In practice, minor moment along one axis is ignored for simplicity. Biaxial moments are especially important for the corner columns. However, analysis of such columns is not very feasible since it requires many iterations in trial and error approach.
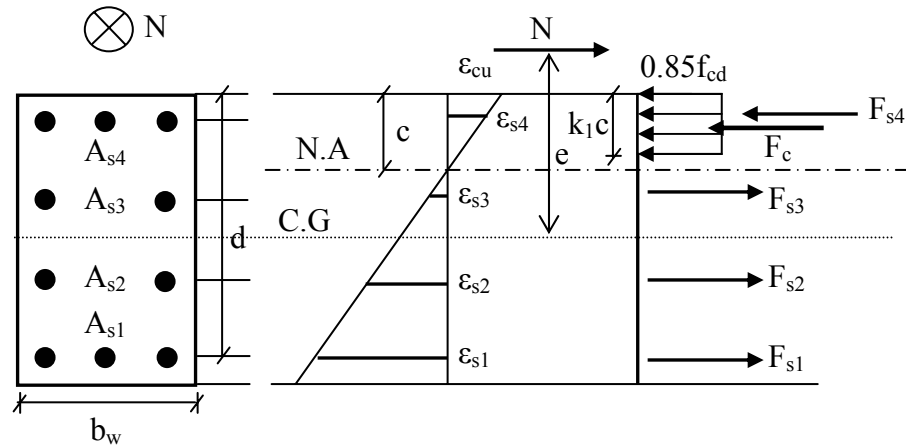
Figure 3.35 - Free Body Diagram of Column Subjected to Axial Load

Different from columns subjected uniaxial bending and axial load, (N,M) interaction in case of combined biaxial bending and axial load is defined by a surface formed by series of two dimensional diagrams (Figure 3.36). Each point on the surface represents a set of axial load and moments about both axes. Every horizontal plane obtained by cutting the surface corresponds to interaction between two moments, M_{xy} and M_{xz} under the constant axial load.
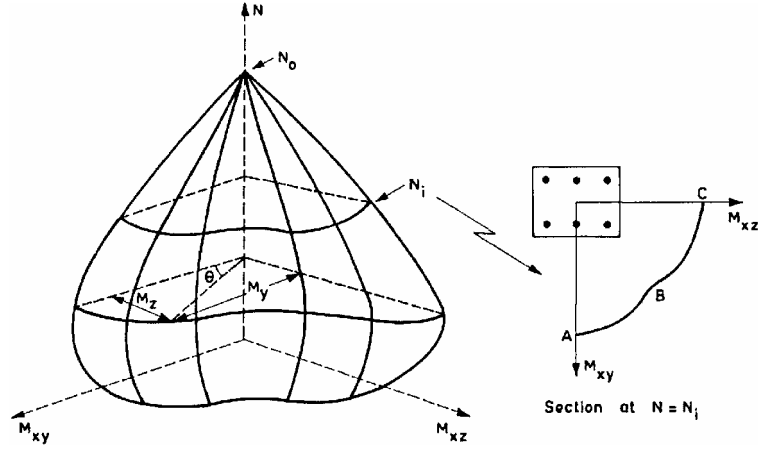
Figure 3.36 - Interaction Surface for Combined Biaxial Bending and Axial Load
[9]

Approximate method for combined biaxial bending and axial load action implemented in the program is the following;

$$\left(\frac{M_{xz}}{M_{xz0}}\right)^{\alpha 1} + \left(\frac{M_{xy}}{M_{xy0}}\right)^{\alpha 2} \leq 1 \qquad (3.92)$$

where

M_{xz} : moment about the z-axis

M_{xy} : moment about the y-axis

M_{xz0} : Uniaxial flexural strength about the z-axis under applied axial load

M_{xy0} : Uniaxial flexural strength about the y-axis under applied axial load

The values of α_1 and α_2 depend on the column properties and the level of axial load. They linearly change between 1.0 and 2.0. Following relations are suggested in British Code (CP110-72) for their variations based on ratio of design axial load, N_d, to the uniaxial strength, N_{or};

$$\alpha_1 = \alpha_2 = 1.0 \quad \text{for} \quad \frac{N_d}{N_{or}} < 0.2 \qquad (3.93)$$

$$\alpha_1 = \alpha_2 = 0.67 + 1.67\left(\frac{N_d}{N_{or}}\right) \quad \text{for} \quad 0.2 \le \frac{N_d}{N_{or}} \le 0.8 \tag{3.94}$$

$$\alpha_1 = \alpha_2 = 2.0 \quad \text{for} \quad \frac{N_d}{N_{or}} > 0.8 \tag{3.95}$$

In the developed program code, interaction between shear & torsion and uniaxial bending & axial load provides good estimation as far as the column safety is concerned. Flexural and shear safety of beams is directly found from their demand-capacity ratios. Flexural strength of beams is compared with maximum moment on beams which mostly occurs at the supports. Although uniaxial compression for columns is unlikely to happen, safety of columns in terms of pure axial compression are also checkhed from corresponding demand-capacity ratios.

CHAPTER 4

INTERPRETATION OF RESULTS: SEISMIC VULNERABILITY ASSESSMENT

4.1 INTRODUCTION

In this chapter, analyses results produced by the developed software are discussed and validated. Proposed methods for the seismic vulnerability assessment of buildings are explained. Detailed assessment method is tested by using 36 buildings from Düzce damage database to define cutoff values to predict the damage levels of building on possible future earthquakes. In addition, the developed software's structural analysis module is verified by two example buildings.

4.2 PROGRAM VERIFICATION

In order to test the consistency of the program two buildings are selected. First one is the structural mechanics laboratory extension building (K7). Second one is İş Bankası (Kabataş Branch) building in Istanbul. They are modeled and analyzed using both EQMASTER and SAP2000 [8]. Static and response spectrum analyses are run in SAP2000 [8]. Then, results such as periods, modal shapes, base reactions, and member forces are compared.

4.2.1 Structural Mechanics Building, K7

K7 building belongs to the Civil Engineering Department of METU in Ankara. K7 has two stories and is a prefabricated reinforced concrete building. The first and second storey heights are 4.4 m and 3.25 m, respectively. Floor plans of both stories are rectangular having 6.3 m width and 30 m length. External view of the building is shown in Figure 4.1.

Figure 4.1 - Structural Mechanics Building, K7

Structural system consists of five frames in short direction and two frames in long direction. Frames in short direction have single-bay width of 6.3 m while frames in long direction include four bays having equal width of 7.5 m. Floor plans for the two stories are given in Figure 4.2. All columns are 40 cm by 40 cm size and located at the axes intersections. Beams in short direction are 40 cm by 65 cm size whereas the ones in long direction have cross-sections of 40 cm by 55 cm size. Slabs are put in place as prefabricated blocks having 15 cm thickness.

There are no irregularities in structural system configuration. However, existence of partition and outer walls disturb the symmetric floor plan of the building. The first story is designed for laboratory use and therefore large empty spaces are set aside. Small part of this story is reserved for office use. The second story is

completely designed for offices and contains eight rooms. Location of partition and outer walls are also shown in Figure 4.2.
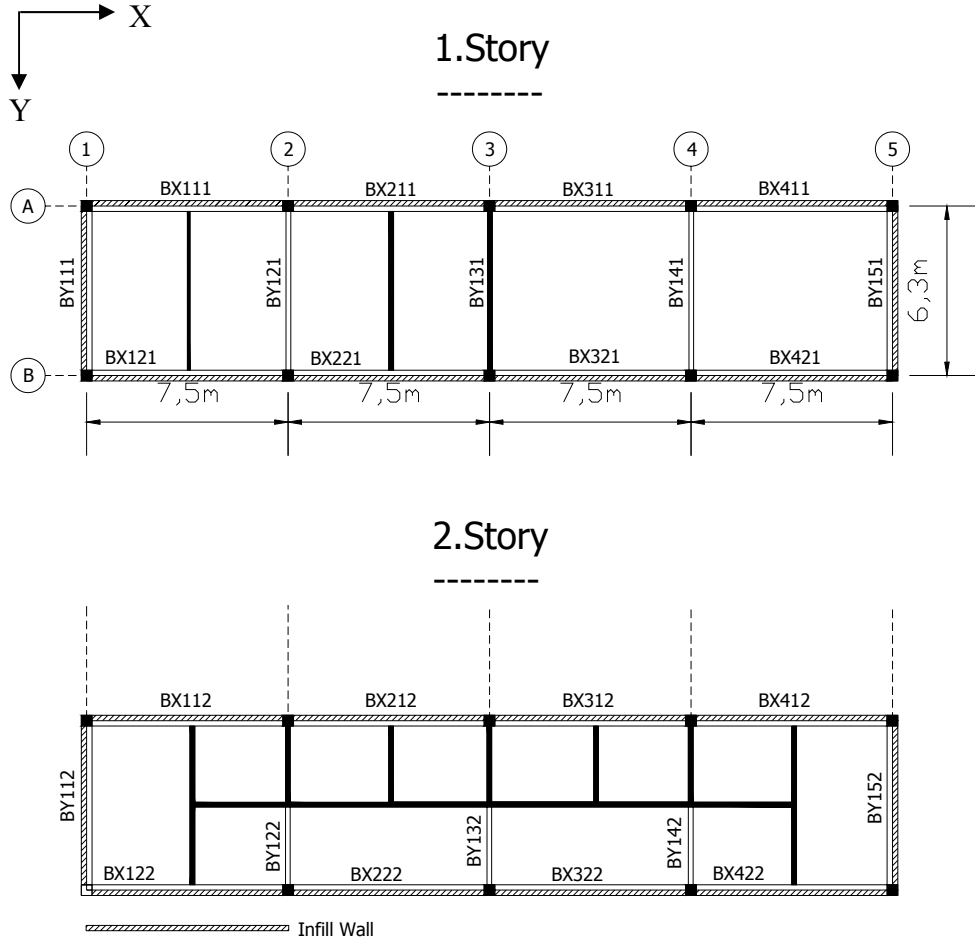
Figure 4.2 - Structural Floor Plan and Wall Locations

Çelik [6], tested this building to measure the first two periods and modal shapes. In that study, building is modeled as bare frame and with infill walls. Test results are compared with analytical study in which good agreement is observed. These test results are also used in this study for comparison purposes.

In order to check the infill wall application in the program, K7 building was modeled as bare frame and with infill walls in EQMASTER's graphical interface. 2D view of the both models is shown in Figure 4.3 and Figure 4.4. K7 analytical models analysis results are compared against SAP2000 analysis results not only

for vibration periods, but also modal shapes, base reactions, and member forces to cover both static and dynamic results.
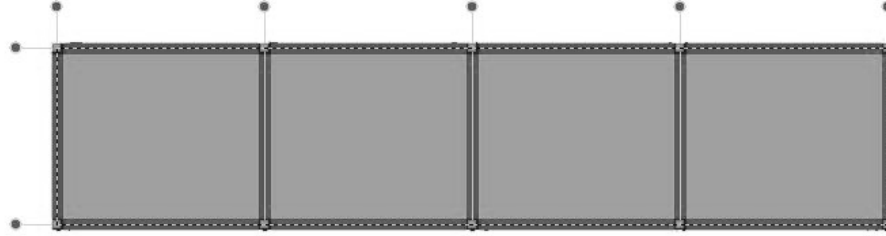
Figure 4.3 - 2D Model for K7 Building as Bare Frame (same for two stories)
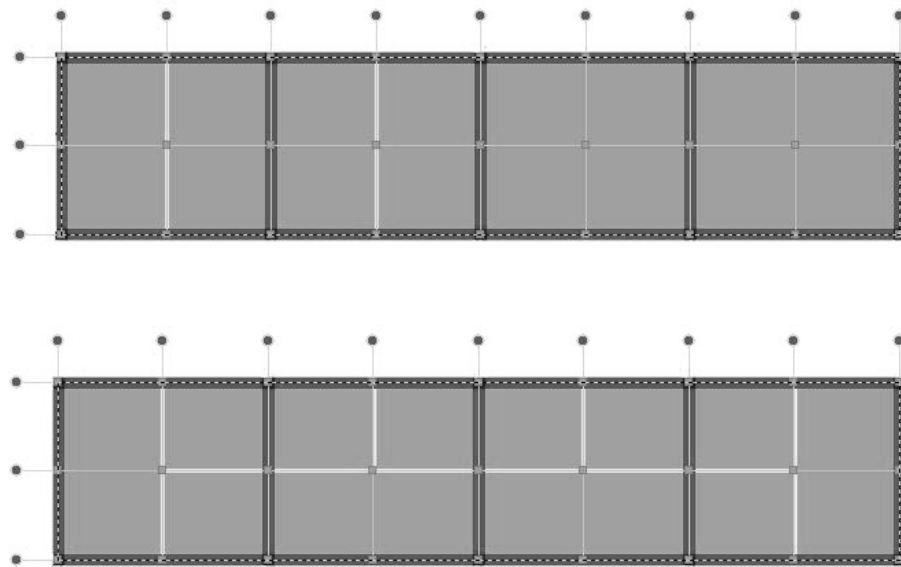
Figure 4.4 - 2D Model for K7 Building with Infill Walls (1st and 2nd story)

The analysis results obtained from both programs for K7 building are discussed below. Results are presented for both bare frame and with infill wall models. Comparison of base reactions, vibration periods, and modal shapes may be seen from Figure 4.5 through Figure 4.7. Due to large number of members, comparison of member forces is limited to the first story columns and beams. Note that these forces are combined loading condition for 1G+1Q+1E. Designations used for beam and column names are shown in Figure 4.2. X and Y directions stand for long and short directions, respectively.

79
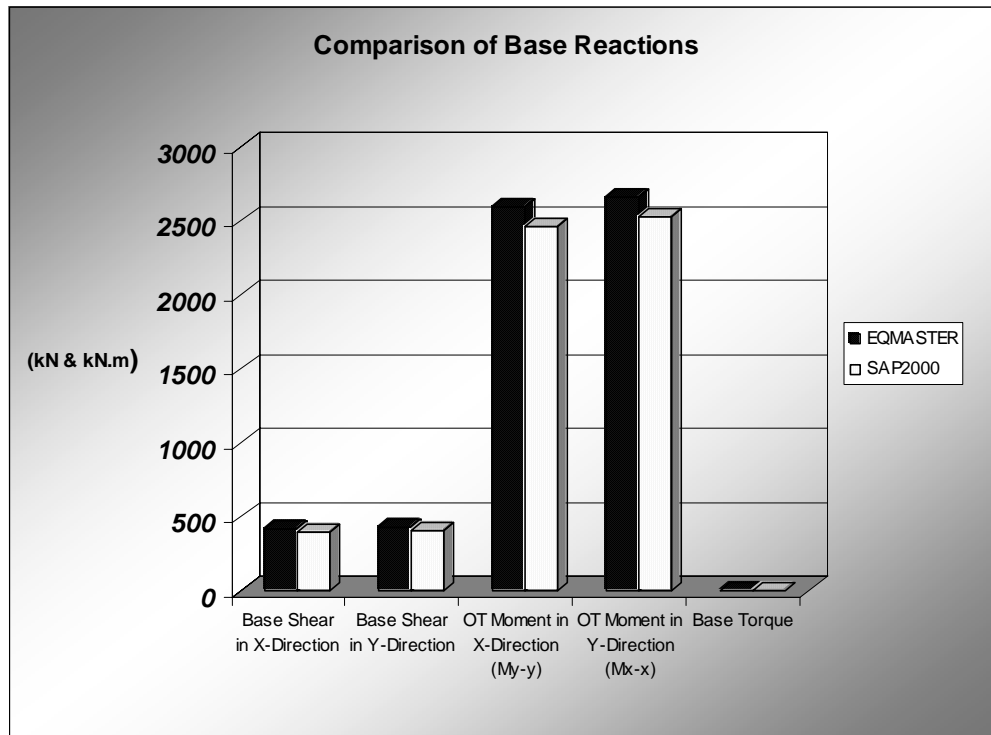
Figure 4.5 - Comparison of Base Reactions for K7 (Bare Frame Model)
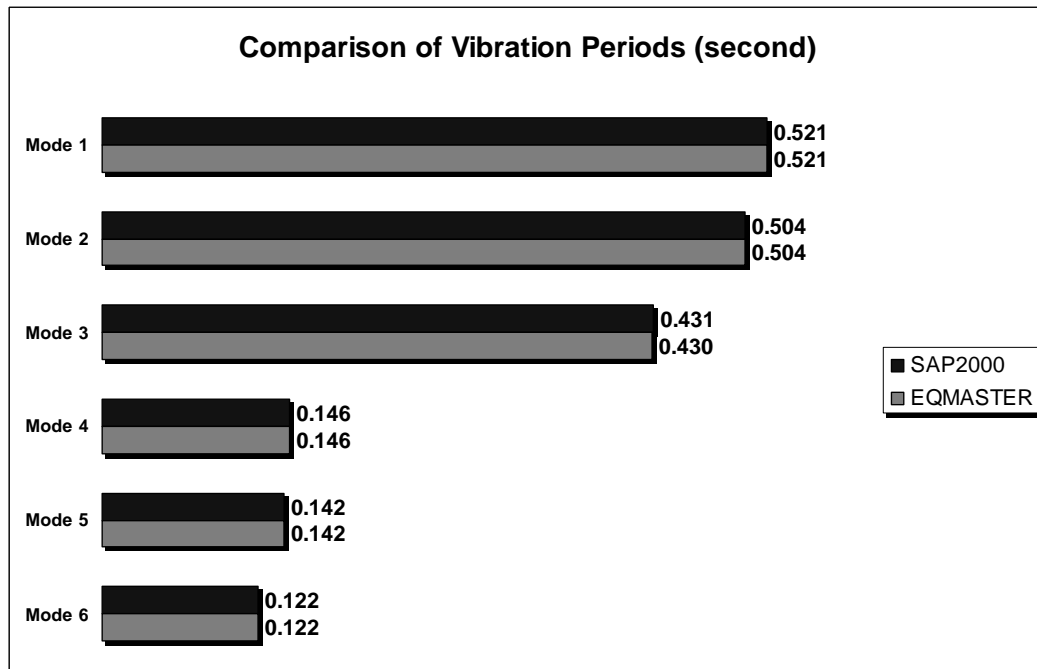
Figure 4.6 - Comparison of Vibration Periods for K7 (Bare Frame Model)
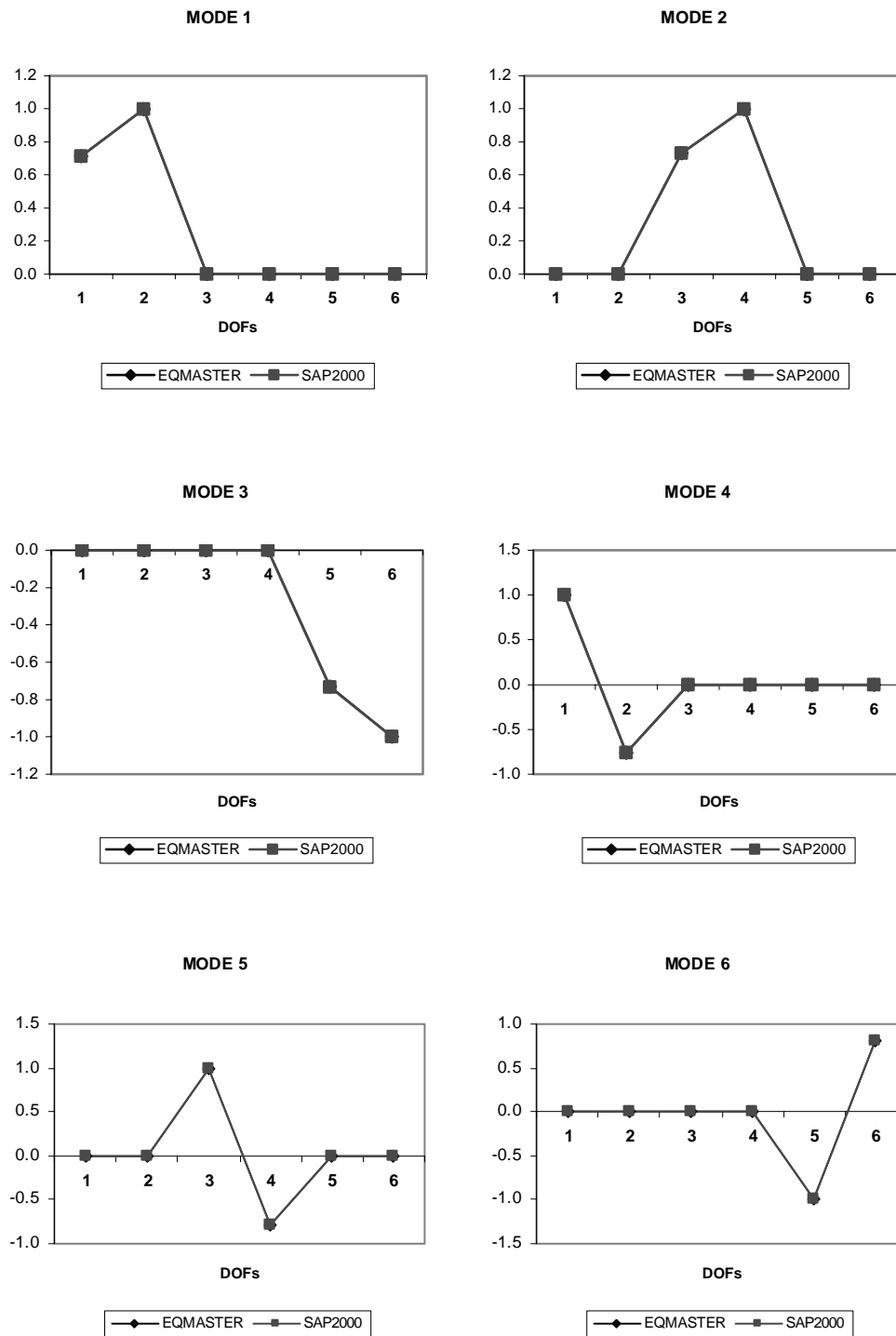
Figure 4.7 - Comparison of Modal Shapes for K7 (Bare Frame Model)

Note that the dimensionless numbers on the vertical axes of the graphs in Figure 4.7 represent the relative movements of all dofs (scaled to unity). Numbers on

horizontal axis stand for dofs assigned based on lumped mass model. The first two modal shapes correspond to translations in Y and X directions respectively. Torsional mode appears in the third mode. Second bending modes in X and Y directions and the second torsional mode follows the order of the first three modes. Comparison of maximum member forces is given in Table 4.1 and Table 4.2.

Table 4.1 - Comparison of Column Forces for K7 (Bare Frame Model)

COLUMNS – EQMASTER

Element ID	Moment in X-Direction (M_{y-y}) (kN.m)	Shear in X-Direction (kN)	Moment in Y-Direction (M_{x-x}) (kN.m)	Shear in Y-Direction (kN)	Axial Load (kN)
A1-1	101.13	42.44	105.46	45.93	258.9
A2-1	104.49	44.73	107.8	47.52	444.96
A3-1	102.31	43.24	107.8	47.52	425.79
A4-1	104.49	44.73	107.8	47.52	444.96
A5-1	101.13	42.44	105.46	45.93	258.9
B1-1	101.13	42.44	105.46	45.93	258.9
B2-1	104.49	44.73	107.8	47.52	444.96
B3-1	102.31	43.24	107.8	47.52	425.79
B4-1	104.49	44.73	107.8	47.52	444.96
B5-1	101.13	42.44	105.46	45.93	258.9

COLUMNS - SAP2000

Element ID	Moment in X-Direction (M_{y-y}) (kN.m)	Shear in X-Direction (kN)	Moment in Y-Direction (M_{x-x}) (kN.m)	Shear in Y-Direction (kN)	Axial Load (kN)
A1-1	96.43	40.55	100.48	43.81	254.73
A2-1	99.34	42.53	102.82	45.41	439.6
A3-1	97.23	41.09	102.82	45.41	420.74
A4-1	99.34	42.53	102.82	45.41	439.6
A5-1	96.43	40.55	100.48	43.81	254.73
B1-1	96.43	40.55	100.48	43.81	254.73
B2-1	99.34	42.53	102.82	45.41	439.6
B3-1	97.23	41.09	102.82	45.41	420.74
B4-1	99.34	42.53	102.82	45.41	439.6
B5-1	96.43	40.55	100.48	43.81	254.73

Table 4.2 - Comparison of Beam Forces for K7 (Bare Frame Model)

BEAMS - EQMASTER				BEAMS - SAP2000		
Element ID	Moment (kN.m)	Shear (kN)		Element ID	Moment (kN.m)	Shear (kN)
BX11-1	144	75.37		BX11-1	140.38	74.31
BX21-1	126.63	67.53		BX21-1	123.59	66.71
BX31-1	126.63	67.53		BX31-1	123.59	66.71
BX41-1	144	75.37		BX41-1	140.38	74.31
BX12-1	144	75.37		BX12-1	140.38	74.31
BX22-1	126.63	67.53		BX22-1	123.59	66.71
BX32-1	126.63	67.53		BX32-1	123.59	66.71
BX42-1	144	75.37		BX42-1	140.38	74.31
BY11-1	151.23	80.38		BY11-1	145.28	78.49
BY12-1	166.87	101.96		BY12-1	160.92	100.08
BY13-1	166.87	101.96		BY13-1	160.92	100.08
BY14-1	166.87	101.96		BY14-1	160.92	100.08
BY15-1	151.23	80.38		BY15-1	145.28	78.49

A good match between base reactions is observed as shown in Figure 4.5. Correlations in periods and modal shapes are even better. Moreover, member forces turned out to be satisfactorily close.

The following analysis results belong to the same building which is modeled with infill walls. Acceptable conformity between base reactions is seen in Figure 4.8. Maximum error for base reactions is less than %5. Comparison of vibration periods and modal shapes is given in Figure 4.9 and Figure 4.10, respectively. Although there is 26.7% difference in the second fundamental mode periods, the mode shapes are almost exactly matched. Note that the second mode is dominantly torsional but also includes translation. Existence of infill walls makes it difficult to attain a perfect agreement especially in the coupled modes (i.e., modes 2 and 5). Experimental results for K7 building are also quite close to those determined by EQMASTER. Comparison of fundamental periods provided by Celik [6] with analytical values is given in Table 4.3.

Table 4.3 – Fundamental Period Comparison

	Celik [6]	EQMASTER
K7 (Bare Frame)	-	0.521 (sec)
K7 (Infill Walls)	0.17 (sec)	0.205 (sec)
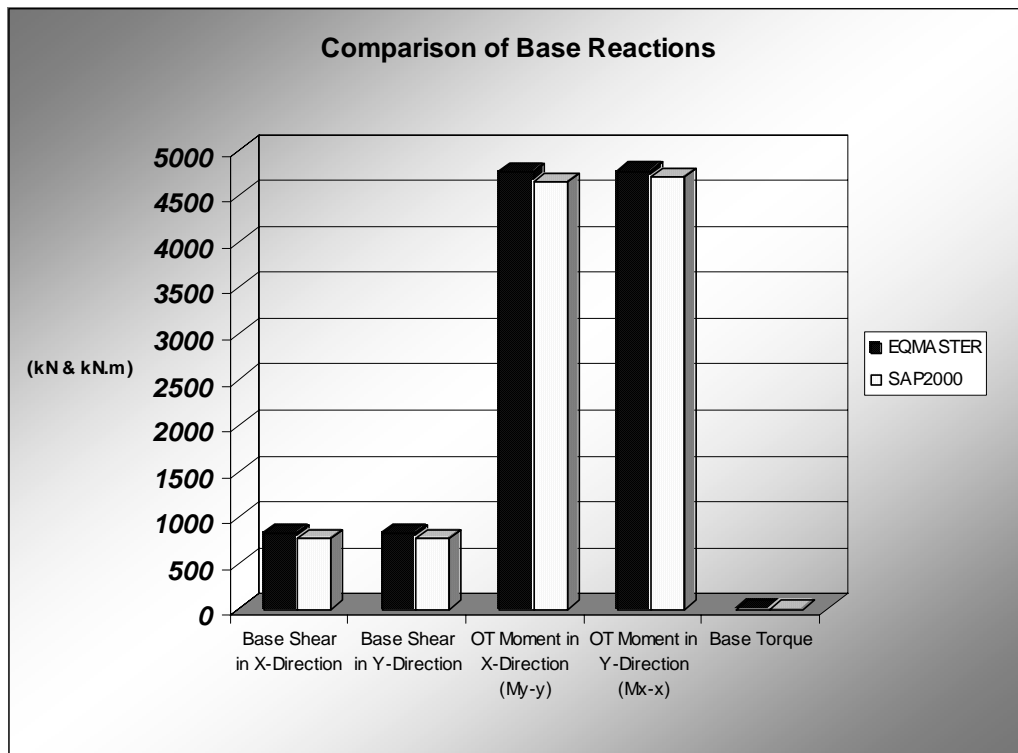
Figure 4.8 - Comparison of Base Reactions for K7 (Infill wall model)
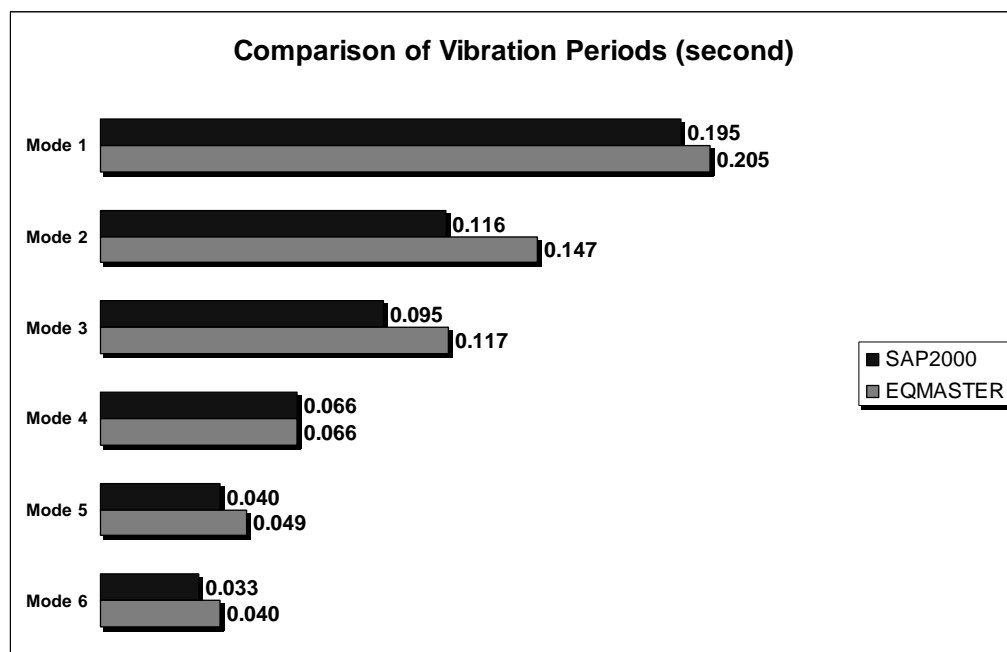
Figure 4.9 - Comparison of Vibration Periods for K7 (Infill wall model)
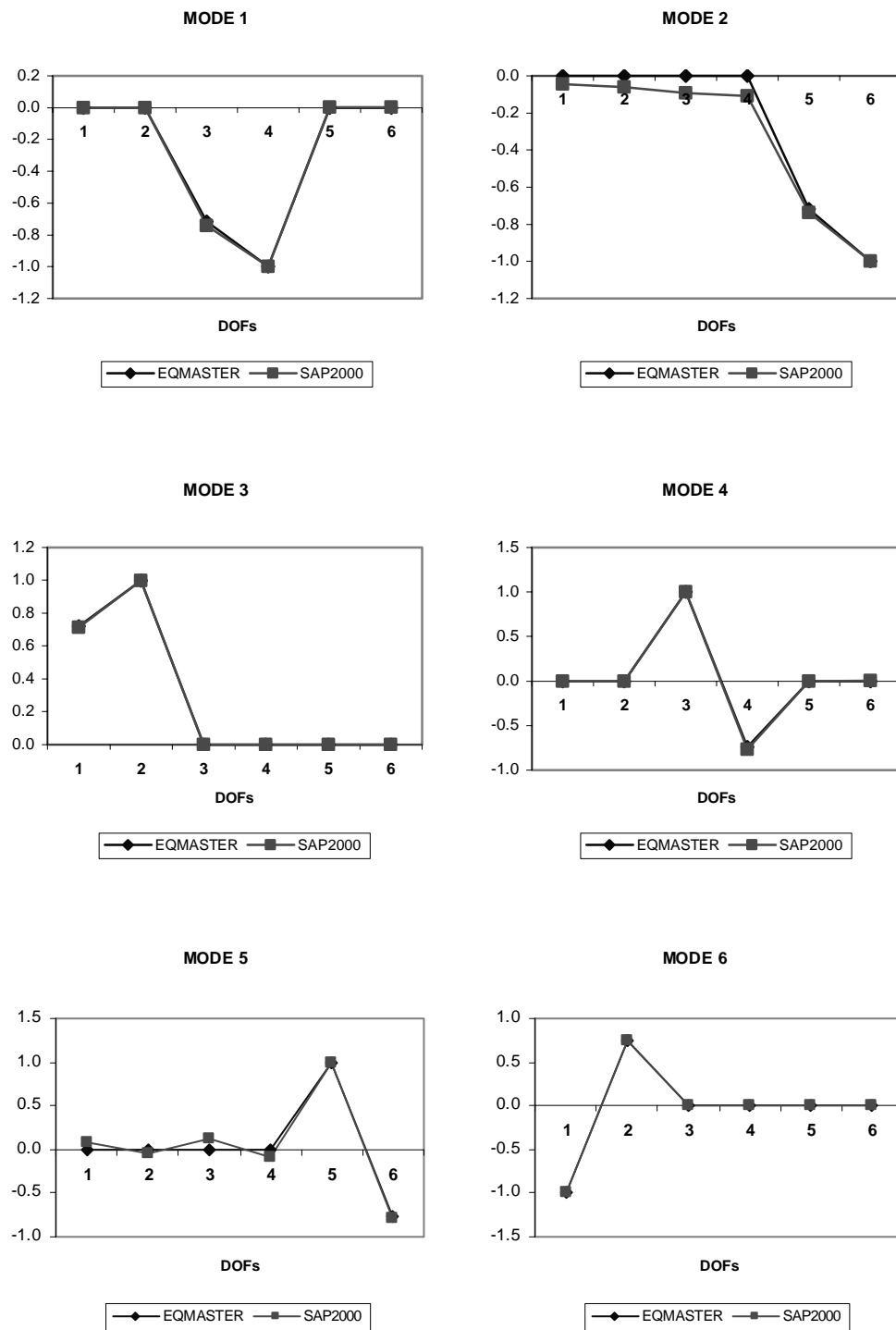
Figure 4.10 - Comparison of Modal Shapes for K7 (Infill Wall Model)

In general, agreement of results from infill wall model is inferior to the bare frame comparison but still quite satisfactory. Observed deviations from the SAP2000 [8] model are most probably due to differences in the infill wall modeling, although the wall model of EQMASTER is verified using a simple wall model solved by SAP2000 [8] using meshed shell element. Existence of additional parameters in a wall model in SAP2000 [8] may also cause this difference.

4.2.2   İş Bankası Kabataş Branch Building

This reinforced concrete building is one of the branches of İş Bankası located in Istanbul. It has four stories in which the first story height is 3.10 m and remaining three stories are 2.90 m. Outside view of the building is given in Figure 4.11.

Figure 4.11 - İş Bankası Kabataş Branch Building, Istanbul

Several types of column and beam cross-sections exist in the structural system. Almost all beams are located between columns. All floors are in rectangular shape having 16.7 m by 16 m in size. Floor plan includes four frames in each direction. Slab consists of small opening for landing located at the upper right region. Floor plan of the first and the other stories can be seen in Figure 4.12 and Figure 4.13. Model view in graphical interface is also given in Figure 4.14.
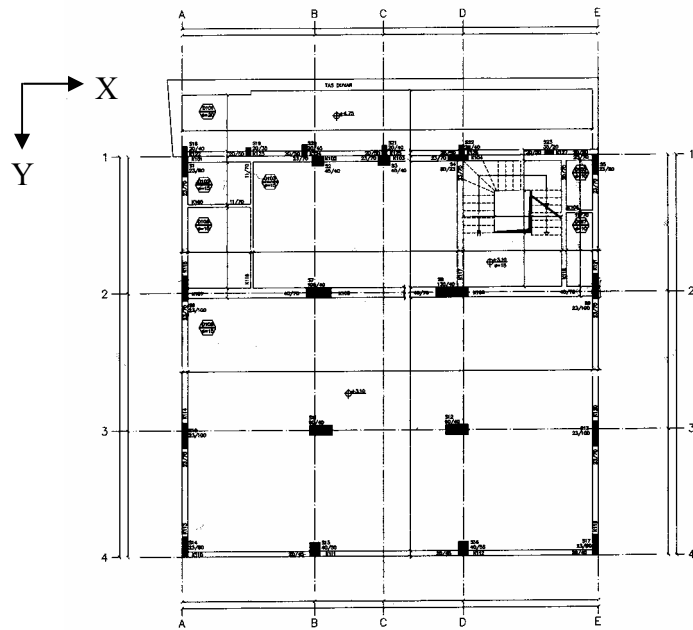
Figure 4.12 - Structural Floor Plan for Story 1
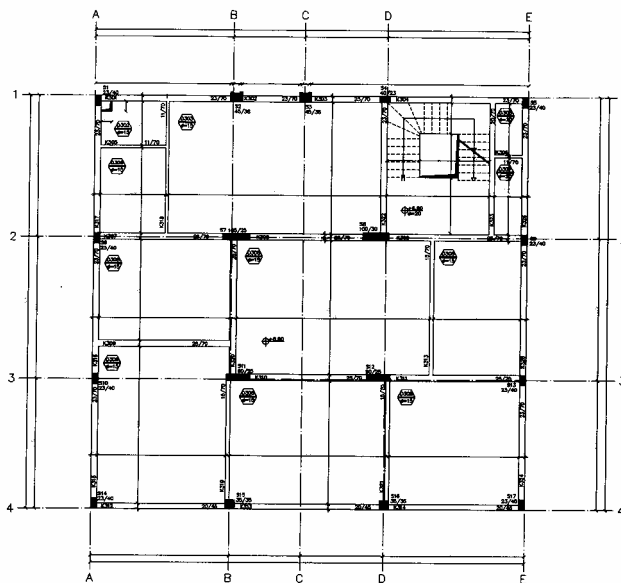
Figure 4.13 - Structural Floor Plan for Stories 2, 3 and 4

87
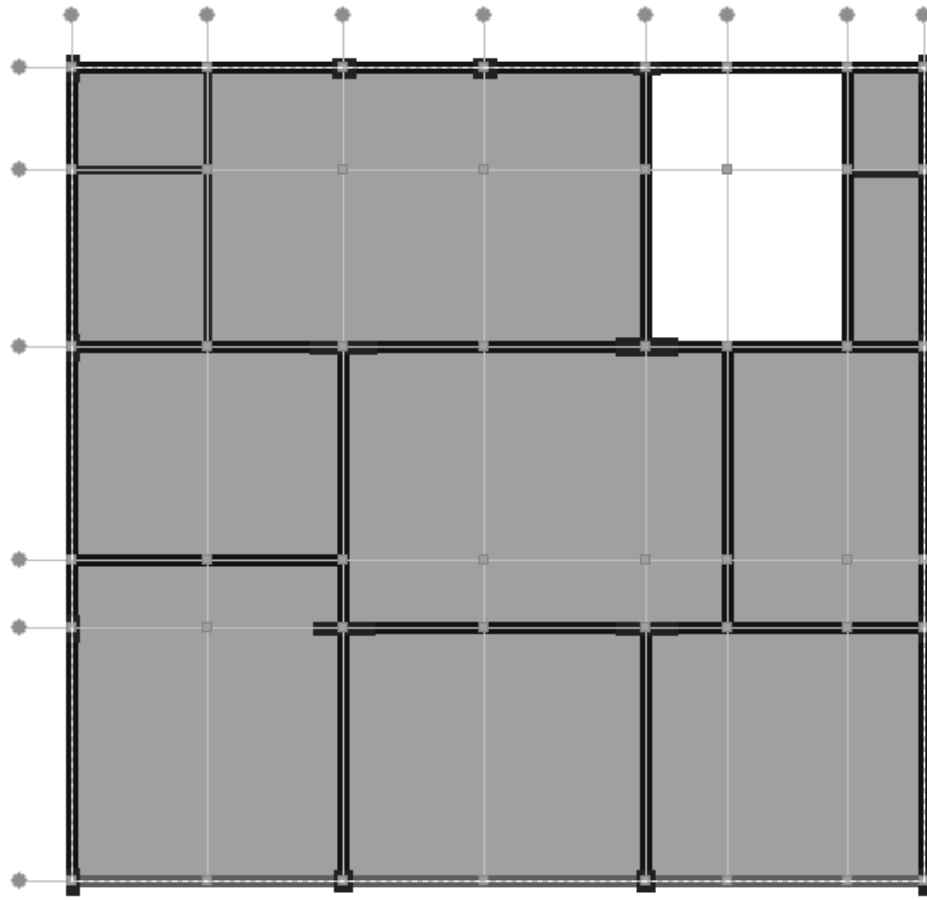
Figure 4.14 – Model View of İş Bankası Building (stories 2, 3 and 4)

There is no vertical discontinuity. Dimensions of some columns slightly change through the height of the building. Four columns located in the middle have relatively larger cross-sections. Most of the perimeter and inner beams are 23 cm by 70 cm in size. Building location corresponds to earthquake zone 2. Building importance factor is unity and local site class according to Turkish Earthquake Code [16] is Z4.

Analysis results from two programs are given below. Note that building is modeled without infill walls. Tolerable differences appear in the base reactions. Different from previous models, considerable base torque exist for this building due to unsymmetrical floor plan. Vibration periods and modal shapes are compared in Figure 4.16 and Figure 4.17 respectively.
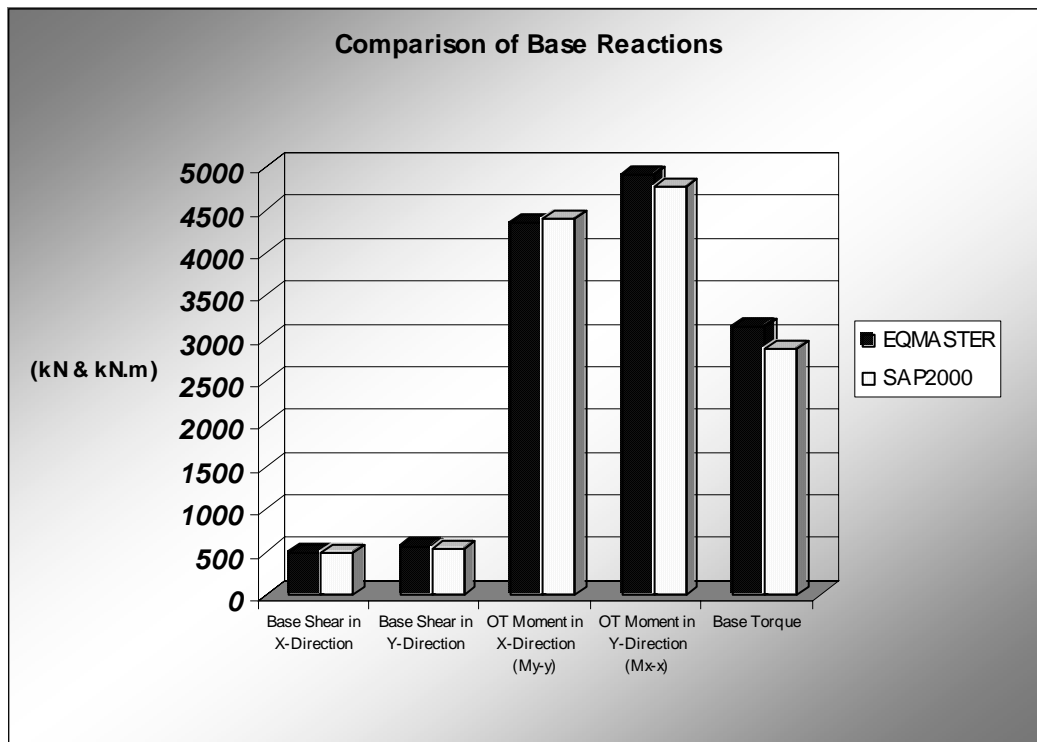
Figure 4.15 - Comparison of Base Reactions for İş Bankası Building
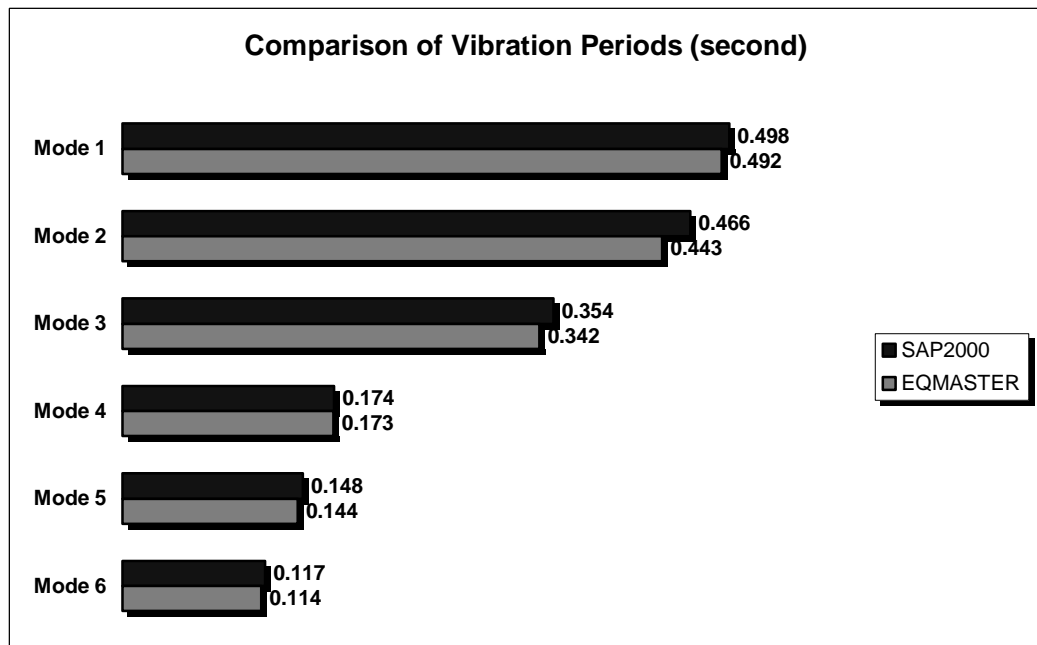
Figure 4.16 - Comparison of Vibration Periods for İş Bankası Building

MODE 1

MODE 2

MODE 3
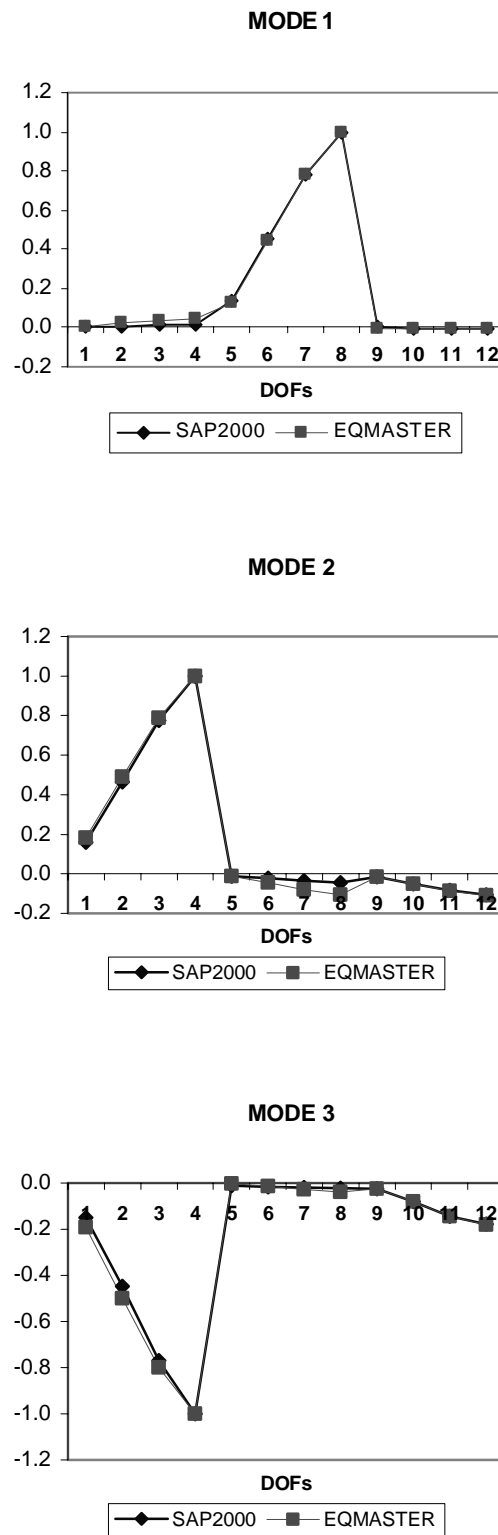
Figure 4.17 – (a) Comparison of Modal Shapes for İş Bankası Building

(modes 1, 2 and 3)

MODE 4

MODE 5

MODE 6
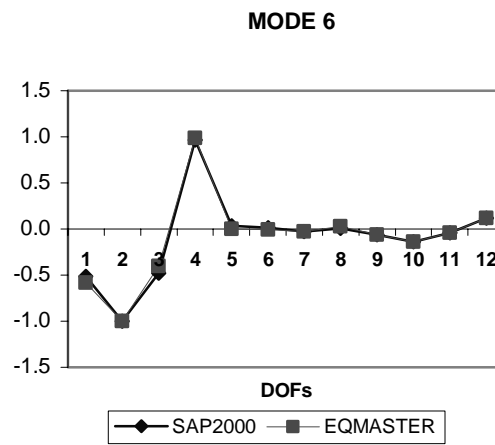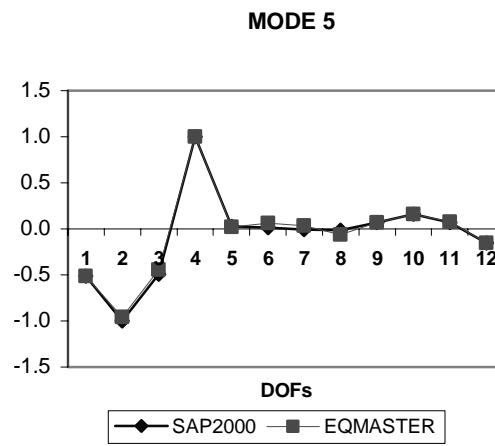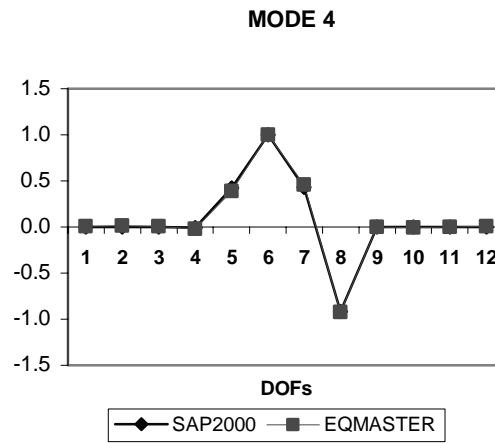
Figure 4.17 – (b) Comparison of Modal Shapes for İş Bankası Building

(modes 4, 5 and 6)

91

Although there are totally twelve modes, the first six modes are enough to examine similarities between modal shapes produced by two programs. The first translational mode is in Y-direction. The second and third modes include translation in X-direction and torsion. It is clear that satisfactory agreement is observed in all periods and modal shapes. Same level of conformity is also seen in member force comparisons which are given in Table 4.4 and Table 4.5. The last number in element ID stands for the corresponding story number. Due to large number of members existing in this building, only beam and column forces at the first story are tabulated.

Table 4.4 - Comparison of Column Forces for İş Bankası Building

COLUMNS – EQMASTER

Element ID	Moment in X-Direction (My-y) (kN.m)	Shear in X-Direction (kN)	Moment in Y-Direction (Mx-x) (kN.m)	Shear in Y-Direction (kN)
A1-1	10.91	6.99	132.35	56.06
B1-1	33.83	19.78	15.77	1.79
C1-1	35.00	21.06	14.29	1.71
D1-1	92.17	47.92	15.47	9.65
E1-1	11.07	7.09	89.98	38.74
A2-1	18.15	10.93	282.28	132.33
B2-1	247.03	98.17	36.52	4.61
D2-1	515.07	189.10	53.03	19.62
E2-1	17.57	10.62	189.84	89.09
A3-1	7.71	2.09	273.77	124.09
B3-1	167.29	35.59	33.24	3.33
D3-1	159.01	30.05	27.83	3.46
E3-1	6.29	0.99	184.14	83.58
A4-1	13.03	7.30	135.11	58.67
B4-1	39.25	18.78	36.97	4.30
D4-1	38.79	18.38	33.26	4.69
E4-1	12.76	7.05	91.46	40.11

Maximum error in member force calculation is around %10. The developed software consideres frame stiffness in a global reduced number of dofs and development of software producing exactly the same analysis results as SAP2000 [8] requires professional computer programming which is beyond the scope of this study. Thus, such approximate results may be within acceptable limits as the complexity of the structure and approximate nature of this program is concerned.

Table 4.4 – (continued)

COLUMNS - SAP2000

Element ID	Moment in X-Direction (My-y) (kN.m)	Shear in X-Direction (kN)	Moment in Y-Direction (Mx-x) (kN.m)	Shear in Y-Direction (kN)
A1-1	14.00	8.45	118.73	51.75
B1-1	34.86	21.23	14.65	0.85
C1-1	33.98	20.31	14.13	0.82
D1-1	94.15	50.46	15.32	9.64
E1-1	13.29	8.10	112.06	47.89
A2-1	21.21	12.59	238.00	107.65
B2-1	255.22	93.89	34.05	3.89
D2-1	539.12	185.11	61.08	22.15
E2-1	20.41	12.21	226.33	100.92
A3-1	8.46	2.26	239.85	108.75
B3-1	180.51	33.38	31.47	2.63
D3-1	175.85	29.98	28.52	2.61
E3-1	7.52	1.05	228.63	102.96
A4-1	14.55	8.12	117.81	51.22
B4-1	41.33	18.43	34.46	2.88
D4-1	41.73	18.58	33.43	2.73
E4-1	14.36	7.86	110.71	48.00

Table 4.5 – Comparison of Beam Forces for İş Bankası Building

BEAMS - EQMASTER			BEAMS - SAP2000		
Element ID	Moment (kN.m)	Shear (kN)	Element ID	Moment (kN.m)	Shear (kN)
AB-1-1	62.12	35.96	AB-1-1	60.10	42.12
BC-1-1	61.04	46.17	BC-1-1	57.93	41.69
CD-1-1	68.28	45.03	CD-1-1	63.22	42.24
DE-1-1	45.65	47.13	DE-1-1	54.00	32.56
AB-2-1	138.65	74.49	AB-2-1	142.20	73.52
BD-2-1	141.58	73.56	BD-2-1	158.31	77.49
DE-2-1	105.20	53.29	DE-2-1	125.61	56.97
AB-4-1	31.25	26.95	AB-4-1	35.42	21.58
BD-4-1	31.55	27.15	BD-4-1	35.93	21.93
DE-4-1	29.98	34.09	DE-4-1	33.17	19.34
12-A-1	115.30	60.88	12-A-1	109.42	55.24
23-A-1	110.02	62.55	23-A-1	101.53	49.39
34-A-1	125.02	63.67	34-A-1	108.50	56.7
12-D-1	74.58	35.85	12-D-1	82.27	38.54
12-E-1	100.94	43.77	12-E-1	101.21	48.92
23-E-1	97.44	45.99	23-E-1	95.80	45.75
34-E-1	106.98	46.11	34-E-1	101.50	52.05

As far as the user-friendly content of the program is considered all of the above results are served to the user in much more effective format. Explicable graphical representations are used for the results of member forces besides their tabular form. Simple 3D animation is utilized to demonstrate modal shapes. All related graphs and other visual materials are described in Appendix A.

4.3   Proposed Methods

Two different seismic vulnerability assessment methods are proposed in this study. The first one is relatively more complicated and based on the analysis results produced by EQMASTER. The second approach contains several questions and in the form of simple questionnaire which may be directly used through a HTML based internet page. However, complete analysis of the building is required for the first approach. Reply to the user is in the online report format for both methods. Explanation of the second approach is given in Appendix B.

4.3.1   Approach 1: Detailed Analysis

The first method uses demand-capacity ratios of beams and columns as two major variables which are then factored by their importance factors (Equation 4.1). Demand-capacity ratios are checked in terms of both shear&torsion and flexure&axial load as explained in section 3.3.13. Shear&torsion interaction may be considered as relatively less critical than flexure&axial interaction especially if the axial load on a column is below the balanced point (Figure 3.32). Hence, the shear&torsion and flexure&axial demand capacity ratios are modified by coefficients of 1.2 and 2, respectively. Same modifications are done for beams and columns. Note that torsion is considered together with shear. Axial load - moment relationship is taken into account when the flexural safety is concerned for columns. Corresponding maximum values are selected as their final demand-capacity ratios.

Building is given a damage score using the following formulation;

$$DS_{building} = \frac{IF_{beam} * \left(\frac{F}{C} \right)_{beam} + IF_{column} * \sum_{i=1}^{n} \left(IF \right)_{column}^{i} * \left(\frac{F}{C} \right)_{column}^{i}}{IF_{beam} + IF_{column}}$$ **(4.1)**

where

$\left(\frac{F}{C} \right)_{beam}$: demand-capacity ratio of beams on a building scale

$\left(IF \right)_{column}^{i}$: importance factor of columns at the ith story

$\left(\frac{F}{C} \right)_{column}^{i}$: average demand-capacity ratio of columns at the ith story

$\left(IF \right)_{beam}$: importance factor of beams on a building scale

$\left(IF \right)_{column}$: importance factor of columns on a building scale

Development of importance factors is based on energy dissipation capacity of beams. Two limiting cases are investigated for this purpose. In the first case all beams are considered as infinitely flexible meaning that hinges carrying zero moment are formed at the ends (Figure 4.18) and beams transmit axial forces between columns. Cantilever behaviour of columns is observed under such condition. All floors are assumed to be equal height.
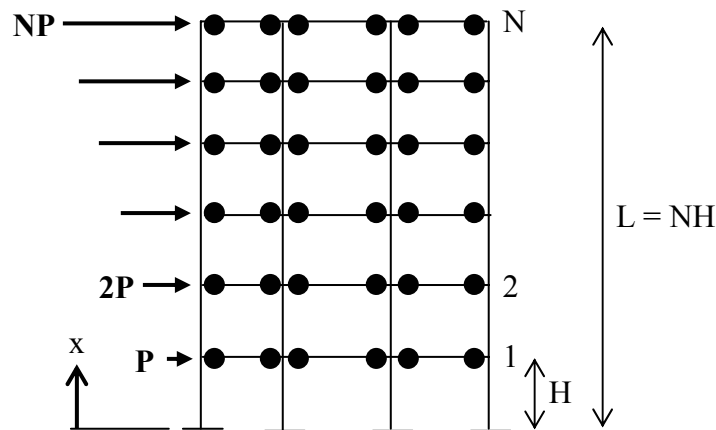
Figure 4.18 – Infinitely Flexible Beams

Then all beams are assumed as infinitely rigid in the second case (Figure 4.19). Bilinear capacity curves relating base shear to top floor displacement are defined for infinitely rigid and infinitely flexible beam cases. The difference in areas under these curves reflects the energy dissipated by beams which quantifies their level of importance. The area between these two curves is normalized by the area under rigid-beam curve. Derivation of this process is given below. Referring to Figure 4.18, displacement at the top floor due to applied earthquake load at the ith floor is given by;

$$\delta_{top} = \frac{(iH)^3 (iP)}{3EI} + \frac{(iH)^2 (iP)}{2EI}(N-i)H \qquad (4.2)$$

The first term in Equation 4.2 is the lateral top floor displacement due to applied load at the ith floor. Second term is rotation multiplied by the distance of the applied load to the top floor which results in additional lateral top floor displacement. Summing up Equation 4.2 for all floors leads to the total top floor displacement;

$$\delta_{top}{}^{flexible} = \frac{PH^3}{6EI}\left(3N\sum_{i=1}^{N} i^3 - \sum_{i=1}^{N} i^4 \right) \qquad (4.3)$$

Similar calculations are performed for the second case in which beams are considered as infinitely rigid. However, displacement pattern is different due to rigid beams as shown in Figure 4.19.
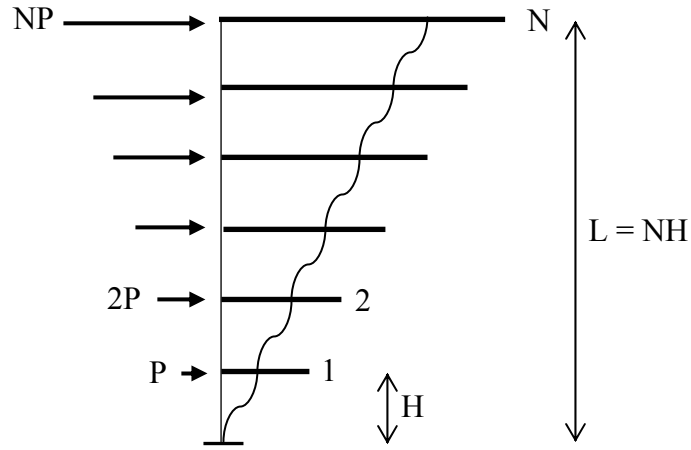
Figure 4.19 - Infinitely Rigid Beams

Displacement at the top floor due to earthquake load at i[th] floor in Figure 4.19 is given by;

$$\delta_i = \left[\frac{N(N+1)}{2} - \frac{(i-1)i}{2} \right] \frac{PH^3}{12EI} \tag{4.4}$$

Note that the displacement at the first floor when number of story is equal to one becomes $PH^3/12EI$ which is the ratio of P to the stiffness of a fixed ended column. Then, top floor displacement is obtained through summation of each floor displacement;

$$\delta_{top}{}^{rigid} = \frac{PH^3}{12EI} \left[\frac{N^2(N+1)}{2} - \sum_{i=1}^{N} \frac{i(i-1)}{2} \right] \tag{4.5}$$

The last part of the derivation is to construct base shear vs. top displacement graphs for both cases (Figure 4.21). When the beams are infinitely flexible, system has a tendency to form a mechanism earlier as compared to "rigid case" and the yielding base shear is smaller than the rigid beam case. Thus, shear corresponding to yield point of "rigid case" is reduced by a factor of γ in order to obtain yielding shear force for "flexible case" ($V_f = \gamma * V_r$ as shown in Figure

97

4.21). Coefficient γ is calculated by equating plastic moment at the base column for both cases by referring the free body diagrams as shown in Figure 4.20.

$$M_p = V_t \frac{H}{2}$$

Rigid Case

$$M_p = \gamma V_t H^*$$
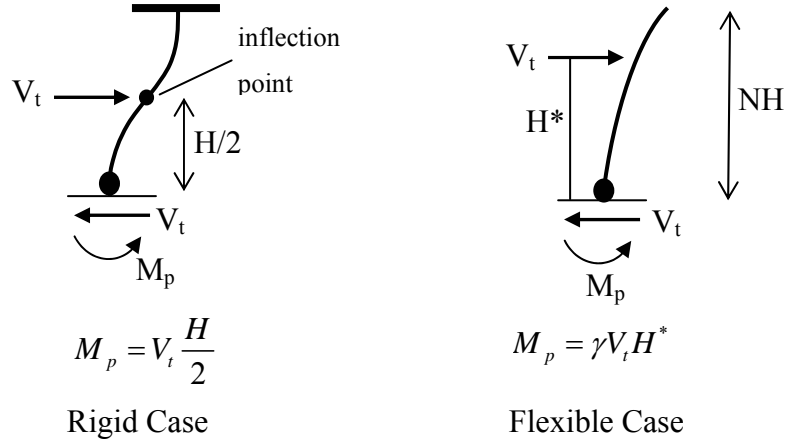
Flexible Case

Figure 4.20 – Free Body Diagrams for "Rigid" and "Flexible" Cases

Note that base shear is applied on the inflection point of the base column for the "rigid case" whereas base shear acts on the height [$H^* = H^*(2N+1)/3$] in case of infinitely flexible beams. Base shear for flexible case (Figure 4.18) is given by;

$$V_t = \frac{N(N+1)}{2}P \tag{4.6}$$

After equating M_p values in Figure 4.20 and substituting Equation 4.6;

$$\frac{N(N+1)P}{2}\frac{H}{2} = \gamma V_t H^* \tag{4.7}$$

Note that $V_t H^*$ can be replaced by overturning moment in Figure 4.18;

$$M_{overturning} = PH \sum_{i=1}^{N} i^2 \tag{4.8}$$

Hence, substituting Equation 4.8 into Equation 4.7 yields;

$$\gamma = \frac{N(N+1)}{4\sum\limits_{i=1}^{N} i^2} = \frac{3}{4N+2} \tag{4.9}$$
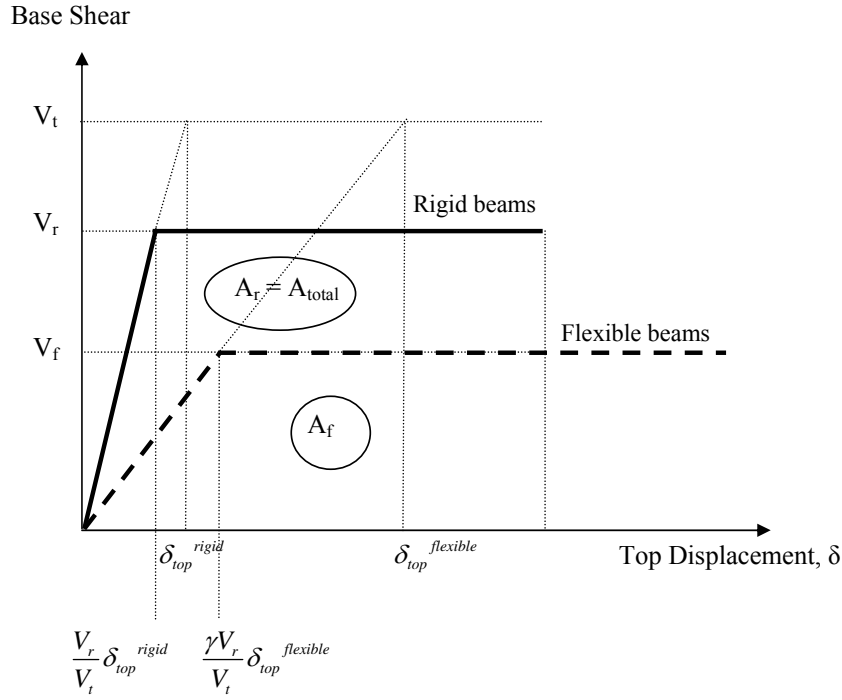
Figure 4.21 – Base Shear vs. Top Floor Displacement Curves

Displacements corresponding to yield points of both cases are determined by dividing base shear values with their corresponding stiffness (slope) values. Areas under the curves shown in Figure 4.21 can now be calculated. The area A_f relates to the energy dissipation due to columns only, whereas A_r relates energy dissipation due to beams and columns together. Column importance factor is therefore calculated as the ratio of area under dashed line curve (A_f) to the area under rigid beam curve (A_r). A_f is given by;

$$A_f = \frac{\gamma V_r}{V_t} \delta_{top}^{\;flexible} \gamma V_r \left(R^f - \frac{1}{2} \right) \tag{4.10}$$

99

Finally, column importance factor becomes;

$$IF_{column} = \frac{A_f}{A_{total}} = \frac{\delta_{top}^{flexible} \gamma^2 \left(R^f - \dfrac{1}{2} \right)}{\delta_{top}^{rigid} \left(R^r - \dfrac{1}{2} \right)} \qquad (4.11)$$

where R^f and R^r, which are taken as 2.5 and 5 respectively, stand for the ratio of top displacement resulting in failure to that corresponding to yielding for "flexible case" and "rigid case" respectively. That ratio is smaller for "flexible case" since system in this case is on the verge of a mechanism. Selection of R^f and R^r also affects the variation of importance factors with the total number of story in a building (Figure 4.22). Thus, above values may be used accordingly. Note that importance factor for beams is identical throughout the building. However, importance of columns should decrease for those located in higher floors since they are different in the sense of their contribution to the energy dissipation. Therefore, the distribution shown in Table 4.6 is utilized in order to signify column importance factor assigned for each floor.

Table 4.6 - Column Importance Factor Distribution for Floors

Floor	1	2	3	4	5	6	7	8	9	10
1	100%									
2	100%	44%								
3	100%	69%	25%							
4	100%	81%	49%	16%						
5	100%	87%	64%	36%	11%					
6	100%	91%	73%	51%	27%	8%				
7	100%	93%	80%	62%	41%	22%	6%			
8	100%	95%	84%	69%	52%	34%	17%	5%		
9	100%	96%	87%	75%	60%	44%	28%	14%	4%	
10	100%	96%	89%	79%	67%	53%	38%	24%	12%	3%

When the interstorey drift is taken as a linear function of the interstorey shear, the energy dissipated at each floor would be a function of shear square. Relative importance factors can be assigned to each floor's columns as a function of interstorey shear value square. Percentages shown in Table 4.6 are obtained from the ratio of the squares of shear forces at each floor to the base shear square. The

energy dissipations of higher storey columns are assumed to be smaller than the lower storey columns. The summation of factors in Table 4.6 is larger than unity; therefore, these factors are scaled for better interpretation so that the summation of all floors becomes unity (Table 4.7).

Table 4.7 - Column Importance Factor Distribution for Floors (Scaled)

Floor	1	2	3	4	5	6	7	8	9	10
1	100%									
2	69%	31%								
3	51%	36%	13%							
4	41%	33%	20%	7%						
5	34%	29%	21%	12%	4%					
6	29%	26%	21%	15%	8%	2%				
7	25%	23%	20%	15%	10%	5%	2%			
8	22%	21%	18%	15%	11%	7%	4%	1%		
9	20%	19%	17%	15%	12%	9%	6%	3%	1%	
10	18%	17%	16%	14%	12%	9%	7%	4%	2%	1%

Importance of a column at a particular story changes according to the total story number of that building. For instance, a column at the second story has 0.36 importance in a three story building. This number reduces to 0.21 as in the case of an eighth story building.

Importance of beams is also related to their energy dissipation capacity and equal to the ratio of difference between areas of the two curves (A_f and A_r) to total area (A_r) as shown in the following equation;

$$IF_{beam} = \frac{A_r - A_f}{A_r} = 1 - \frac{\delta_{top}^{flexible} \gamma^2 \left(R^f - \frac{1}{2} \right)}{\delta_{top}^{rigid} \left(R^r - \frac{1}{2} \right)} \tag{4.12}$$

Similar to columns, different factors are used to represent beam importance for buildings with different total number of storeys. Figure 4.22 illustrates the variation of beam and column importance factors with the total number of storeys. The beam importance factors for different storeys are assumed to be constant in a building.

101

Importance Factors vs. Number of Story
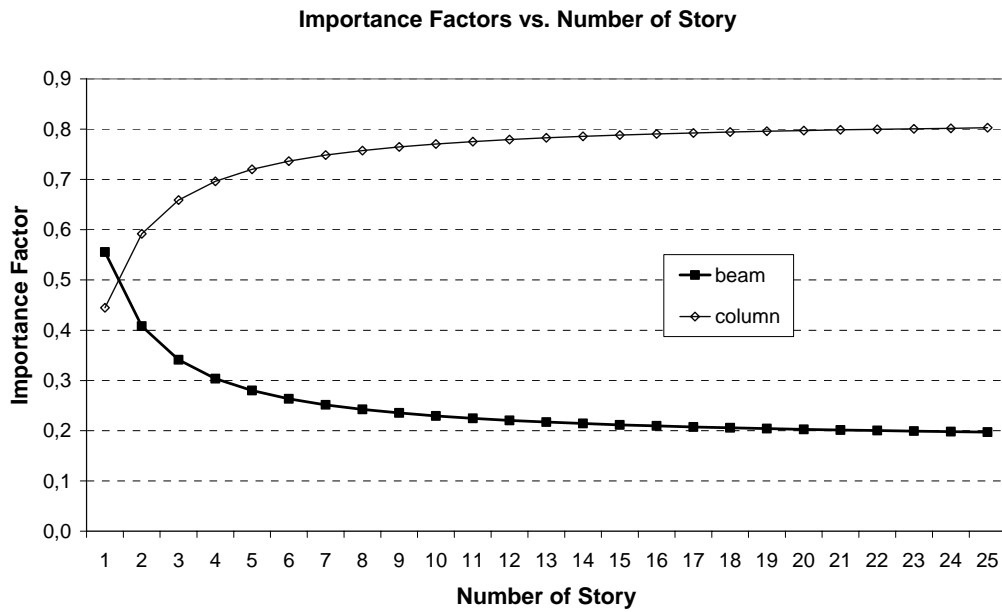
Figure 4.22 - Variation of Importance Factors with Number of Story

Figure 4.22 shows that the beams are more critical in a single story building compared to higher buildings. Change in beam importance factor gets smaller as the number of story increases and the factor itself approaches to 0.2 after fifteen story buildings. Similar change is observed in columns approaching to a value of 0.8 after 15 storeys. Note that the summation of beam and column importance factors is always unity.

Importance factors developed for beams and columns are similar in terms of their theoretical derivations. Columns are always relatively more critical from ductility and collapse point of view in practice (strong column – weak beam concept) which is supported by the suggested method as well.

4.3.2   Application of Approach 1 on Example Buildings

Although the derivation for damage score of the building is little complicated, application on a building is quite simple and requires several program runs. Damage score assigned to the building is out of 100; however the damage score may exceed 100 based on the overall demand-capacity ratios. Clearly, the more score the building has, the more damage it is expected or the more vulnerable it

will be during an earthquake. Calculation of the ultimate capacities shown in Equation 4.1, requires information on reinforcement details of members. This kind of difficulty is prevented in the program by an option where minimum reinforcement amounts specified in the Turkish Earthquake Code [16] can be automatically assigned. Application of the first approach using these minimum values may lead to extreme damage scores. On the other hand, infill walls may significantly contribute to the overall performance of a building. Table 4.8 shows the damage scores of the example buildings based on minimum level of reinforcement.

Table 4.8 – Damage Scores of the Example Buildings

	K7 Building (Bare)	**K7 Building (Infill)**	**İş Bankası Building**
Damage Score	981.6	139.8	175.6

It is observed that damage score for the bare frame of K7 building is extremely high. This is simply because minimum reinforcement specifications are not adequate despite favorable conditions of the building such as earthquake zone, number of storeys etc. On the other hand, the damage score reduces to an acceptable level when infill walls are considered. Load carrying members still have minimum reinforcement amounts in this case. Existence of infill walls significantly diminishes the earthquake demand on beams and columns. Damage score of the İş Bankası building is also obtained from its bare frame model. However, cross-sectional areas of members (columns in particularly) are considerably large compared to K7 building. This leads to relatively greater reinforcement amounts and decreases the damage score significantly. Beams are also effective in such situation where only 20% exceeded their flexural capacity. That ratio is around %80 for K7 building (bare frame).

4.3.3 Application of Previous Methods on Example Buildings

Additional observations are done based on previous assessment approaches. The methodology developed by Ersoy and Tankut [10] is applied to example buildings. Detail procedure of this method is given in 2.5.3. The aim, at this point, is to provide supplementary idea about possible damage that the building will suffer during earthquake. Figure 4.23 and Figure 4.24 illustrates the application of the method on example buildings shown by larger square. Figures also demonstrate the distribution of buildings obtained from Düzce damage database in order to show the reliability of the method to the user. Note that existence of infill walls for K7 building does not affect the result since they are not included in the procedure.
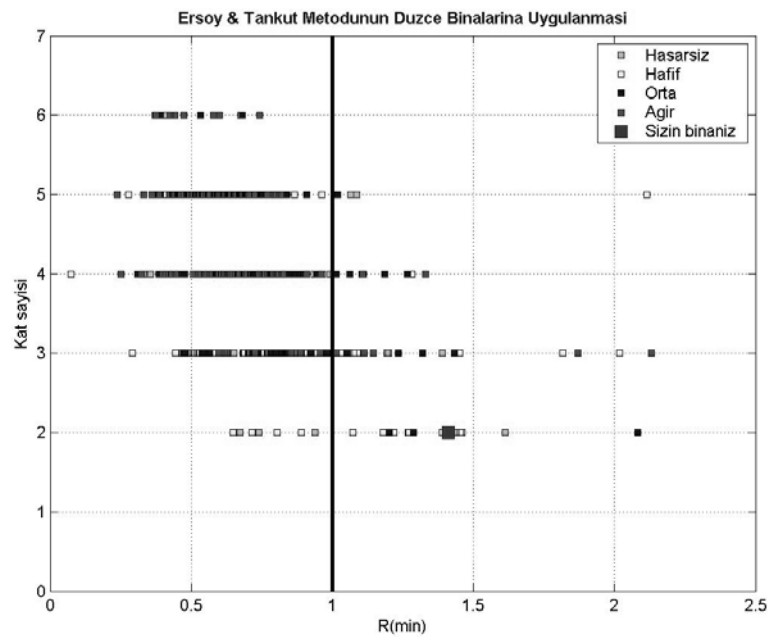
Figure 4.23 – Application of Ersoy & Tankut Method [10] on K7 Building

Based on Ersoy and Tankut [10] method, İş Bankası building comes out to be comparatively safer than K7 building.
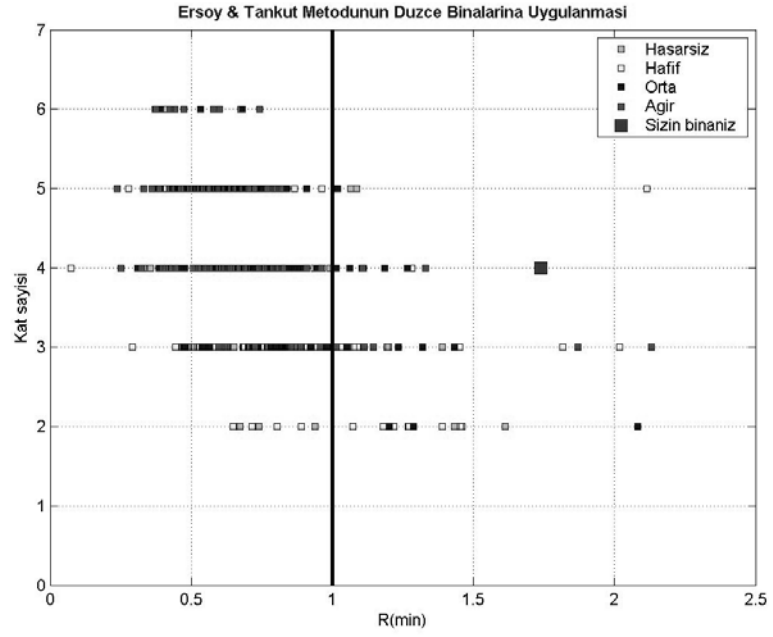
Figure 4.24 - Application of Ersoy & Tankut Method [10] on İş Bankası Building

Similar representation is performed using another assessment method proposed by Hassan and Sozen [14]. Application of method on example buildings together with Düzce damage database shown in Figure 4.25, Figure 4.26 and Figure 4.27. Note that boundary lines used in the figures were suggested by authors for the 1992 Erzincan Earthquake. Although these boundary lines were suitable for the Erzincan damage database, they seem to be unconservative for Düzce records. Method also includes the existence of infill walls. Detail explanation of the method is given in 2.5.1.
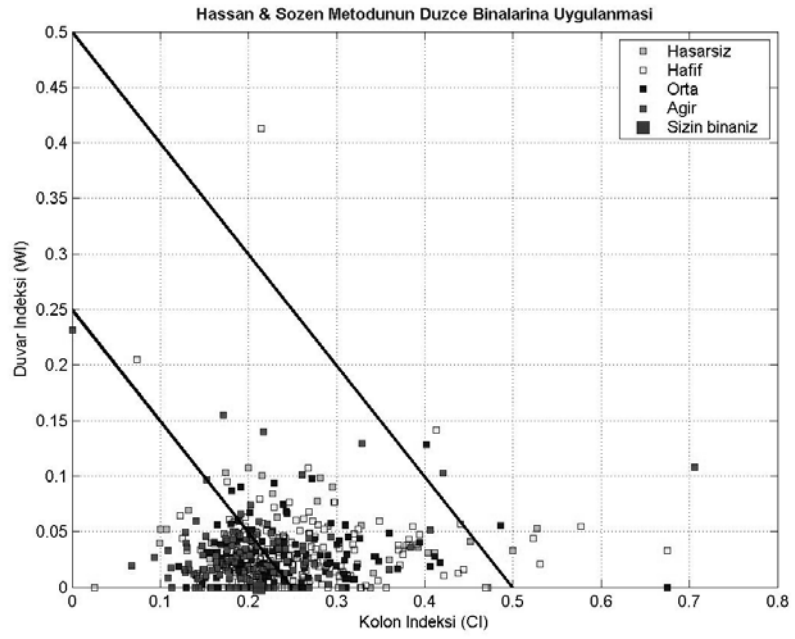
Figure 4.25 - Application of Hassan & Sozen Method [14] on K7 (Bare frame)
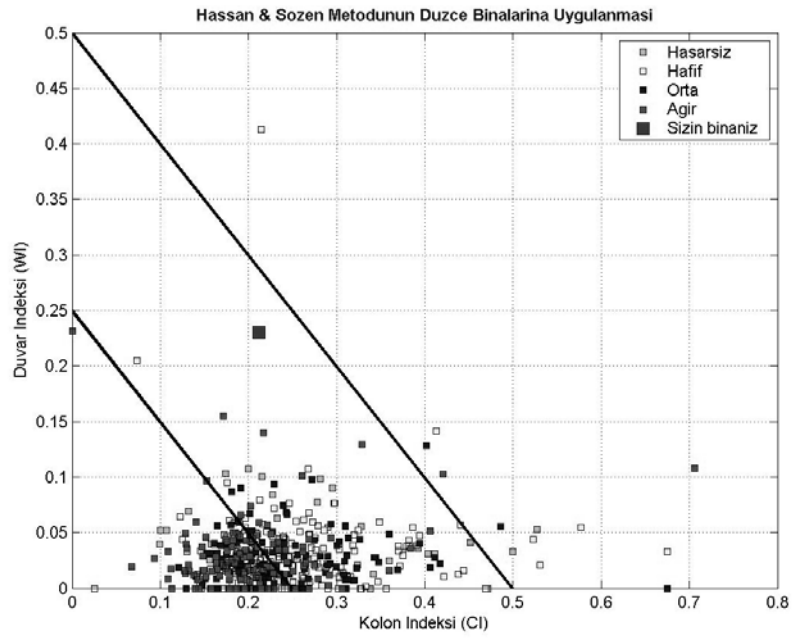
Figure 4.26 - Application of Hassan & Sozen Method [14] on K7 (Infill walls)
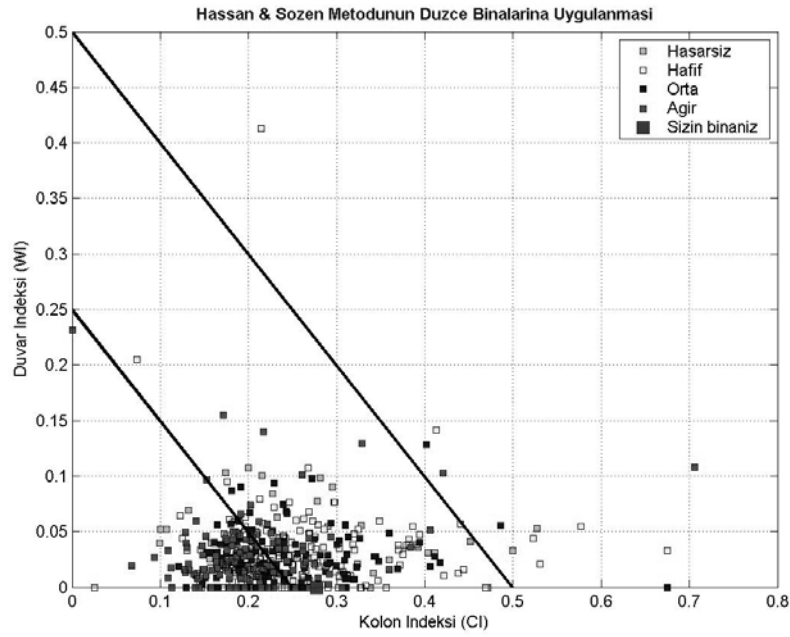
Figure 4.27 - Application of Hassan & Sozen Method [14] on İş Bankası Building

Effect of infill walls on priority index is clear when compared with bare frame. Priority index for the bare frame is within boundary lines indicating its relative weakness. On the other hand, İş Bankası building falls inbetween of the margins and comes out to be safer according to this method.

4.3.4   Application of Approach 1 on Düzce Damage Database

In order to observe the correlation between building damage score and corresponding damage level, 36 buildings from Düzce damage database are analyzed. Four groups of damage levels, namely, none, light, medium and severe are defined for Düzce buildings. 9 buildings from each damage level are selected. Buildings from each damage level are equally distributed as three, four and five story buildings. For the buildings having same number of story, the ones with different overhang ratios (OR) and minimum lateral stiffness indexes (MNLSTFI) are picked up to represent complete building stock as much as possible.

After each building is analyzed in EQMASTER, damage score is plotted against observed damage level. Boundary lines for damage levels are then determined on the graph given in Figure 4.28. Buildings used in the analysis and their damage scores are shown in Table 4.9.

Table 4.9 - Damage Scores of the Buildings from Düzce Database

ID	Time of Construction	# of Stories	IRREQULARITIES							Damage in R/C members	MNLSTFI	OR	Building Damage Score
			A1	A2	A3	A4	B1	B2	B3				
E-A-4	1975	3	1	2	2	2	2	2	2	L	0,0580	0,1160	141,6
E-G-20	1987	3	2	2	2	2	2	1	2	L	0,0660	0,0000	136,4
E-NB-146	1980	3	2	2	2	2	2	2	2	L	0,0563	0,0461	126,0
A-20-EKS-36	1985	4	2	2	2	2	2	2	2	L	0,1215	0,0750	160,0
E-G-3	1974	4	2	2	2	2	2	1	2	L	0,0189	0,0000	102,8
E-J-30	1990	4	2	2	2	2	1	1	2	L	0,0579	0,1178	130,4
A-38-EKS-60	1990	5	2	2	2	2	2	1	2	L	0,0466	0,0864	162,8
A-9-EKS-19	1995	5	2	2	2	2	2	1	2	L	0,1239	0,1059	176,4
E-G-17	1992	5	2	1	2	2	2	1	2	L	0,0367	0,0000	164,8
C-B10-144	1988	3	2	2	2	2	2	2	2	M	0,0171	0,0000	166,4
C-B20-237	1982	3	2	2	2	2	2	1	2	M	0,1745	0,0909	171,2
M-EKS-36	1990	3	1	2	2	2	2	2	2	M	0,0940	0,0659	191,6
A-5-EKS-41	1989	4	2	2	2	2	2	2	2	M	0,1997	0,1732	242,0
A-5-EKS-42	1989	4	2	2	2	2	2	2	2	M	0,2664	0,0553	126,0
E-NB-127	1980	4	2	2	2	2	2	1	2	M	0,0699	0,0000	166,0
A-55-EKS-97	1984	5	2	1	2	2	2	1	2	M	0,0787	0,0000	274,4
I-E-32	1980	5	2	2	2	2	2	2	2	M	0,0675	0,1110	198,8
M-7-EKS-11	1985	5	1	2	2	2	2	1	2	M	0,0468	0,1145	173,2
C-B6-101	1995	3	2	2	2	1	2	2	2	N	0,0749	0,0702	118,0
I-A-2	1950	3	2	2	2	2	2	1	2	N	0,0181	0,0000	132,0
I-F-44	1975	3	2	2	2	2	2	2	2	N	0,1316	0,0908	135,6
C-B21-38	1982	4	1	2	2	1	2	1	2	N	0,0764	0,0393	116,4
C-B4-88	1979	4	1	2	2	2	2	1	2	N	0,0738	0,0884	121,6
I-C-21	1976	4	2	2	2	2	2	1	2	N	0,0356	0,0000	105,6
C-B21-37	1989	5	2	2	2	1	2	1	2	N	0,0857	0,0848	99,6
I-E-33	1985	5	2	2	2	2	2	2	2	N	0,1187	0,0000	150,4
I-E-35	1993	5	2	2	2	1	1	1	2	N	0,1610	0,1884	86,0
C-B1-1	1988	3	1	2	1	1	2	1	2	S	0,0631	0,3489	397,6
E-I-42	1980	3	2	2	2	2	2	1	2	S	0,0648	0,0000	325,2
G-C-40	1983	3	2	2	2	2	2	2	2	S	0,1628	0,0452	216,8
E-G-14	1980	4	2	2	2	2	2	1	2	S	0,0711	0,1105	273,6
E-G-19	1976	4	2	2	2	2	2	1	2	S	0,0293	0,0331	325,2
E-NB-106	1975	4	2	2	2	1	2	1	2	S	0,0421	0,0435	246,4
E-G-13	1980	5	2	2	1	2	2	1	1	S	0,0378	0,0000	243,6
E-K-39	1985	5	1	2	2	2	2	1	2	S	0,0673	0,1148	240,4
M-7-EKS-10	1985	5	1	2	2	2	2	1	2	S	0,1385	0,0469	262,8

Irregularities 1: Exist 2: Not Exist

Figure 4.28 shows the damage score distribution for the buildings from Düzce database. As can be seen from Figure 4.28, buildings are categorized under three different damage levels. None and light damage levels are combined whereas medium and severe damage levels are considered separately. Finally, the following cut-off values are chosen for three damage levels:

$$0 < None + Light \leq 165$$
$$165 < Medium \leq 210$$
$$210 < Severe$$

Within the above boundary values, %94.4 of none and light damaged buildings fall into the selected range while that ratio becomes %66.7 for medium damaged buildings. On the other hand, %100 of severely damaged buildings is successfully detached by corresponding cut-off value.
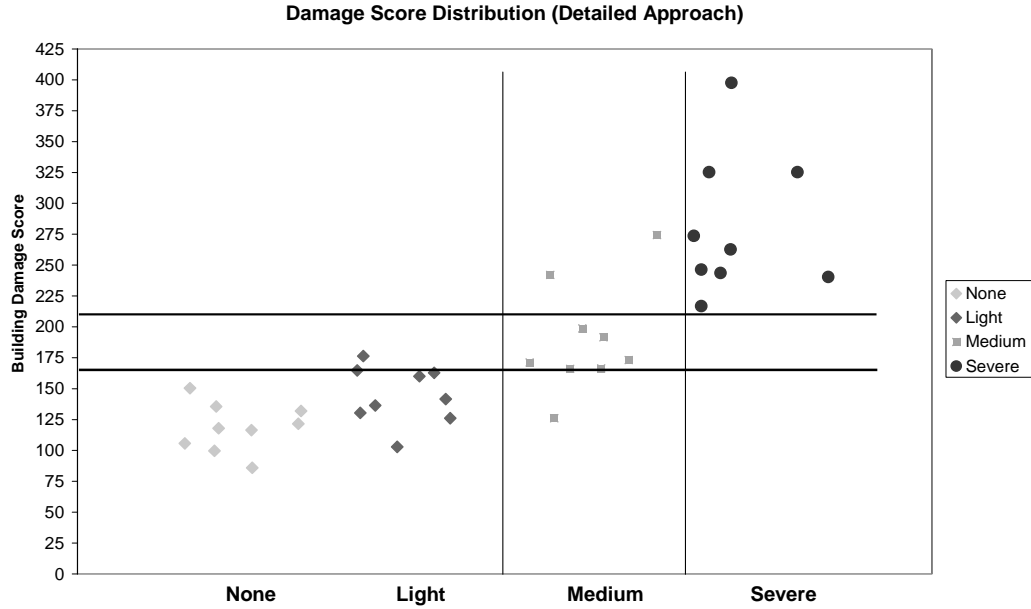

Figure 4.28 – Damage Score Distribution (Detailed Approach)

Additional 9 buildings from Düzce damage database (one is from Bingöl database) are randomly selected in order to verify the consistency of boundary values. Two buildings from none, light and medium damage levels and three buildings from severe damage level are tested and damage scores are checked whether the buildings are correctly classified. Observed damage levels and damage scores of the test buildings are given in Table 4.10.

Table 4.10 – Damage Scores of the Test Buildings

ID	Time of Construction	# of Stories	IRREQULARITIES							Damage in R/C members	*MNLSTFI*	*OR*	*Building Damage Score*
			A1	A2	A3	A4	B1	B2	B3				
E-G-16	1990	3	2	2	2	1	2	2	2	L	0,1507	0,0684	158,8
E-J-23	1986	4	1	2	2	2	2	1	2	L	0,0582	0,0171	131,6
C-B20-246	1970	3	2	2	2	2	2	2	2	M	0,0487	0,1230	178,8
A-5-EKS-15	1981	4	2	2	2	2	2	2	2	M	0,0677	0,0681	180,0
I-D-27	1987	3	2	2	2	2	2	1	2	N	0,2648	0,0620	140,8
I-C-19	1973	4	2	2	2	1	2	1	2	N	0,0489	0,0000	146,0
C-B2-77	1980	3	1	2	2	1	1	1	2	S	0,0490	0,1446	228,4
E-H-25	1983	4	2	2	1	2	2	1	2	S	0,0459	0,0929	257,2
BNG-6-2-8	1980	2	1	2	1	2	2	1	2	S		0,2429	422,7

Note that four buildings with none and light damage have damage scores less than 40. Two buildings with medium damage fall into the range between 40 and 52. Severely damaged two buildings, on the other hand, have damage scores above 52.

Relatively simplified method is also proposed as an alternative to detailed approach. Discussions and explanations are given in Appendix B & C.

CHAPTER 5

SUMMARY AND CONCLUSIONS

5.1   SUMMARY

In this study, a web-based computer program is developed for seismic vulnerability assessment of existing reinforced concrete buildings. Developed software includes two different levels of evaluation methods.

Simple:

The simplified method (Appendix B & C) targets to produce building *evaluation index* by means of several simple questions in the form of a questionnaire. Evaluation index is calculated according to response to each question which reveals possible seismic defects of a building. All questions are tried to be designed as self explanatory addressing average internet users in Turkey.

Detailed:

The second method, which is much more detailed compared to the first simplified method, computes a *damage score* for a building based on linear structural analysis. The building properties are entered by the user through a user-friendly graphical interface. The analysis results are used to compute capacity demand ratios for all beams and columns. Building damage score is obtained by calculating weighted average of all members based on their assigned importance factors. The ranges of *damage score* values corresponding to building damage levels (severe, medium, none-light damage) are determined by using 36 different

111

buildings from Düzce damage database. Buildings are randomly selected to represent the entire building stock as much as possible. Nine buildings are selected for each one of the four damage levels. Among each nine building group, subgroups of three buildings are selected for three, four, and five storey buildings. Each three building subgroup has different properties such as overhang ratios, lateral stiffness terms, etc. None and light damage states are combined as none-to-light, whereas medium and severe damage states are considered separately during damage estimation stage. Cutoff values for the three groups of damage classifications are determined as the building damage scores obtained from detailed method are plotted against damage levels. The cutoff values and ranges are then tested by using randomly selected 9 buildings from the same database (one is from Bingöl database) with two buildings from each of none, light and medium damage levels and three buildings from severe damage level. In the detailed method, the user has to download a user interface and need to define structural properties (e.g., dimensions, coordinates, reinforcement, etc.). Different than the simplified method, setting up a building model and execution of analysis for the detailed method require intermediate level of civil engineering background and higher level of computer competency.

5.2 CONCLUSIONS

Under the light of the results of this analytical study, following conclusions can be drawn;

- Methods of two complexity levels are proposed for the seismic vulnerability assessment and simple evaluation of existing R/C buildings. The detailed method is found to be reliable and effective in assigning building damage score and predicting corresponding damage level. Simplified method (Appendix B & C) addresses average level of internet users, questions are easy to answer, and the resulting report is more socially oriented than engineering. The report also intents to give general

information about commonly known facts on building parameters and their effects on seismic performance, in an attempt to educate public.

- 36 + 9 buildings are used from Düzce damage database to correlate damage scores against damage level. The 36 building training set is successfully separated into three damage level groups (severe damage 100%, medium damage 66.7%, none-light 94.4 % success rate). The medium damage level is subjective to the naked eye. Two of the three misclassified buildings in the medium damage level are assigned to severe damage, which is on the safe side. One misclassified building in the none-light damage level is assigned to medium damage level, which is again on the safe side. All of the nine test buildings are successfully coupled with their corresponding observed damage levels (100% success rate). Using a larger number of buildings might affect the calculated success rates.

- In its current form, simplified approach (Appendix B & C) may be used to quickly calculate online building evaluation index. Although there is no damage estimation due to lack of appropriate database, this method may provide an idea about the *relative* seismic vulnerability of a reinforced concrete building by comparing building evaluation index against indices obtained for other buildings. A histogram of all building evaluation indices in the database might give an idea about the evaluation index of a building relative to all buildings in the database.

- Numerous earlier (nonlinear analysis, regression, approximate, etc.) studies on understanding and linking structural parameters to observed damage have not been as successful as it is desired. Although current study involves linear solution and uncertainties regarding reinforcement, the results are much superior to any earlier studies on separating the observed damage using a single analysis tool for classification. Sensitivity studies showed that the infill wall contribution is a very important parameter, which probably underestimated by previous linear/nonlinear analyses. Reducing the infill wall contribution makes the damage score distribution versus observed damage inseparable.

113

5.3   FUTURE RECOMMENDATIONS

- More buildings should be involved in determination of cut-off values for building damage level prediction for the detailed approach. Number of buildings for testing of cut-off values should also be increased.
- Damage level estimation should be done in case of simplified method after appropriate database with large number of building stock is generated.
- Further complicated nonlinear analyses (pushover, time history etc.) should be performed by using different professional softwares to improve the seismic vulnerability assessment technique and compare the results with linear analysis.

REFERENCES

1. Applied Technology Council, "A Handbook for Seismic Evaluation of Existing Building" (ATC-22), Federal Management Agency Report FEMA-178, California, 1989.

2. Applied Technology Council, "NEHRP Guidelines for the Seismic Rehabilitation of Buildings" (ATC 33), Federal Management Agency Report FEMA-273, Washington, 1997.

3. Applied Technology Council, "Rapid Visual Screening of Buildings for Potential Hazards" A Handbook, (ATC-21), Federal Management Agency Report FEMA-154, California, 1988.

4. Aydogan, V., "Seismic Vulnerability Assessment of Existing Reinforced Concrete Buildings in Turkey", M.Sc. Thesis, Middle East Technical University, Ankara, 2003.

5. Bagci, G., Yatman, A., Ozdemir, S., Altin, N., "Türkiye'de Hasar Yapan Depremler", Deprem Araştırma Bülteni, No.69, pp. 113-126

6. Celik, O.C., "Forced Vibration Testing of Existing Reinforced Concrete Buildings", M.Sc. Thesis, Middle East Technical University, Ankara, 2002.

7. Chopra, A.K., "Dynamics of Structures: Theory and Applications to Earthquake Engineering", Second Edition, Prentice Hall, Inc., 2001.

8. Computer and Structures, Inc., SAP2000 Version 8.1.5, California, 2003.

9. Ersoy, U., Ozcebe, G., Tankut, T., "Reinforced Concrete", Middle Technical University, Ankara, 2003.

10. Ersoy, U., Tankut, T., "Az Katlı Yapıların Deprem Tasarımına İlişkin Bir Öneri", Türkiye Mühendislik Haberleri, No.386, pp. 40-43, 1996.

11. Fajfar, P., "A Simplified Nonlinear Method for Seismic Damage Analysis of Structures", Workshop on Seismic Design Methodologies for the Next Generation of Codes, Slovenia, 1997.

12. Gulkan, P., Sozen, M.A., "Procedure for Determining Seismic Vulnerability of Building Structures", ACI Structural Journal, Vol. 96, No.3, pp.336-342, 1999.

13. Gulkan, P., Yakut, A., "An Expert System for Reinforced Concrete Structural Damage Quantification" in ACI SP-162, Mete A. Sozen Symposium: Edited by J.K. Wight and M.E. Kreger, 1996, pp 53-71.

14. Hassan, A.F., Sozen, M.A., "Seismic Vulnerability Assessment of Low-Rise Buildings in Regions with Infrequent Earthquakes", ACI Structural Journal, Vol.94, No.1, pp.31-39, 1997.

15. Japan Building Disaster Prevention Association, "Standard and Commentary for Evaluation of Seismic Capacity of Existing Reinforced Concrete Buildings", Tokyo, 2001.

16. Ministry of Public Works and Settlement. General Directorate of Disaster Affairs, "Specifications for Structures to be Built in Disaster Areas", Ankara, 1998.

17. Open System for Earthquake Engineering Simulation, "OpenSees", Pacific Earthquake Engineering Research Center, University of California Berkeley.

18. Pay, C., "A New Methodology for the Seismic Vulnerability Assessment of Existing Buildings in Turkey", M.Sc. Thesis, Middle East Technical University, Ankara, 2001.

19. Rodriguez, M.E., Aristizabal, J.C., "Evaluation of a Seismic Damage Parameter", Earthquake Engineering and Structural Dynamics, pp.463-477, 1999.

20. Sucuoglu, H., Yazgan, U., "Simple Survey Procedures for Seismic Risk Assessment in Urban Building Stocks", Proceedings of the NATO Science for Piece Workshop on Seismic Assessment and Rehabilitation of Existing Buildings, edited by S.Tanvir Wasti and Guney Ozcebe, pp.97-118, Izmir 2003

21. The MathWorks, Inc., MATLAB, Version 6.5 Release 13, Massachusetts, 2002.

22. TS-498, "Design Loads for Buildings", Turkish Standards Institute, Ankara, 1997.

23. TS-500, "Requirements for Design and Construction of Reinforced Concrete Structures", Turkish Standards Institute, Ankara, 2000.

24. Wasti, S.W., Sucuoglu, H., Utku, M., "Structural Rehabilitation of Damaged RC Buildings After the 1 October 1995 Dinar Earthquake" Journal of Earthquake Engineering, Vol. 5, No. 2, pp.131-151, 2001.
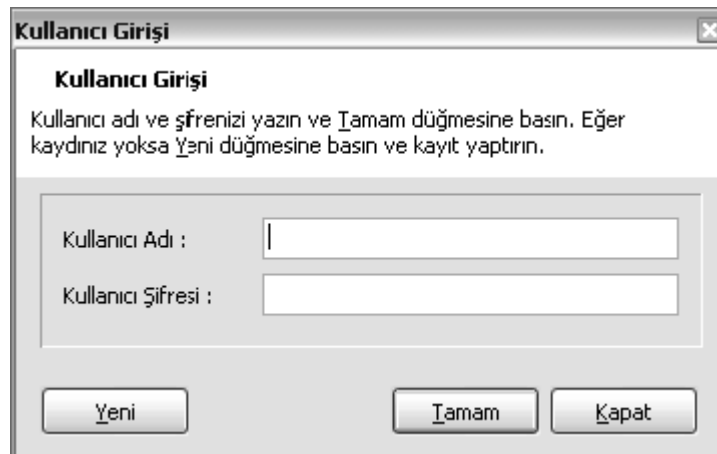
25. Wilson, E.L., Kiureghian, A.D., Bayo, E.P., "A Replacement of the SRSS Method in Seismic Analysis", Earthquake Engineering and Structural Dynamics, Vol.9, pp.187-194, 1981.

APPENDIX A

ANALYSIS WIZARD FOR EQMASTER

Step by step explanations may provide better understanding in order to use the program effectively. Details on how to analyze a building from the beginning and getting final report are given in this part. One of the example buildings (K7) is selected for this purpose.

Since this is internet-based software, user must receive his own account from the server before starting analysis. Such process is achieved by using additional utility called "communication". User is to specify his username and password on the welcome screen shown below. If user uninstalls the software there is no need to indicate different username & password on reinstallation. User can obtain his past information by selecting "receive from server" option after pressing "new" button.

Figure A.1 - Welcome Screen

User must select a folder on the computer to locate his projects. Having specified required information, following communication tool appears on the screen (Figure A.2). User may see his projects grouped under different headings. Before sending the project for analysis, they are located in "projects to be sent" folder. They pass to "projects in analysis" during analysis. Final analysis report is saved in "analysis reports".
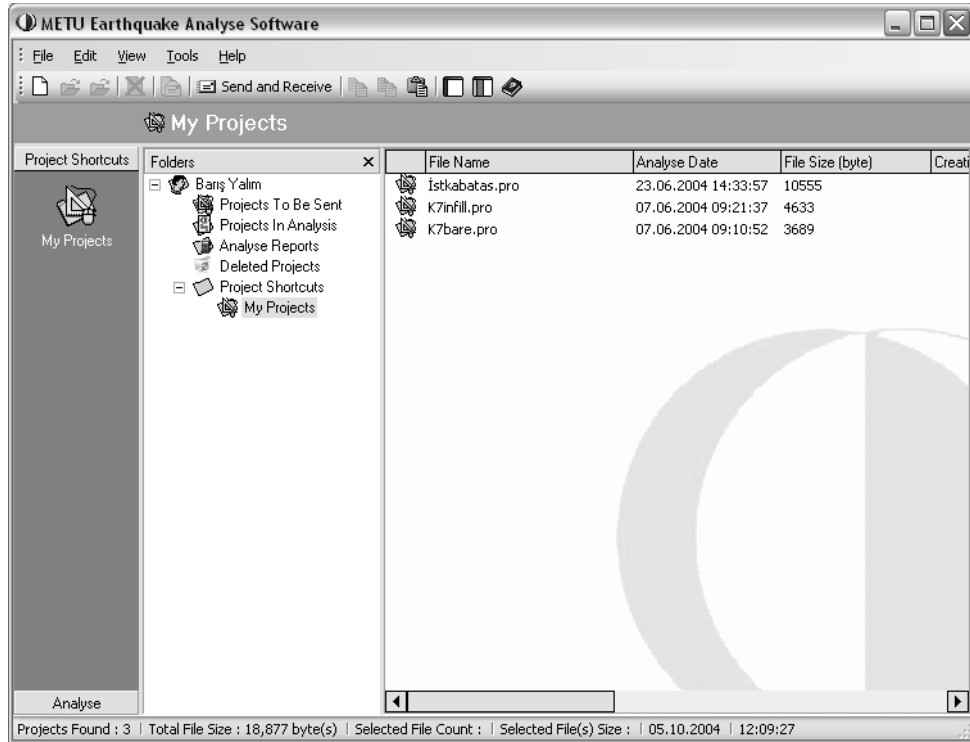

Figure A.2 – Interface for Communication Tool

Project arrangements can easily be done using communication tool. Projects can be opened, modified or deleted on this utility.

The next step is modeling of the building using EQMASTER's graphical user interface (GUI) which can be run by selecting "design" from start menu. Design of GUI has been prepared as simple as possible for all kind of users. New model is created by clicking "new project". At this stage, user must sign and accept the agreement (disclaimer) determined by software developers. Window shown in Figure A.3 is then displayed on the screen.

Figure A.3 – New Project Window

General properties of the building such as the location, soil type, geometric layout etc. are provided on this window. Height and slab thickness for each floor is entered in "storey information". Location of horizontal and vertical axis can also be arranged using this menu. These properties can later be modified. However, change in unit is not possible therefore user must be careful about unit selection before carrying on. Initial view of the building for these properties is shown in Figure A.4.

Next part is identification of members. Columns, beams, infill walls and shear walls are all defined using template manager. Once sectional properties are specified for a member it is recorded as unique in the template. Such an option is extremely useful in buildings having numerous same types of members. Member properties are automatically updated when changed on the template. New member is defined using the buttons located on the left (Figure A.5).
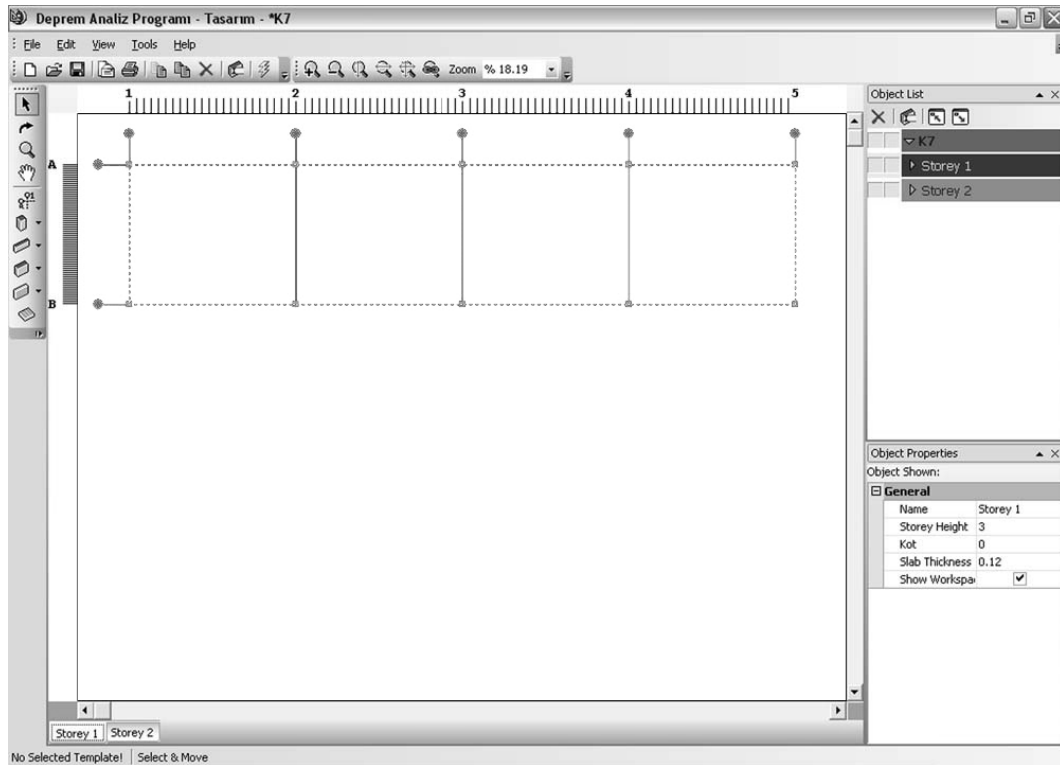
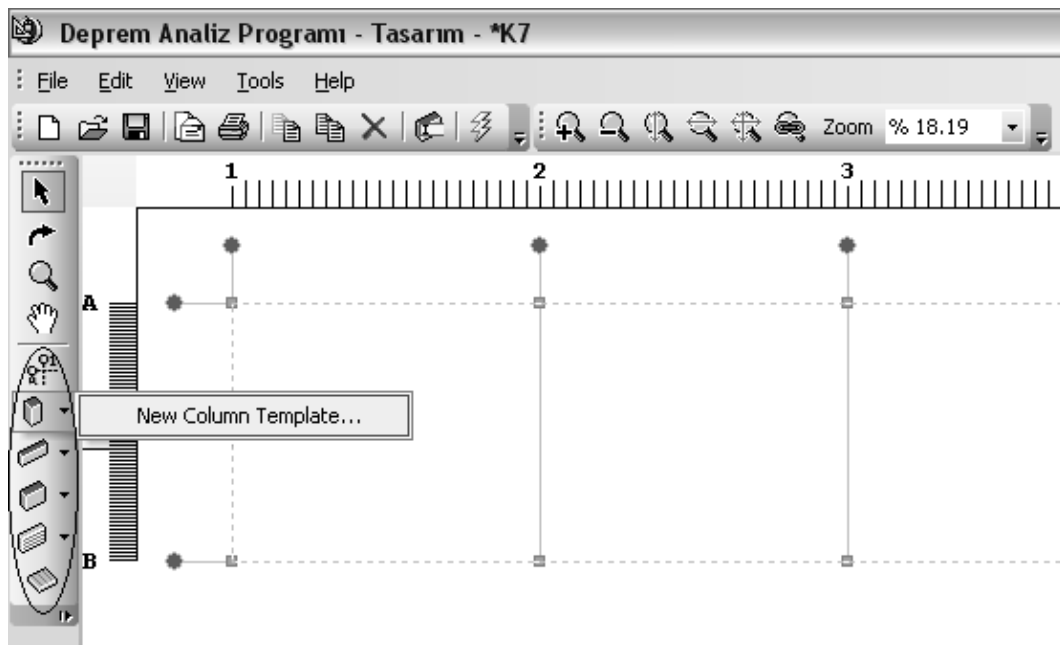**Figure A.4 -** Initial View of the Building (Axes System)

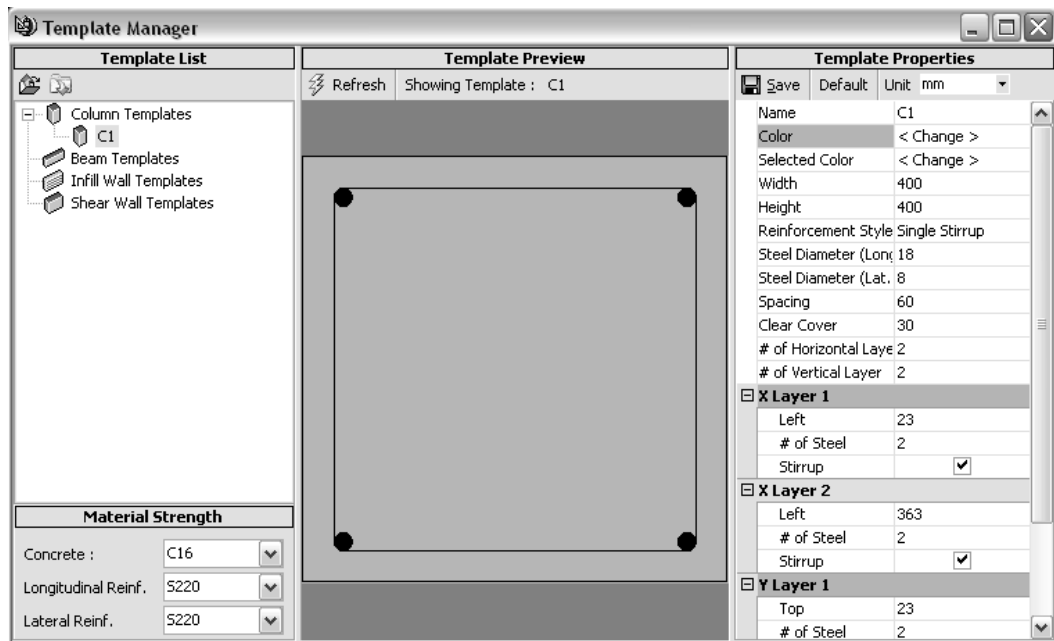**Figure A.5 –** Template Buttons

122

Figure A.6 – Template Manager

Reinforcement details are also required while defining new section. In case not knowing such details user can assign minimum amounts by clicking "default" button. Parameters related to material strength are also provided in the template. Same operations are done for each member type. Slabs are defined for each floor by clicking on empty areas formed by axes intersections after selecting "slab button".

Members can now be drawn on the interface using corresponding buttons on the left. After selecting any type of member its property is shown on the right. If no member is selected general project properties are listed. Axes are very flexible to use. Rotations and relative distances can be specified both by keyboard and mouse. Another important property is provided in "object list". Every single element can be reached from this menu. In addition to each element, floors can also be locked so that any change in the floor is not permitted. If building contains floors with same structural elements then there is a chance to copy complete floor to any destination floor which may save considerable time. Project of a typical

building can be finished in fifteen minutes. User does not need complete a project in single session. It can be saved at any time to be continued later.

As long as modeling is finished, the only thing that user must do is sending the project to the server for analysis. This is done by clicking "send" button located under "file" menu. Note that such process requires internet connection and takes few minutes depending on connection speed and project size. Project moves to "project in analysis" folder in communication tool. User may disconnect from internet at this time. Analysis report may be received at any time later by means of internet connection. "Send and receive" button is used in the communication tool for this purpose. Reports are then put in "analysis reports" folder and opened by double clicking.

Analysis report includes general information about building (building summary), properties of structural members, stiffness & mass properties of both frames and building. Member forces, floor displacements and overall building forces are also listed. Graphical representation is used to show member forces more comprehensibly. Parts of the analysis report are given in following figures.
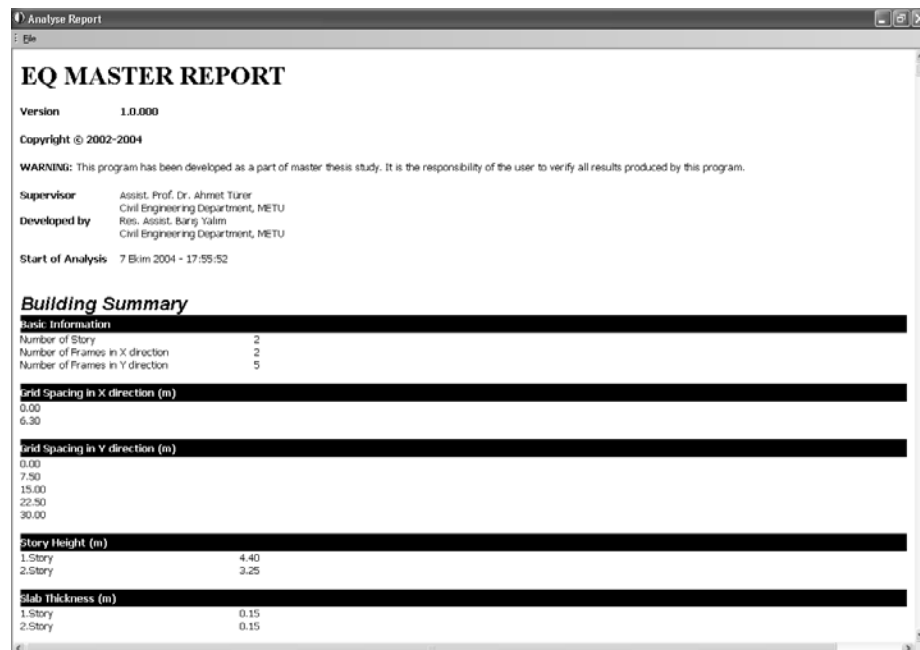

Figure A.7 –Analysis Report (Building Summary)

124

Analyse Report

Geometric Properties

Column Dimensions in X-Direction (m)

1.Story

| 0.4000 | 0.4000 | 0.4000 | 0.4000 | 0.4000 |
| 0.4000 | 0.4000 | 0.4000 | 0.4000 | 0.4000 |

2.Story

| 0.4000 | 0.4000 | 0.4000 | 0.4000 | 0.4000 |
| 0.4000 | 0.4000 | 0.4000 | 0.4000 | 0.4000 |

Column Dimensions in Y-Direction (m)

1.Story

| 0.4000 | 0.4000 | 0.4000 | 0.4000 | 0.4000 |
| 0.4000 | 0.4000 | 0.4000 | 0.4000 | 0.4000 |

2.Story

| 0.4000 | 0.4000 | 0.4000 | 0.4000 | 0.4000 |
| 0.4000 | 0.4000 | 0.4000 | 0.4000 | 0.4000 |

Moment of Inertia of Columns about X-Direction (m^4)

1.Story

| 2.1333e-003 | 2.1333e-003 | 2.1333e-003 | 2.1333e-003 | 2.1333e-003 |
| 2.1333e-003 | 2.1333e-003 | 2.1333e-003 | 2.1333e-003 | 2.1333e-003 |

2.Story

| 2.1333e-003 | 2.1333e-003 | 2.1333e-003 | 2.1333e-003 | 2.1333e-003 |
| 2.1333e-003 | 2.1333e-003 | 2.1333e-003 | 2.1333e-003 | 2.1333e-003 |

Moment of Inertia of Columns about Y-Direction (m^4)

1.Story

| 2.1333e-003 | 2.1333e-003 | 2.1333e-003 | 2.1333e-003 | 2.1333e-003 |
| 2.1333e-003 | 2.1333e-003 | 2.1333e-003 | 2.1333e-003 | 2.1333e-003 |

2.Story

| 2.1333e-003 | 2.1333e-003 | 2.1333e-003 | 2.1333e-003 | 2.1333e-003 |
| 2.1333e-003 | 2.1333e-003 | 2.1333e-003 | 2.1333e-003 | 2.1333e-003 |

Figure A.8 – Analysis Report (Geometric Properties)

Analyse Report

Depth of Beams in X-Direction (m)

1.Story

| 0.5500 | 0.5500 | 0.5500 | 0.5500 |
| 0.5500 | 0.5500 | 0.5500 | 0.5500 |

2.Story

| 0.5500 | 0.5500 | 0.5500 | 0.5500 |
| 0.5500 | 0.5500 | 0.5500 | 0.5500 |

Width of Beams in X-Direction (m)

1.Story

| 0.4000 | 0.4000 | 0.4000 | 0.4000 |
| 0.4000 | 0.4000 | 0.4000 | 0.4000 |

2.Story

| 0.4000 | 0.4000 | 0.4000 | 0.4000 |
| 0.4000 | 0.4000 | 0.4000 | 0.4000 |

Moment of Inertia of Beams in X-Direction (m^4)

1.Story

| 5.5458e-003 | 5.5458e-003 | 5.5458e-003 | 5.5458e-003 |
| 5.5458e-003 | 5.5458e-003 | 5.5458e-003 | 5.5458e-003 |

2.Story

| 5.5458e-003 | 5.5458e-003 | 5.5458e-003 | 5.5458e-003 |
| 5.5458e-003 | 5.5458e-003 | 5.5458e-003 | 5.5458e-003 |

Figure A.8 – Analysis Report (Geometric Properties, continued)

125

Depth of Beams in Y-Direction (m)

1.Story

0.6500	0.6500	0.6500	0.6500	0.6500

2.Story

0.6500	0.6500	0.6500	0.6500	0.6500

Width of Beams in Y-Direction (m)

1.Story

0.4000	0.4000	0.4000	0.4000	0.4000

2.Story

0.4000	0.4000	0.4000	0.4000	0.4000

Moment of Inertia of Beams in Y-Direction (m^4)

1.Story

9.1542e-003	9.1542e-003	9.1542e-003	9.1542e-003	9.1542e-003

2.Story

9.1542e-003	9.1542e-003	9.1542e-003	9.1542e-003	9.1542e-003

GridInfo

X-Coordinates of Grid Intersections

0.00	7.50	15.00	22.50	30.00
0.00	7.50	15.00	22.50	30.00

Y-Coordinates of Grid Intersections

0.00	0.00	0.00	0.00	0.00
6.30	6.30	6.30	6.30	6.30

Figure A.8 – Analysis Report (Geometric Properties, continued)

All results for beams and columns are arranged according to following style: Size of the matrices for columns is equal to number of axes in x & y directions in floor plan. For instance, the first element of any column matrix corresponds to column at upper left corner of that floor. Style for beams on the other hand are little different. They are grouped into two parts: beams defined in x-direction (parallel to x-axis) and beams defined in y-direction (parallel to y-axis). All matrices for beams in x-direction resemble those beam locations on the floor plan. Therefore, its row & column size is always equal to number of axes in x-direction and one less of number of axes in y-direction respectively. Similar style is valid for all matrices for beams in y-direction. In this case, size of the matrices is equal to one less of number of axes in x-direction by number of axes in y-direction.

Stiffness matrices for frames are obviously always symmetric and square (Figure A.9). Note that condensed forms are given so that size is n by n where n is the number of story.

Figure A.9 – Analysis Report (Frame Properties)

Mass and stiffness matrices for building are in same size (3n x 3n). Note that building mass matrix is always diagonal while building stiffness matrix is square and symmetric (Figure A.10).

Figure A.10 – Analysis Report (Mass & Stiffness Properties)

In addition to structural matrices, mass of each floor (translational & rotational), total building mass, mass and stiffness centers in both directions and corresponding eccentricities are also given. They are listed for each floor as shown in Figure A10.
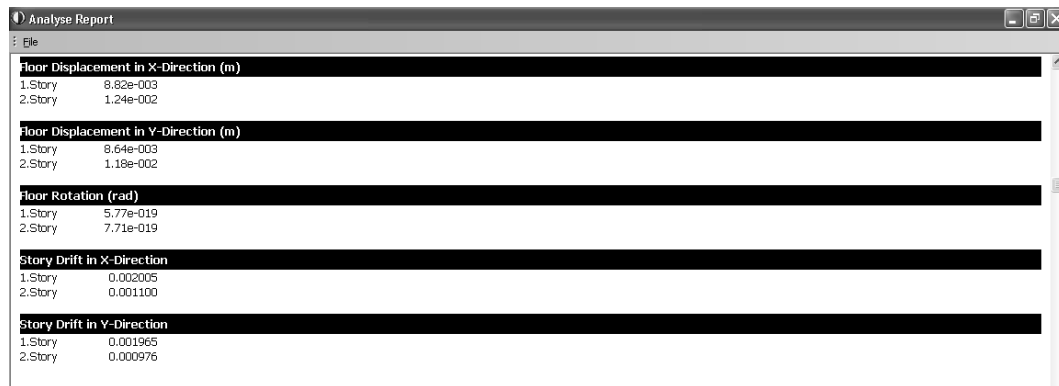
Figure A.10 – Analysis Report (Mass & Stiffness Properties, continued)

Maximum forces developed at each floor and at the base of building are shown in Figure A.11. Results from now on are based on analysis by EQMASTER.

Figure A.11 – Analysis Report (Story Forces & Base Reactions)

128

In addition to forces, floor displacements (translational and rotational) and story drifts are listed as shown in Figure A.12.
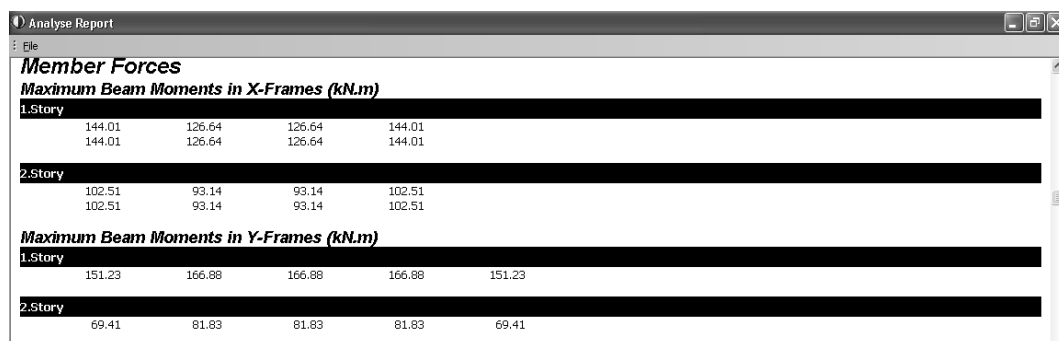
Figure A.12 – Analysis Report (Floor Displacements & Story Drifts)

Graphical representation is utilized to for member forces. Style for numerical results is exactly the same as those used for geometric properties (Figure A.13). Beam graphics are in the form of 3D plates located in floor plan. Interpolated color scale makes it much more efficient and user friendly. Shear and moment graphs of beams are shown separately for each floor. Due to large number of such graphs only those representing beam moments for the two floors are presented in Figure A.14 and Figure A.15.

Figure A.13 – Analysis Report (Numerical Representation of Member Forces, Beams)
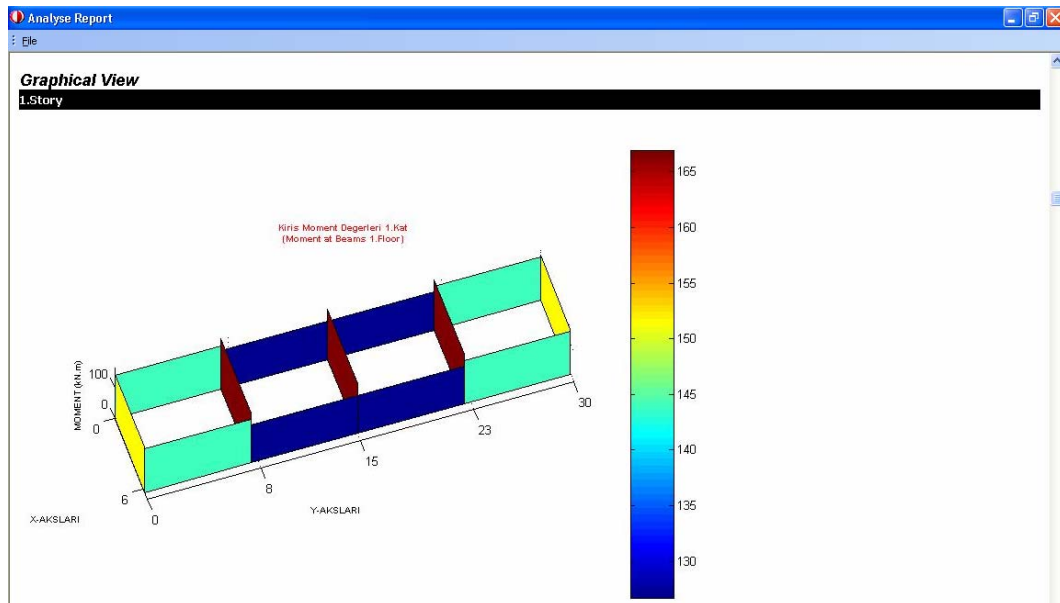
Figure A.14 – Analysis Report (Graphical View of Beam Moments, 1st floor)
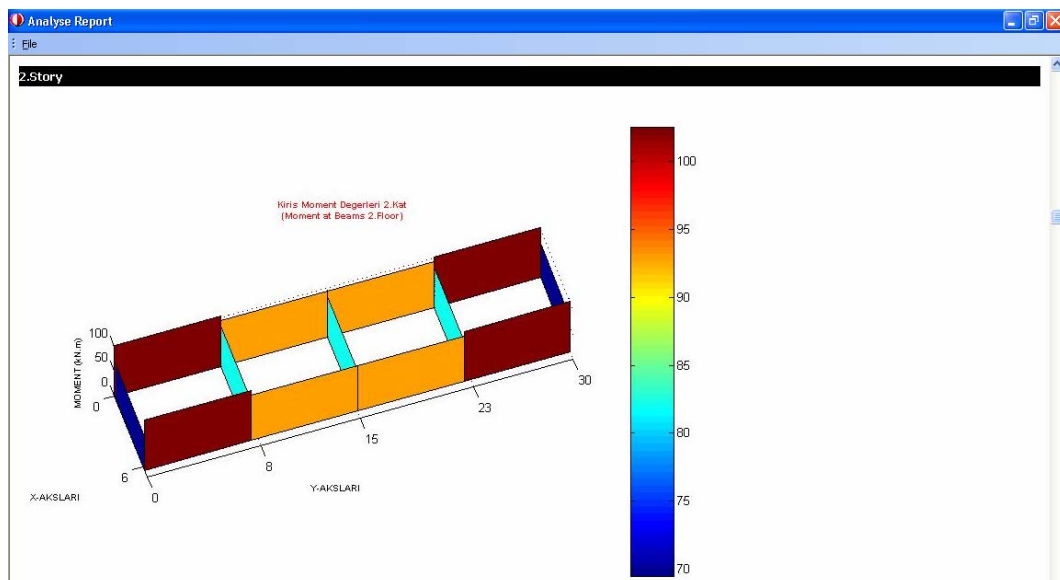
Figure A.15 - Analysis Report (Graphical View of Beam Moments, 2nd floor)

Visual style for columns, on the other hand, is based on 2D top view of floor plan. Distribution of column forces on the floor plan is symbolized using interpolated color scaling. Two selected graphs are shown in below.
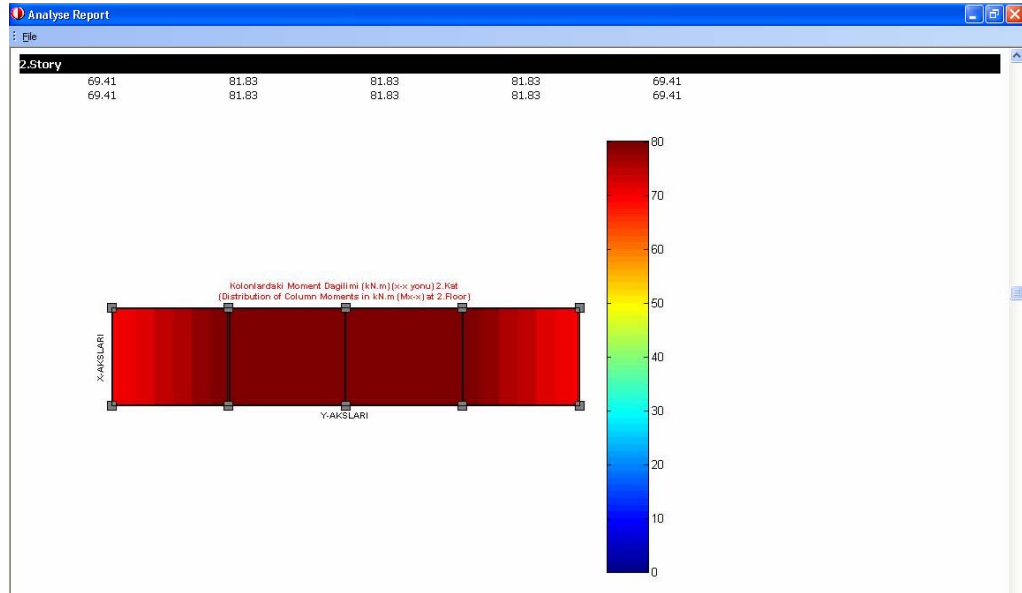
Figure A.16 - Analysis Report (Graphical View of Column Moments, 2nd floor)
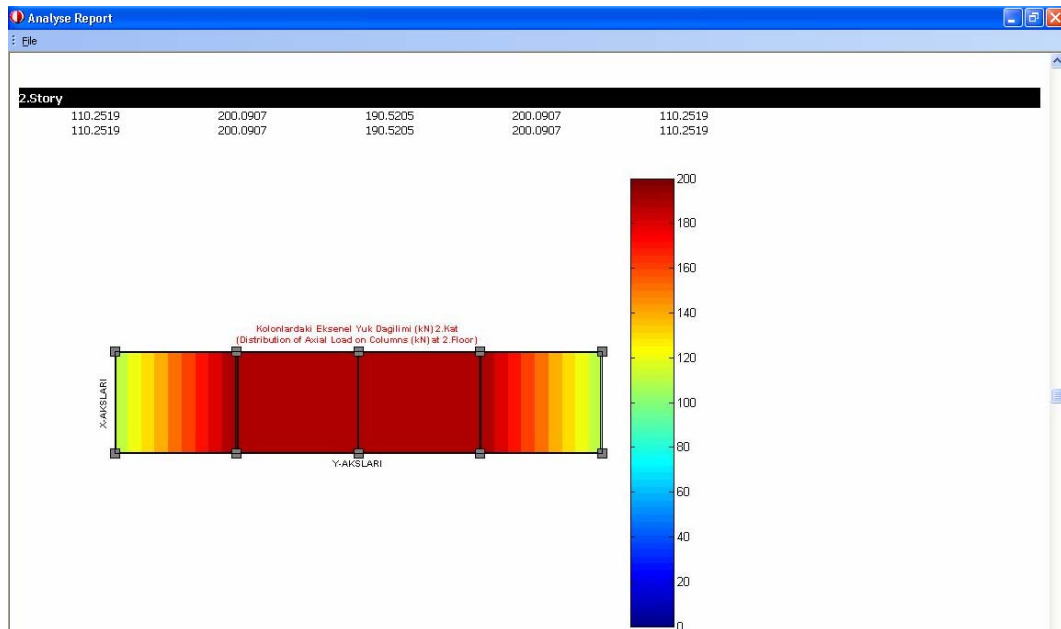
Figure A.17 - Analysis Report (Graphical View of Column Axial Load, 2nd floor)

Demand-capacity ratio for each member is given in the report as well. Same graphical styles as above are used for this purpose. Shear limits of columns are shown in 3D graphical format to observe any brittle failure (Figure A.18). Same format is employed for axial load limit for columns. Beams are also graphically illustrated whether they exceeded shear brittle limit or not.
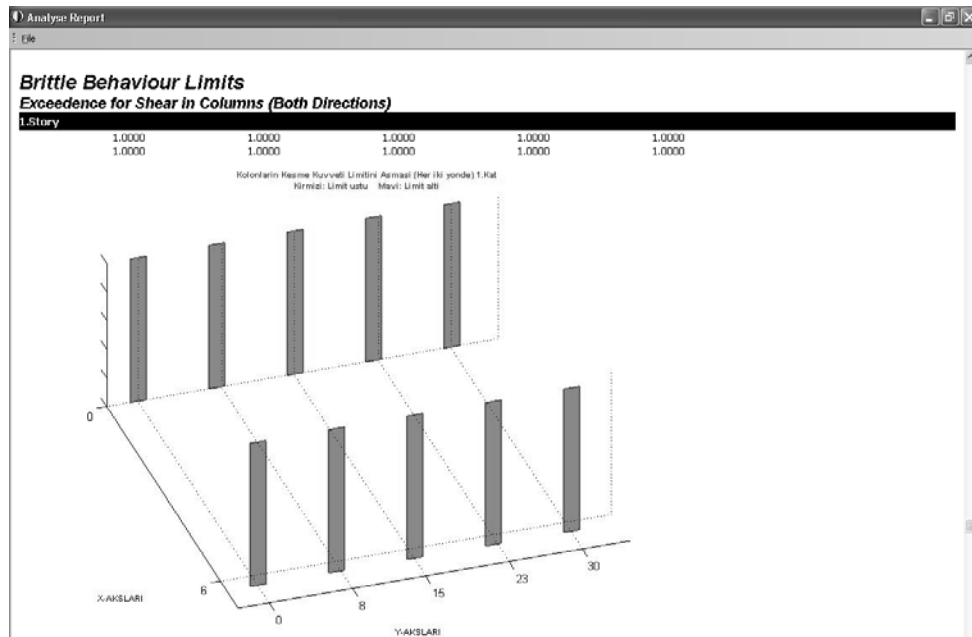
Figure A.18 – Analysis Report (Shear Brittle Behavior Limits for Columns, 1st floor)

Analysis result related with seismic vulnerability assessment is given as "Building Damage Score" in the report. Application of previous studies is listed together with proposed method (Figure A.19). Relevant graphics for previous methods are already given in chapter 4.
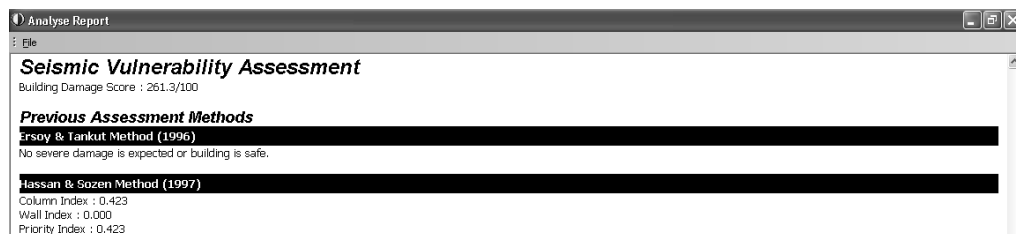
Figure A.19 – Analysis Report (Seismic Vulnerability Assessment**)**

Dynamic properties such as building vibration periods and corresponding modal shapes are presented at the end. Simple 3D animation is developed to simulate modal shapes. In this way, user has a chance to visualize building vibration rather than looking complicated numerical values. Animation speed and view angle is optional to user. Screen shot from the animation of the first mode is shown in Figure A.20.
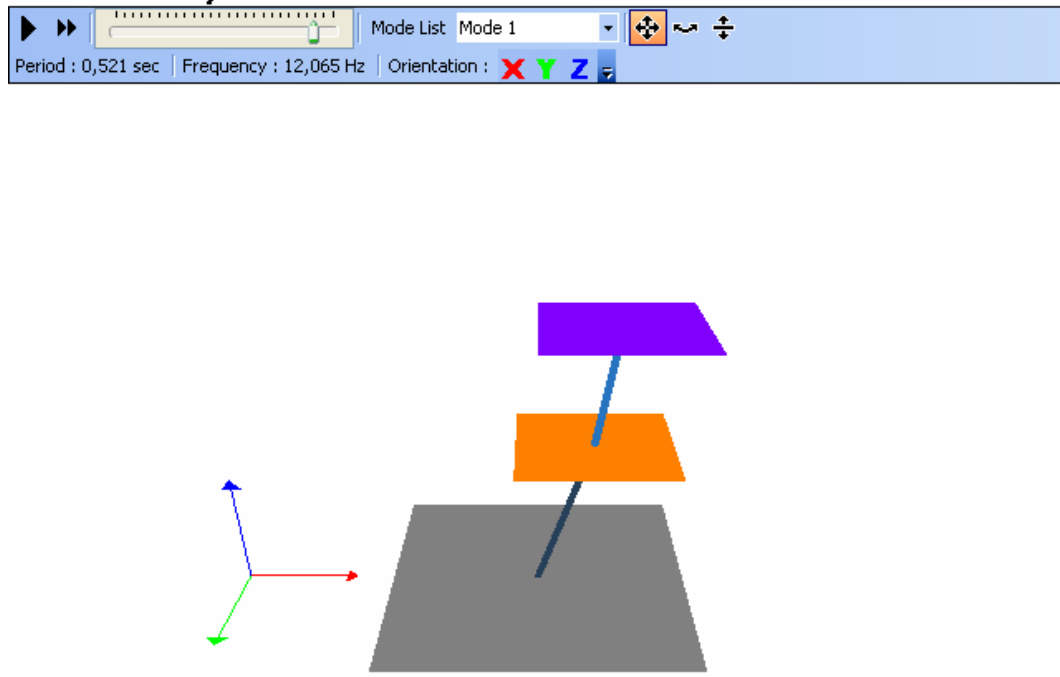
Figure A.20 – Analysis Report (Animation for Modal Shapes)

APPENDIX B

ALTERNATIVE SIMPLIFIED APPROACH

The second method (alternative approach) is quick assessment of the building based on responses to several questions. It is much more simple and straightforward compared to detailed approach. Working scheme on the internet platform is quite similar to detailed analysis in which user responses are obtained, evaluated, and sent back in the report format. All of these processes are performed on internet environment. User responses are recorded in a database.

Key part of the method is to prepare basic questions which can be easily replied by an average internet user in Turkey. Hence, difficulty appears while evaluating the query containing such simple questions. Questions are selected in such a way that they may give some clues about seismic condition of the building and reveal critical points to make quick earthquake vulnerability evaluation. Important parameters used in previous applications in quick assessment are also utilized. The questionnaire is given in the Appendix C.

The most important part of the method is the assessment of the form and assignment of building evaluation index. Method proposed by Sucuoglu and Yazgan [20] is utilized in determination of vulnerability scores for eight of the seventeen questions (number of story, earthquake zone, soft story, overhang, apparent concrete quality, short column, hammering effect, plan irregularity). Vulnerability scores for remaining questions are assigned as much smaller compared to those eight questions since effect of parameters in the remaining

questions on building vulnerability are not known. Both initial scores assigned for each zone according to peak ground velocity and corresponding vulnerability scores for eight parameters are scaled so that initial score always start from 100. Building evaluation index is reduced according to drawbacks of a building determined based upon user responses. Vulnerability scores after scaling of eight parameters from Sucuoglu and Yazgan [20] are shown in Table B.1. Vulnerability scores for the remaining parameters are shown in Table B.2.

Table B.1 – Initial and Vulnerability Scores for Eight Parameters

Story	Zone 1	Zone 2	Zone 3	Soft Story	Heavy Overhang	Apparent Concrete Quality	Short Column	Hammering Effect	Plan Irregularity
	60<PGV<80	40<PGV<60	20<PGV<40						
1,2	95	130	170	0	-5	-5	-5	0	0
3	90	125	160	-10	-5	-10	-5	-2	-2
4	90	115	145	-10	-10	-10	-5	-3	-2
5	90	105	130	-15	-15	-15	-5	-3	-5
6,7	80	90	105	-20	-15	-15	-5	-3	-5

After Scaling of Initial Score to 100									
Story	Zone 1	Zone 2	Zone 3	Zone 4	Soft Story	Heavy Overhang	Apparent Concrete Quality	Short Column	Hammering Effect	Plan Irregularity
1,2	44,2	60,5	79,1	100,0	0,0	-2,3	-2,3	-2,3	0,0	0,0
3	41,9	58,1	74,4	90,7	-4,7	-2,3	-4,7	-2,3	-0,9	-0,9
4	41,9	53,5	67,4	83,7	-7,0	-4,7	-4,7	-2,3	-1,4	-0,9
5	41,9	48,8	60,5	76,7	-7,0	-7,0	-7,0	-2,3	-1,4	-2,3
6,7	37,2	41,9	48,8	58,1	-9,3	-7,0	-7,0	-2,3	-1,4	-2,3

Vulnerability Parameters
Soft Story: No (0); Yes (1)
Heavy Overhangs: No (0); Yes (1)
Apparent Concrete Quality: Good (0); Moderate (1); Poor (2)
Short Column: No (0); Yes (1)
Hammering Effect: No (0); Yes (1)
Plan Irregularity: No (0); Yes (1)

Table B.2 – Vulnerability Scores for the Remaining Nine Parameters

Parameter	Evaluation	Option 1	Option 2	Option 3	Option 4	Option 5
Date of construction (doc)	if $doc < 1975 \rightarrow -1$ if $1975 \leq doc \leq 1998 \rightarrow -0.5$ if $doc \geq 1999 \rightarrow 0$	NA	NA	NA	NA	NA
Vertical Discontinuity (vd)		0	-1	NA	NA	NA
Soil Type (st)		0	-0,5	-0,8	-1	NA
Basement (b)		0	0	-0,3	-0,6	-1
Ground inclination (gi)		0	-0,3	-0,8	NA	NA
Window size (ws)		0	-0,2	-0,5	NA	NA
Mezzanine (m)		0	-1	NA	NA	NA
Strong Beam - Weak Column (sb-wc)		0	-1	NA	NA	NA

It should be noted that output of the method should be as understandable as possible. User is preferred to get useful information in order to relate his building with earthquake concepts which are currently very popular in Turkey. On the other hand, giving a reliable building evaluation index requires a large database consisting of all necessary information applicable to questionnaire. Therefore, at this stage, it is better to provide user report mainly for educational purposes.

Index criterion in date of construction depends on the release date of the code at that time. The worst case is assigned to those constructed before 1975 since they are potentially out of date in terms of current construction requirements. Building is additionally punished based on its seismic zone. The highest decline is assigned to ones located in the first zone.

In some buildings, the first story is relatively higher than others due to commercial use of that floor. This may cause building to behave like an elevated mass and makes the first storey columns more vulnerable. Ratio of the first story height to typical story height is used to reduce building evaluation index for this purpose. In addition, when lateral stiffness provided by the vertical members at any particular floor is appreciably less than the upper or lower neighboring floor, then that story acts as a "soft story". Although such defect may exist in any floor, ground floor is the most possible location. Building is given negative points based on the number of sides surrounded mainly by windows.

Beside structural configuration, architectural properties of buildings are effective in earthquake resistance if not properly designed. Unsymmetrical floor plans strengthen torsional effect on columns. Sudden changes in stiffness throughout the elevation or in the plan significantly modify lateral load distribution on the building. Evaluation index of the building is decreased considering above conditions. In case the area of the ground floor is considerably smaller than that of typical floors, earthquake resistance of structural members on these floors is affected. Elevated masses such as heavy balconies are among main problems.

Expected damage of the building is related with overhang values in four directions.

Hammering of two neighboring buildings may produce additional structural damage. Column collapse is also possible if the neighbouring building slabs are not at the same elevation and hammers against columns. Negative points are given based on these criteria.

Apparent concrete quality may be considered as one of the significant factors in building vulnerability. Despite properly selected cross-sections of load carrying members, local or total failures may be observed due to poor concrete quality.

Existence of "short column" in a building may lead to brittle shear failure of such columns and should also be taken into account.

"Strong beam – weak column" concept may be another parameter for building vulnerability. Failure of columns lead direct failure of a building, while prior failure of beams would still keep the building standing while adding additional damping and ductility. The columns should be designed stronger than beams for a preferred earthquake response. Evaluation index of the building is reduced based on whether such defect exists in the building or not.

Other helpful parameters in assigning building evaluation index are soil type, ground water level, ground inclination, window sizes, and existence of mezzanine. These are detailed questions and may have relatively small contribution to building evaluation index. Some of them may be removed if a database study is carried out. Older version of the vulnerability scores for each of the seventeen questions is shown in Table B.3. Different questions have different number of options; therefore, the irrelevant options are shown as "NA" for some questions. The remaining point from 100 after all questions is equal to the evaluation index for the building. Explanations of options can be seen in the questionnaire given in Appendix C.

Table B.3 – Old Evaluation Method (abandoned)

Question #	Explanation	Evaluation	Option 1	Option 2	Option 3	Option 4	Option 5
User Info. 2							
1	Seismic zone (sz)	$-2(4-sz)$	NA	NA	NA	NA	NA
2	Number of story (n)	$if\ n\le4 \to 0$ $if\ n\ge5 \to -2(n-4)$	NA	NA	NA	NA	NA
3	Date of construction (doc)	$if\ doc<1975 \to -4$ $if\ 1975\le doc\le1998 \to -2$ $if\ doc\ge1999 \to 0$	NA	NA	NA	NA	NA
4	First story height (h1)	$if\ \dfrac{h1}{ht} >1.2 \to 15\left(\dfrac{h1}{ht}-1.2\right)$	NA	NA	NA	NA	NA
5	Typical story height (ht)	$if\ \dfrac{h1}{ht} \le1.2 \to 0$	NA	NA	NA	NA	NA
5	Building Geometry (bg)		0	-2	-2	-2	-2
6	Vertical Discontinuity (vd)		0	-5	NA	NA	NA
7	Soil Type (st)		0	-3	-6	-10	NA
8	Basement (b)		0	0	-1	-2	-4
9	Ground inclination (gi)		0	-1	-3	NA	NA
10	Window size (ws)		0	-1	-3	NA	NA
11	Mezzanine (m)		0	-4	NA	NA	NA
12	Soft story (ss)		0	-2	-3	-5	-5
13	Apparent Concrete Quality (qc)		0	-3	-6	NA	NA
14	Short Column (sc)		0	-4	NA	NA	NA
15	Strong Beam - Weak Column (sb-wc)		0	-4	NA	NA	NA
16	Overhang in four directions (o_1, o_2, o_3, o_4)	$\displaystyle\sum_{i=1}^{4} -o_i$	NA	NA	NA	NA	NA
17	Hammering effect in three directions & Floor level $(h_1,h_2,h_3,fl_1,fl_2,fl_3)$	$\displaystyle\sum_{i=1}^{3} -h_i\left(2fl_i+1\right)$	NA	NA	NA	NA	NA

Application of Approach 2 on Düzce Damage Database

The same buildings analyzed in the first approach are also utilized for the simplified case to observe the relation between damage level and building evaluation index. However, the Düzce damage database does not include information for all of the questions asked in the simple approach. Therefore, only a subset of questions is answered, while keeping the answers to other questions constant. For instance, soil type is taken as Z1 [16] and window size is chosen as medium for all buildings. "Short column" and "strong beam – weak column" existence is discarded. The answers to the answered questions are also generally similar for a vast majority of the buildings causing a small variation in the building evaluation index. Table B.4 shows damage levels and corresponding evaluation indexes of the buildings.

Table B.4 – Evaluation Indices of the Buildings from Düzce Database

ID	Time of Construction	# of Stories	A1	A2	A3	A4	B1	B2	B3	Damage in R/C members	*MNLSTFI*	*OR*	*Building Evaluation Index*
E-A-4	1975	3	1	2	2	2	2	2	2	L	0,0580	0,1160	35,7
E-G-20	1987	3	2	2	2	2	2	1	2	L	0,0660	0,0000	20,0
E-NB-146	1980	3	2	2	2	2	2	2	2	L	0,0563	0,0461	34,6
A-20-EKS-36	1985	4	2	2	2	2	2	2	2	L	0,1215	0,0750	33,7
E-G-3	1974	4	2	2	2	2	2	1	2	L	0,0189	0,0000	24,7
E-J-30	1990	4	2	2	2	2	1	1	2	L	0,0579	0,1178	29,0
A-38-EKS-60	1990	5	2	2	2	2	2	1	2	L	0,0466	0,0864	25,3
A-9-EKS-19	1995	5	2	2	2	2	2	1	2	L	0,1239	0,1059	26,7
E-G-17	1992	5	2	1	2	2	2	1	2	L	0,0367	0,0000	17,7
C-B10-144	1988	3	2	2	2	2	2	2	2	M	0,0171	0,0000	36,0
C-B20-237	1982	3	2	2	2	2	2	1	2	M	0,1745	0,0909	29,0
M-EKS-36	1990	3	1	2	2	2	2	2	2	M	0,0940	0,0659	36,0
A-5-EKS-41	1989	4	2	2	2	2	2	2	2	M	0,1997	0,1732	32,3
A-5-EKS-42	1989	4	2	2	2	2	2	2	2	M	0,2664	0,0553	32,3
E-NB-127	1980	4	2	2	2	2	2	1	2	M	0,0699	0,0000	27,6
A-55-EKS-97	1984	5	2	1	2	2	2	1	2	M	0,0787	0,0000	24,7
I-E-32	1980	5	2	2	2	2	2	2	2	M	0,0675	0,1110	32,3
M-7-EKS-11	1985	5	1	2	2	2	2	1	2	M	0,0468	0,1145	18,3
C-B6-101	1995	3	2	2	2	1	2	2	2	N	0,0749	0,0702	35,1
I-A-2	1950	3	2	2	2	2	2	1	2	N	0,0181	0,0000	27,8
I-F-44	1975	3	2	2	2	2	2	2	2	N	0,1316	0,0908	34,3
C-B21-38	1982	4	1	2	2	1	2	1	2	N	0,0764	0,0393	24,4
C-B4-88	1979	4	1	2	2	2	2	1	2	N	0,0738	0,0884	28,1
I-C-21	1976	4	2	2	2	2	2	1	2	N	0,0356	0,0000	25,0
C-B21-37	1989	5	2	2	2	1	2	1	2	N	0,0857	0,0848	17,4
I-E-33	1985	5	2	2	2	2	2	2	2	N	0,1187	0,0000	25,3
I-E-35	1993	5	2	2	2	1	1	1	2	N	0,1610	0,1884	15,5
C-B1-1	1988	3	1	2	1	1	2	1	2	S	0,0631	0,3489	26,2
E-I-42	1980	3	2	2	2	2	2	1	2	S	0,0648	0,0000	28,7
G-C-40	1983	3	2	2	2	2	2	2	2	S	0,1628	0,0452	34,6
E-G-14	1980	4	2	2	2	2	2	1	2	S	0,0711	0,1105	19,7
E-G-19	1976	4	2	2	2	2	2	1	2	S	0,0293	0,0331	27,6
E-NB-106	1975	4	2	2	2	1	2	1	2	S	0,0421	0,0435	27,8
E-G-13	1980	5	2	2	1	2	2	1	1	S	0,0378	0,0000	16,0
E-K-39	1985	5	1	2	2	2	2	1	2	S	0,0673	0,1148	34,6
M-7-EKS-10	1985	5	1	2	2	2	2	1	2	S	0,1385	0,0469	27,6

Irregularities 1: Exist 2: Not Exist

Correlation between building evaluation index and damage level can be better observed if a suitable database is prepared to serve the questionnaire. Thus, simplified method, at this stage may be useful in terms of only giving general information and creating public more conscious about future earthquakes.

APPENDIX C

QUESTIONNAIRE FORM & REPORT

User Information 1

E-Posta Adresiniz	

User Information 2

Adresiniz

Şehir ADANA ▼   **Posta Kodu** (06610 gibi)

Question 1

Toplam Kat Sayısı (bodrum dahil)

Question 2

**Binanın İnşaat Tarihi** yıl (örnek: 1997)

Question 3

Giriş Kat Yüksekliği metre (Ondalık sayı girmek için virgül kullanınız)

Question 4

Tipik Kat Yüksekliği metre (Ondalık sayı girmek için virgül kullanınız)

Question 5

	Dikdörtgen	L Bina	3 Blok	Yamuk	Diğer
Binanın Şekli	☐	☐	☐	☐	☐

a	[ ]	metre (Ondalık sayı girmek için virgül kullanınız)
b	[ ]	metre (Ondalık sayı girmek için virgül kullanınız)

a ve b değerleri sadece dikdörtgen şeklindeki binalar için geçerlidir.

Question 6

Bina Düzeni	**Her katın şekli aynı mı? (Binada düzensizlik var mı?) Örneğin, ilk üç kattan sonra geniş bir teras ve devam eden daha küçük alanlı (birden fazla) katlar, bir katın toplam alanının %20'sinden büyük döşemede boşluklar, ani değişen kolon boyutları gibi...**
	☐ Evet, her katın şekli aynı (Binada düzensizlik yok)
	☐ Hayır, her katın şekli aynı değil (Binada düzensizlik var)

Question 7

Zemin Türü	☐ Çok sıkı kum, çakıl, sert kil ve siltli kil (Z1)
	☐ Sıkı kum, çakıl, çok katı kil ve siltli kil (Z2)
	☐ Orta sıkı kum, çakıl, katı kil ve siltli kil (Z3)
	☐ Gevşek kum, Yumuşak kil, siltli kil (Z4)

Question 8

Bodrum	**Bodrum katta su problemi var mı?**
	☐ Bodrum yok
	☐ Tümüyle kuru
	☐ Duvarlar nemli ve küflü
	☐ Hafif seviyede su sızıntısı var
	☐ Bodrum su doluyor veya pompa ile su sürekli boşaltılıyor

Question 9

	Binanın bulunduğu arazinin eğimi,
Arazi Bilgileri	⬚ Düze yakın ⬚ Hafif eğimli ⬚ Dik eğimli (yamaç gibi)

Question 10

	Pencerelerin büyüklüğü,
Pencereler	⬚ Küçük ⬚ Orta ⬚ Büyük

Question 11

Asma Kat	⬚ Asma kat yok ⬚ Asma kat var

Question 12

	Giriş katın kaç yüzü camekan ağırlıklı,
Giriş Kat	⬚ Giriş kat mesken, camlar normal ⬚ Giriş katın ön cephesi dükkan/camekan ağırlıklı ⬚ Giriş ve yan cephe dikkan/camekan ⬚ Üç cephe camekan ⬚ Dört cephe camekan

Question 13

	Gözle görülür beton kalitesi,
Beton Kalitesi	○ İyi ○ Orta ○ Kötü

Question 14

Kısa Kolon	○ Kısa kolon yok ○ Kısa kolon var
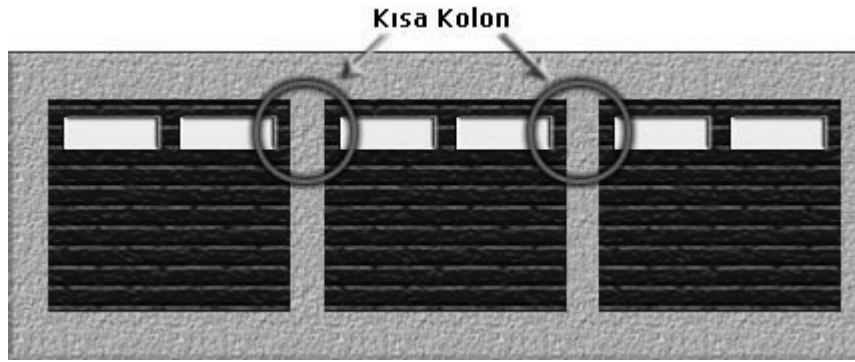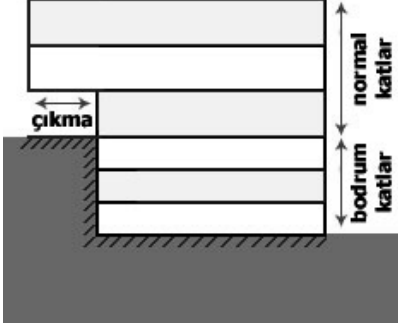
Question 15

Kuvvetli Kiriş - Zayıf Kolon	○ Kuvvetli Kiriş - Zayıf Kolon yok ○ Kuvvetli Kiriş - Zayıf Kolon var

Kolonlar kirişlerden daha kalın ve kuvvetli
"Zayıf kolon - kuvvetli kiriş" yok

Kolonlar kirişler daha zayıf
"Zayıf kolon - kuvvetli kiriş" var
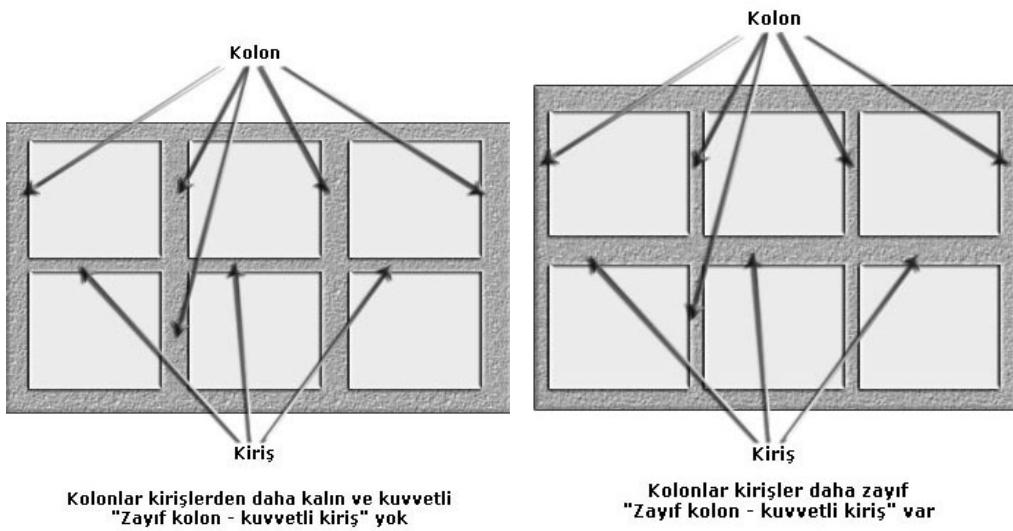
Question 16

Bina Yapısı

Bodrum Kat Sayısı		
Normal Kat Sayısı		Resimde görüldüğü gibi
Ön Cephenin Çıkması		metre (Ondalık sayı girmek için virgül kullanınız)
Arka Cephenin Çıkması		metre (Ondalık sayı girmek için virgül kullanınız)
Sağ Cephenin Çıkması		metre (Ondalık sayı girmek için virgül kullanınız)
Sol Cephenin Çıkması		metre (Ondalık sayı girmek için virgül kullanınız)

Question 17

	Yapışık bina var mı?		
	Yön	**Var**	**Kat Seviyeleri Aynı**
Yapışık Bina	Sol taraf	☐	☐
	Sağ taraf	☐	☐
	Arka taraf	☐	☐

Analiz Et   Sıfırla

Figure B.1 – Questionnaire Form

Analysis report based on filling out above form is immediately shown on the screen by pressing "analyze" button. Before getting report, user is warned if there are any missing or incorrect entries. User must be connected to the internet to fill the form and obtain report. Analysis report consists of building summary and general explanations according to response to each question. Earthquake zone map of the province is also included. Educational comments are added. Score reduction due to each question and resulting building evaluation index is given. Sample report for K7 building is shown below.

Basit Analiz Raporu

Size sunulan bu rapor bir deprem emniyet değerlendirmesi değildir. Amerikan FEMA-154 ve ATC-21 kodlarından faydalanılarak Düzce depremi bina hasarları için Prof. Dr. Haluk Sucuoğlu tarafından kalibre edilen metod ve tekniklerden esinlenerek elde edilmiş bu puanlama binalar için bir ön eleme niteliği taşımaktadır. Yaklaşımın basitliği ve parametrelerin yetersizliği sebebiyle güvenilirliği düşüktür. Elde edilen puan, binanın deprem performansını göstermez fakat göreceli, yaklaşık bir fikir verir. Verilerin tecrübeli inşaat mühendisleri tarafından girilmemiş olabilmesi ve soruların herkesin cevaplayabileceği kadar basitleştirilmesi ihtiyacı ise ek belirsizlikler getirmektedir. Basit soruları cevaplayarak oluşturulmuş bu rapor, akademik çalışma ve eğitim amaçlıdır. Başka bir amaç için kullanılamaz. Ücretsiz sunulan rapor, kullanıcının sorumluluğundadır ve üniversite ile çalışanlarını bağlayamaz.

Başlangıç Skorunuz	100

Girilen Bilgiler		**Puan**
Bulunduğunuz İl ve İlçe	Ankara - Çankaya	
Deprem Bölgesi	4	
Bina İnşaat Tarihi	2000	0
Bina Kat Sayısı	2	
Giriş Kat Yüksekliği	4,4 metre	
Tipik Kat Yüksekliği	3,25 metre	

146

Zemin Tipi	Çok sıkı kum, çakıl, sert kil ve siltli kil (Z1)	0
Zayıf Kat	Yok (Giriş kat mesken)	0
Bitişik Bina Sayısı	0	0
Çıkma Sayısı	0	0
Bina Geometrisi	Dikdörtgen	0
Binada Düzensizlik	Yok	0
Pencereler	Orta	-0,2
Asma Kat	Yok	0
Bodrum	Yok	0
Arazi Eğimi	Düze yakın	0
Beton Kalitesi	Orta	-2,3
Kısa Kolon	Yok	0
Kuvvetli Kiriş-Zayıf Kolon	Var	-0,5

Değerlendirme	
Bina Değerlendirme Puanı	**97 / 100**

Lütfen açıklamaları okuyunuz.

Açıklamalar

Sert zeminlerde ve çok yüksek olmayan binalarda deprem dalgaları yumuşak ve dolgu zeminlerde olduğu gibi fazla büyümez ve binalar bazı dizayn ve inşaat hatalarını tolere edebilir. Hem zeminin kuvvetli olması hem de kat sayısının az olmasına rağmen kolon - kiriş boyutları, donatı miktarı, beton kalitesi, etriye sıklaştırması yapılması, ankraj boyu ve bükülme şekli, temel tipi, bağ kirişi, perde duvarların varlığı, düzenli çerçeve sisteminin bulunması, zayıf kat ve düzensizlikler olası depremde oluşacak hasarın büyüklüğünü doğrudan etkileyecek önemli faktörlerdir. Bunlara ek olarak, yapınızın bulunduğu bölgenin hangi deprem bölgesi olduğu ve aktif faylara uzaklığı da çok önemlidir.

Binanızın bulunduğu ilin Türkiye Deprem Bölgeleri Haritası'na göre ağırlıklı olarak 4. derece deprem bölgesi olduğu görülmektedir. Deprem bölgeleri 1 ile 4 arasında

değişmektedir ve 1. derece en yüksek riske sahip bölgedir. Bu risk 4. bölgeye doğru azalmaktadır. Deprem bölgeleri haritası bölgenin fay hatlarına olan uzaklığı ve geçmiş deprem kayıtları göz önüne alınarak oluşturulmuştur. Bulunduğunuz ilin detaylı deprem haritası aşağıda verilmektedir.
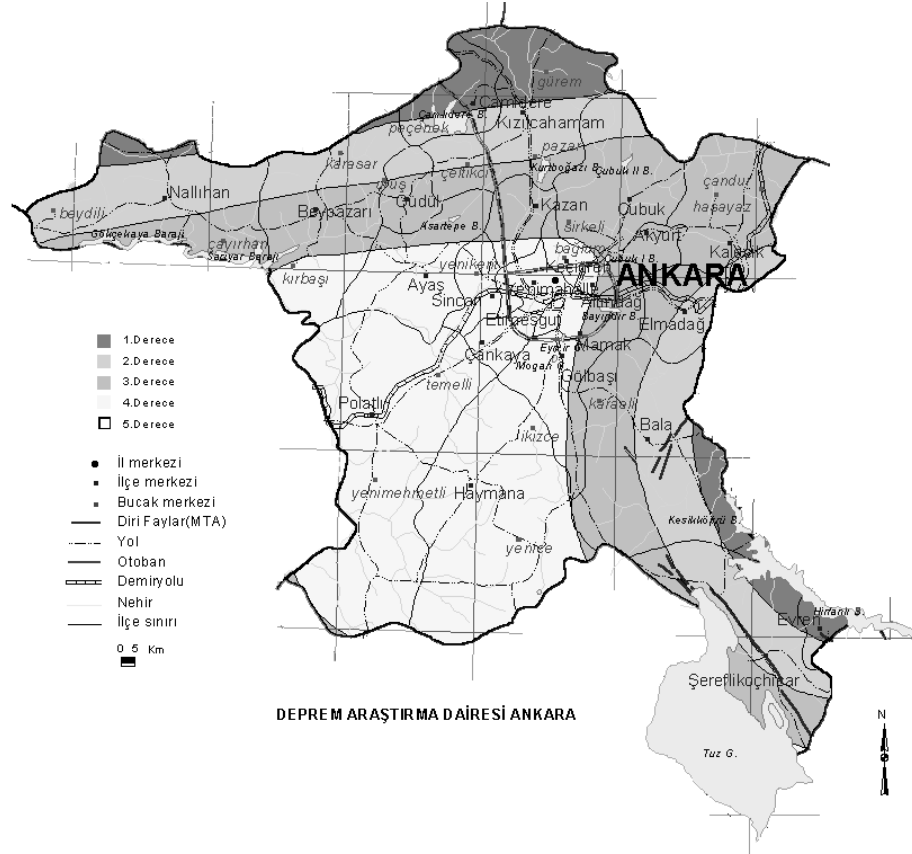
Binanızın projesi 1998 deprem yönetmeliğinden sonra yapılmıştır. Bu yönetmelik öncekilere göre olası depremlere karşı daha güvenli inşaat ve tasarım uygulamaları içermektedir. Fakat bu durumda binanızın tasarımı ve inşaatının yönetmeliğe uygun olarak yapılıp yapılmadığı önem taşımaktadır. Daha geniş bilgi alabilmek için ana sayfa altından 'Detaylı' kısmı tıklanarak indirilecek program kullanılabilir.

Cadde kenarlarında bitişik düzen bina yapılması oldukça yaygındır. Deprem sırasında yapışık düzen binalar, farklı hareket ederek birbirlerine çarparak 'çekiçleme etkisi' yaparlar. Bu binaların depremde yıkılmalarını kolaylaştıran bir etkendir. Yapışık binaların kat seviyelerinin farklı olması durumunda bu etki daha kötü olur: farklı seviyedeki kat döşemeleri diğer binanın kolonlarına çarpar ve ağır hasar görmelerine sebep olur. Binanıza bitişik ayrı bir bina bulunmamaktadır ve çekiçleme etkisi yoktur.

148

Binanın yapısal özellikleri yanında mimari tasarımı da depreme karşı dayanımında büyük önem taşır. Örneğin, simetrik bir yapıya sahip olmayan ve yükseklik boyunca kat planında değişimler (büyüme) görülen binaların depremden daha fazla etkilenmesi beklenir. Bu tür binaların özellikle kolonlarına ek yük gelmesinden dolayı deprem yüklerinin güvenli olarak taşınması zorlaşır. Ayrıca, taşıyıcı sistemin mimari nedenlerden dolayı süreksiz olması (kat alanı boyunca kiriş ve kolonların devam etmemesi) binanın deprem dayanımını olumsuz etkilemektedir. Özellikle Türkiye'de depremlerden sonra görülen hasarların nedenleri arasında bu tür kusurlar gözlemlenmektedir. Unutmamalıdır ki, bu tip olumsuz özellikler binanın deprem dayanımında tek başına etkili değildir. Binanızın geometrisi genel olarak simetrinin en çok ve düzensizliğin en az görüldüğü şekle sahiptir. Bunun yanında tüm kat planlarının aynı olması (ya da birbirine yakın olması) yukarıda sayılan olumsuzlukları ortadan kaldırmaktadır. Bu durum deprem yüklerinin taşıyıcı elemanlara mümkün olduğunca düzgün olarak dağılmasını sağlar.

Betonarme ve dolgu duvarlara karşın pencereler, büyüklüklerine ve bulundukları yere göre binanın deprem dayanımını azaltıcı etken olarak görülebilir. Yine büyüklüklerine bağlı olarak bulundukları katın diğer katlara göre daha zayıf olmasına ve deprem yüklerinin bu bölgede toplanmasına yol açarlar. Dış cephenin camekan ağırlıklı olması (veya büyük pencere alanları bulunması), bulunduğu katın diğerlerine göre daha zayıf olmasına neden olur. Duvarlarda bırakılan pencere boşluklarının dar ve sürekli bir bant halinde olması ise 'kısa kolon' olarak isimlendirilen bir sakınca oluşturur. Kısa kolon ile ilgili detaylı anlatım aşağıda verilmektedir.

Pratikte asma kat kullanımı binaların birinci katı üzerinde görülür ve genelde işyerleri tarafından kullanılır. Fakat bu katın tüm kat alanını kaplamaması ve dolayısıyla o kattaki kolonlara hesapta olmayan ek yük getirmesi sebebiyle tercih edilmemelidir. Binanızda asma kat yoktur.

Giriş kat alanının diğer tipik katlarınkinden büyük ölçüde küçük olması durumu (çıkma), özellikle giriş katındaki kolonlara ek yük bindirir. Genellikle ağır balkonlar ve döşemelerin giriş katından sonra uzatılması binada çıkma yaratmaktadır. Çıkma uzunluğunun bina uzunluğuna göre fazla olması deprem etkilerinin diğer binalara göre daha çok hissedilmesini sağlar. Dolayısıyla bu durumdan mümkün oldukça kaçınılmalıdır. Binanızda herhangi bir yönde çıkma bulunmamaktadır. Pratikte önerilen en ideal durumdur.

Bodrum katta su probleminin olması yeraltı su seviyesinin (su tablası) yüzeye yakın olduğunun göstergesi olabilir. Yüksek su tablası bulunan bölgelerde, sırf kum, siltli kum

veya kumlu siltten oluşan suya doygun zeminler deprem sırasında yükselen boşluk basıncı sebebiyle sıvılaşabilir. Böyle zeminlerde deprem sırasında zemin sıvılaşarak binada büyük oturmalar, yan dönmeler, vb. hareketler görülebilir. 1999 Marmara depremlerinde bu duruma özellikle deniz veya dere kenarındaki binalarda sık rastlanmıştır. Bu depremlerde binada hasar olmamasına rağmen denizin içine girmiş veya olduğu yerde yan yatmış binalar sıvılaşma etkisinin bir sonucudur. Bodrum katta görülen su miktarı sıvılaşmanın olup olmayacağı konusunda kesin bir yargı getirmemekle beraber bu konuda bir parametre olarak kullanılabilir. Binanızın bodrum katında su problemi görünmüyor. Bu durum bodrum katınızda iyi derecede su izolasyonu olduğunu ya da su tablasının düşük olduğunu gösterir.

Binanın oturduğu zeminin yanı sıra bulunduğu arazinin eğimi de depreme karşı bina tasarımında etkili bir faktördür. Yumuşak zeminli dik yamaçlara inşa edilen binalarda zemin kayma riski vardır. Diğer yandan düz veya düze yakın araziye yapılmış binalarda zemin kayma riski minimumdur. Daha genel bakılacak olursa, zemin tipine, arazi eğimine ve zemin suyu seviyesine bağlı olarak olası depremde oluşacak zemin kayması riski değişmektedir. Binanız düze yakın bir arazide bulunmaktadır. Zemin kayması ihtimali düşüktür.

Binaların deprem davranışını etkileyen faktörlerden birisi beton kalitesidir. Beton kalitesi genellikle 'schmit hammer' denilen el büyüklüğünde bir cihaz vasıtası ile yüzeysel olarak ya da 10cm çapında 15-20 cm boyunda silindirik çekirdek (karot) numunesi alıp laboratuvarda test ederek öğrenilir. Bu teknik ve cihazların bulunmadığı durumlarda üzerinde sıva boya olmayan, açık olarak görülen beton kısımlara bakarak genel olarak betonun kalitesi hakkında fikir sahibi olunabilir. Ölçüme dayalı olmayan bu gözlem, kişinin tecrübesi ve görebildiği beton yüzeyi ile sınırlıdır ve kişiye özeldir (subjektiftir). Beton yüzeyinde görülen iri boşluklar betonun iyi yerleşemediğinin göstergesidir. İri taşlar genellikle kötü kaliteye işarettir. Donatının (demirlerin) beton yüzeyine yakın olarak görülebilmesi, donatının bir kısmının açıkta kalarak gözle görülebilmesi kötü işçilik ve/ya kötü betonarme göstergeleridir. Sulanmamış ve yanmış beton ile donmuş beton ya yüzeyde ufalanır ya da köşelerden elle kopartılabilir. Betonun hazır alınmış olması ya da inşaat sahasında imal edilmiş olması, inşaat tarihi, kullanılan agrega ve kum (kontollü kırma taş genellikle deniz-dere yatağı kumuna tercih edilir. kullanılan taşların çok büyük ve yuvarlak ve sadece çok ince olmaması, çeşitli çaplara düzgün dağılmış olması gerekir.), kumun organik madde veya kil içermesi, kullanılan çimento miktarı, kullanılan su ve çimento oranı, işçilik kalitesi, betonun yüksekten dökülmesi (segregasyon), vibrasyon

uygulanması (az yada çok-ikisi de kötü), betonun sıcak havalarda en az 2-3 hafta hergün sulanması, soğuk havalarda donmadan korunması, alkali-silika reaksiyonu, betonun ıslak mekanlarda bulunması gibi faktörlerden etkilenir. Binanızda gözle görünür beton kalitesinin iyi veya orta kalitede olması tek başına binanın depreme dayanıklı olduğu manasına gelmemekle birlikte, olumlu yönde etkili bir durumdur. İyi beton kaitesi genellikle hazır beton alımlarında tutturulabilmektedir. Şantiye ortamında hazırlanan betonlar çoğunlukla düşük kalitede olmaktadır. Beton kalitesinin tek başına iyi olması yeterli değildir ve demirin (donatı) doğru ve eksiksiz yerleştirilmesi ile etriyelerin yeterli aralıkta ve kolon-kiriş bağlantılarında sıklaştırılarak bağlanması ile ilişkilidir.

'KISA KOLON' herhangi bir katta iki kolon arasında örülmüş duvarlarda bırakılan sürekli ve kolona yakın biten küçük ve yayvan pencereler ve açıklıklar ile oluşur. Bu açıklıklar genellikle tuvalet pencereleri, soyunma ve depo odaları olarak kullanılan mekanlarda bulunmaktadır. Çoğunlukla duvarın üst kısımlarında bulunan ve sürekliye yakın bu boşluklara yakın kolonların alt bölgeleri tuğla duvar ile destek görmekte ve kısa pencereye yakın üst kısımları birer 'kısa kolon' oluşturmaktadır. Binanızda sürekli, yayvan ve dar pencerelerin bulunmaması kısa kolon oluşumunu engeller. Bu durum yukarıda belirtilen sebeplerden dolayı binanız için olumlu bir durumdur.
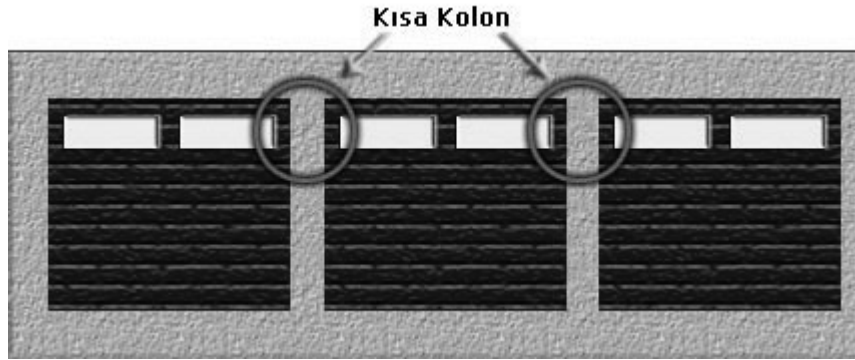
Bir binanın yükünü temellere aktaran ve katları ayakta tutan taşıyıcı sistemin en önemli elemanları (dik yönde duran) kolonlardır. Deprem esnasında, kolonların sistemi taşımaya devam etmesi istenir. Eşyaların ve insanların bulunduğu odaların ve binanın ağırlığını kolonlara aktaran yatay elemanlara kiriş denilir ve kiriş kolon birleşim bölgeleri en çok zorlanan bölgelerdir. Deprem esnasında, kolonların değil, kirişlerin hasar görmesi, taşıyıcı sistemin sağlığı açısından tercih edilir. Kirişlerin kolonlardan daha kuvvetli yapıldığı binalarda, kolon-kiriş birleşim bölgelerindeki hasarlar kolonlar üzerinde yoğunlaşır ve binanın daha çabuk yıkılmasına sebep olur. Kirişlerin kolonlardan daha zayıf olduğu

durumlarda ise, kolonlar yük taşımaya devam eder ve kirişlerde oluşan hasarlar binaya süneklik, deprem enerjisinin emilimi ve sönüm sağlar. 'Kuvvetli kiriş - Zayıf kolon' olması durumunda, tüm kolonların alt ve üst noktalarında plastik mafsallar oluşması ve bunun sonucunda katların birbirleri üzerine yıkılması (su böreği - pan cake) görülebilir. Binanızda 'Kuvvetli kiriş - Zayıf kolon' oluşumu gözlenmektedir. Ancak bu durum diğer birçok olumsuzlukla beraber olduğunda etkilidir.

Kolon

Kiriş

Kolonlar kirişler daha zayıf
"Zayıf kolon - kuvvetli kiriş" var
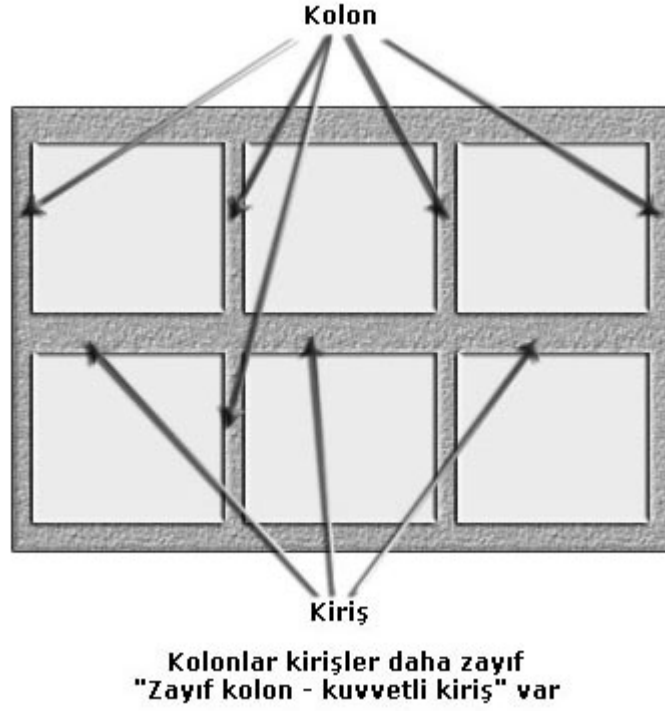
Binanız ile ilgili olarak anket türü sorulara verdiğiniz yanıtlar kullanılarak aşağıda bina değerlendirme puanı oluşturulmuştur. Bu değerlendirme puanı, henüz binanızın deprem performansını belirlememekte, fakat diğer binalar ile göreceli olarak bir değerlendirme imkanı sağlamaktadır. Araştırmanın ilerleyen aşamalarında bina puanı ile depremde beklenen hasar seviyeleri arasında bir bağlantı kurulacaktır. E-mail adresinizi doğru girmiş olmanız durumunda, ileride yapılacak geliştirilmiş yeni değerlendirmeler otomatik olarak e-mail adresinize gönderilecektir. Daha kapsamlı değerlendirme sonucunda 'hasar skoru' ve binanızın (Düzce depremindeki binaların performansları kullanılarak hazırlanan) performans değerlendirmesi için (hafif, orta, ağır hasar gibi) ana sayfamızda bulunan 'detaylı' değerlendirme seçeneğini kullanabilirsiniz. Bu raporun sizin için bilgilendirici ve eğitici olduğunu ümit ederiz. Raporda, ankette ya da sitede anlaşılması güç ve sizin için problemli kısımlar olduğu durumda bize (konu kısmına 'idp' yazarak) e-mail mesajı

152

gönderirseniz, bu görüşleriniz sitemizin iyileştirilmesinde kullanılacaktır. Görüş ve katkılarınız için şimdiden çok teşekkür ederiz.

Bina Değerlendirme Puanı	97 / 100

Veritabanına Kayıtlı Analiz Sonuçları
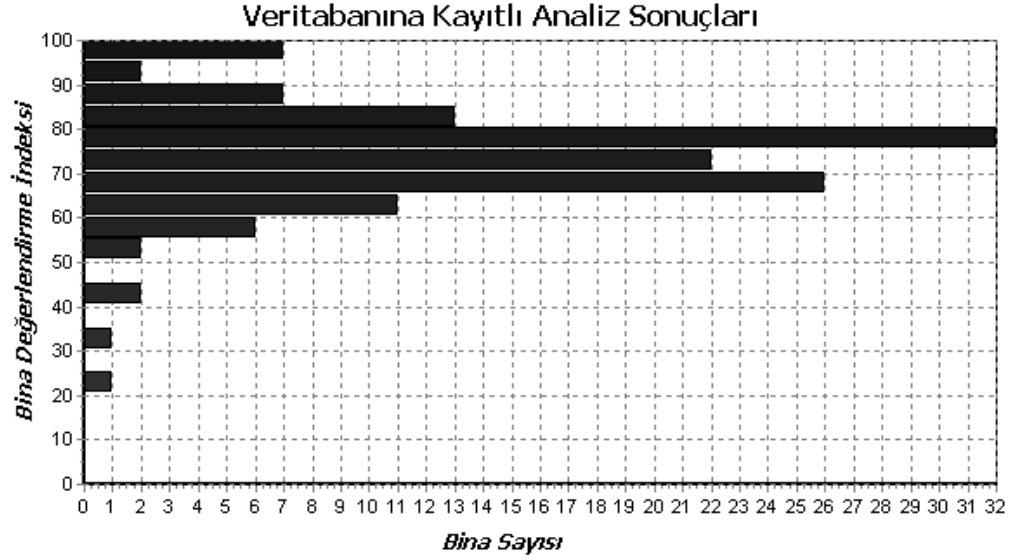
APPENDIX D

DEFINITION OF INPUT VARIABLES

In this section, definition of variables required to carry out an analysis in EQMASTER are given. Input variables are obtained in the form of single text file sent by EQMASTER's graphical interface. All variables are stored in matrices regardless of their sizes which usually depend on number of axes and number of story. Each variable together with its explanation is shown in alphabetical order below. Size is given in parenthesis.

A0 : Effective ground acceleration coefficient. *(1* x *1)*

availSWx : Total available shear wall area in *x-direction* for each story. *(n* x *1)*

availSWy : Total available shear wall area in *y-direction* for each story. *(n* x *1)*

ax : Angle for frames in *x-direction*. Pivot point: Left end of the axis, CW as positive. *(1* x *fx)*

ay : Angle for frames in *y-direction*. Pivot point: Bottom end of the axis, CW as positive. *(1* x *fy)*

b2xd : Depth of beams in *x-direction*. Data for each story are successively added. Matrix is later separated as the number of story. 1st column is the transpose of the 1st *x-axis*. Initial size: *2(fy – 1)* x *fx*

b2xw : Width of beams in *x-direction*. Data for each story are successively added. Matrix is later separated as the number of story. 1st column is the transpose of the 1st *x-axis*. Initial size: *2(fy – 1)* x *fx*

b2yd : Depth of beams in *y-direction*. Data for each story are successively added. Matrix is later separated as the number of story. 1st column is for the 1st y-axis. Initial size: *2(fx – 1)* x *fy*

154

b2yw : Width of beams in *y-direction*. Data for each story are successively added. Matrix is later separated as the number of story. 1st column is for the 1st y-axis. Initial size: *2(fx – 1)* x *fy*

capinfobeamX : Required info for ultimate shear & moment capacity calculation of beams in *x-direction*. It includes eight related data;

- IDX : Identification matrix for the beam.
  - ID(1) : Frame number on which beam is located
  - ID(2) : Order number for the beam in that frame
  - ID(3) : Story number for the beam
- Layer : Number of steel layers
- Steelloc : Steel locations from the top of the section (mm)
- Steelnum : Number of steel at each layer
- Steeldia : Diameter of steel at each layer (mm)
- Stirrupdia : Diameter of stirrup (mm)
- Spacing : Stirrup spacing (mm)
- Cover : Clear cover (mm)

capinfobeamY : Required info for ultimate shear & moment capacity calculation of beams in *y-direction*. It includes eight related data;

- IDY : Identification matrix for the beam.
  - ID(1) : Frame number on which beam is located
  - ID(2) : Order number for the beam in that frame
  - ID(3) : Story number for the beam
- Layer : Number of steel layers
- Steelloc : Steel locations from top of the section (mm)
- Steelnum : Number of steel at each layer
- Steeldia : Diameter of steel at each layer (mm)
- Stirrupdia : Diameter of stirrup (mm)
- Spacing : Stirrup spacing (mm)
- Cover : Clear cover (mm)

col2x : Column dimension parallel to *x-direction*, upper-left corner being the origin. Data for each story are successively added. Matrix is later separated as the number of story. Initial size: *(2fx* x *fy)*

col2y : Column dimension parallel to *y-direction*, upper-left corner being the origin. Data for each story are successively added. Matrix is later separated as the number of story. Initial size: *(2fx* x *fy)*

columncapinfo : Required info for ultimate shear & moment capacity calculation of columns. It includes fourteen related data;

- ID : Identification matrix for the beam.
  - ID(1) : Row index of the column
  - ID(2) : Column index of the column
  - ID(3) : Story number for the column
- LayerX : Number of steel layers for capacity in *x-direction*
- LayerY : Number of steel layers for capacity in *y-direction*
- SteellocX : Steel locations from top of the section for capacity in *x-direction* (mm)
- SteellocY : Steel locations from top of the section for capacity in *y-direction* (mm)
- SteelnumX : Number of steel at each layer for capacity in *x-direction*
- SteelnumY : Number of steel at each layer for capacity in *y-direction*
- SteeldiaX : Diameter of steel at each layer for capacity in *x-direction* (mm)
- SteeldiaY : Diameter of steel at each layer for capacity in *y-direction* (mm)
- Stirrupdia : Diameter of stirrup (mm)
- Spacing : Stirrup spacing (mm)
- CutX : Number of cut for shear capacity in *x-direction* (cut is paralel to Y)
- CutY : Number of cut for shear capacity in *y-direction* (cut is paralel to X)
- Cover : Clear cover (mm)

coorx : x-coordinates of grid intersections. *(fx x fy)*

coory : y-coordinates of grid intersections. *(fx x fy)*

fcd : Design compressive strength of concrete in MPa. *(1 x 1)*

floorarea : Area of each floor in m^2. *(n x 1)*

fx : Number of frames in *x-direction*. *(1 x 1)*

fy : Number of frames in *y-direction*. *(1 x 1)*

fyd : Design yield strength of longitudinal steel in MPa. *(1 x 1)*

fywd : Design yield strength of transverse steel in MPa. *(1 x 1)*

gridx : Distances for axes in *x-direction* to origin in meter. *(1 x fx)*

gridy : Distances for axes in *y-direction* to origin in meter. *(1 x fy)*

h : Height of each floor in meter. *(n x 1)*

jx : Information for joints at each frame in *x-direction*. Data for each story are successively added. Matrix is later separated as the number of story. Numbers corresponding to three different joint types are as below. Initial size: *(2fx x fy)*

- 0 : Regular joint
- -1 : Beam intersecting joint
- -2 : Free end joint (like cantilever)
- -3 : Space joint (not connected to anywhere)

jy : Information for joints at each frame in *y-direction*. Data for each story are successively added. Matrix is later separated as the number of story. Numbers corresponding to three different joint types are as below. Initial size: *(2fy x fx)*

- 0 : Regular joint
- -1 : Beam intersecting joint
- -2 : Free end joint (like cantilever)
- -3 : Space joint (not connected to anywhere)

n : Number of story *(n x 1)*

slab2 : Matrix showing whether *slab* exists or not at each region formed by intersection of axes. Data for each story are successively added. Matrix is later separated as the number of story. Initial size: *2(fx-1) x (fy -1)*

- 0 : Slab exists
- 1 : Slab does not exist

soil : Local site class specified in the code [ref] *(1 x 1)*

spanx : Number of spans for each axis parallel to *x-direction*. Each column of the matrix corresponds to floor. Each element of the column stands for single axis. *Ex*: Element at (1,1) represents the span number for the 1st *x-axis* at the 1st floor. *(fx x n)*

spany : Number of spans for each axis parallel to *y-direction*. Each column of the matrix corresponds to floor. Each element of the column stands for single axis. *Ex*: Element at (2,1) represents the span number for the 2nd *y-axis* at the 1st floor. *(fy x n)*

t : Slab thickness for each floor in meter *(n x 1)*

TA & TB : Spectrum characteristic periods [ref] assigned according to local site class. *(1 x 1)*

wallX2 : Matrix showing whether *infill wall* exists or not on the beams defined in *x-direction*. Data for each story are successively added. Matrix is later separated as the number of story. Initial size: *2(fy – 1) x fx*

- 0 : Infill wall does not exist
- 1 : Infill wall exists

wallY2 : Matrix showing whether *infill wall* exists or not on the beams defined in *y-direction*. Data for each story are successively added. Matrix is later separated as the number of story. Initial size: *2(fx – 1) x fy*

- 0 : Infill wall does not exist
- 1 : Infill wall exists

Xswleft2x : Dimension in *x-direction* for the shear wall defined in *x-direction* corresponding to *width* of the wall. Value in the matrix represents the length contribution due to shear wall to adjacent joint on the *left*. Data for each story are successively added. Matrix is later separated as the number of story. Initial size: *(2fx x fy)*

Xswleft2y : Dimension in *y-direction* for the shear wall defined in *x-direction* corresponding to *thickness* of the wall. Value in the matrix represents the length contribution due to shear wall to adjacent joint on the *left*. Data for each story are successively added. Matrix is later separated as the number of story. Initial size: *(2fx x fy)*

Xswright2x : Dimension in *x-direction* for the shear wall defined in *x-direction* corresponding to *width* of the wall. Value in the matrix represents the length contribution due to shear wall to adjacent joint on the *right*. Data for each story are successively added. Matrix is later separated as the number of story. Initial size: *(2fx x fy)*

Xswright2y : Dimension in *y-direction* for the shear wall defined in *x-direction* corresponding to *thickness* of the wall. Value in the matrix represents the length contribution due to shear wall to adjacent joint on the *right*. Data for each story are successively added. Matrix is later separated as the number of story. Initial size: *(2fx x fy)*

Yswleft2x : Dimension in x-*direction* for the shear wall defined in y-*direction* corresponding to *thickness* of the wall. Value in the matrix represents the length contribution due to shear wall to adjacent joint on the *left*. Data for each story are successively added. Matrix is later separated as the number of story. Initial size: *(2fx x fy)*

158

Yswleft2y : Dimension in y-*direction* for the shear wall defined in y-*direction* corresponding to *width* of the wall. Value in the matrix represents the length contribution due to shear wall to adjacent joint on the *left*. Data for each story are successively added. Matrix is later separated as the number of story. Initial size: *(2fx* x *fy)*

Yswright2x : Dimension in x-*direction* for the shear wall defined in y-*direction* corresponding to *thickness* of the wall. Value in the matrix represents the length contribution due to shear wall to adjacent joint on the *right*. Data for each story are successively added. Matrix is later separated as the number of story. Initial size: *(2fx* x *fy)*

Yswright2y : Dimension in y-*direction* for the shear wall defined in y-*direction* corresponding to *width* of the wall. Value in the matrix represents the length contribution due to shear wall to adjacent joint on the *right*. Data for each story are successively added. Matrix is later separated as the number of story. Initial size: *(2fx* x *fy)*

APPENDIX E

DEMONSTRATION OF TRANFORMATION MATRIX USAGE

In this section, application example of transformation matrices, which relate frame dofs to global dofs, is given for one-story one-bay frame (Figure E.1).
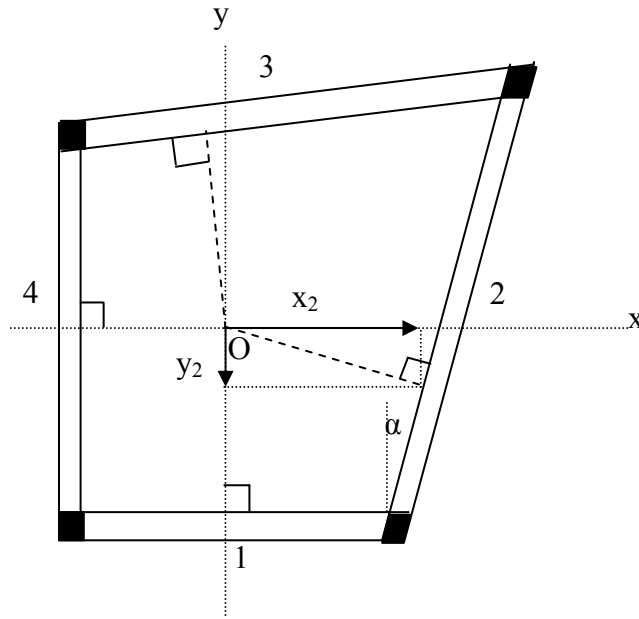

Figure E.1 – Frame Configuration

Frame system shown in Figure E.1 involves two perpendicular and two skewed frames. Stiffness of each frame is defined as 5 units in both directions ($\underline{k}_{x2} = \underline{k}_{y2} = 5$) for demonstration purposes. Distance of the ith frame to the center of mass (point O) is defined by x_i and y_i. Distance of each frame to the mass

center is shown in Table E.. Transformation matrix for each frame is given inTable .

Table E.1 – Frame Distances to Center of Mass

Frame	x (in unit)	y (in unit)
1	0	-2
2	2	-0.5
3	-0.5	2
4	-2	0

Table E.2 – Transformation Matrices of the Frames

Frame	$\underline{a}_{xi} = \begin{bmatrix} \underline{I} & \underline{0} & -y_i \underline{I} \end{bmatrix}$	$\underline{a}_{yi} = \begin{bmatrix} \underline{I} & \underline{0} & x_i \underline{I} \end{bmatrix}$
1	$\begin{bmatrix} 1 & 0 & 2 \end{bmatrix}$	$\begin{bmatrix} 0 & 1 & 0 \end{bmatrix}$
2	$\begin{bmatrix} 1 & 0 & 0.5 \end{bmatrix}$	$\begin{bmatrix} 0 & 1 & 2 \end{bmatrix}$
3	$\begin{bmatrix} 1 & 0 & -2 \end{bmatrix}$	$\begin{bmatrix} 0 & 1 & -0.5 \end{bmatrix}$
4	$\begin{bmatrix} 1 & 0 & 0 \end{bmatrix}$	$\begin{bmatrix} 0 & 1 & -2 \end{bmatrix}$

Contribution of the first frame to the global stiffness matrix is determined by applying Equation 3.29 and 3.30;

$$\underline{k}_{x1} = \underline{a}_{x1}{}^T \underline{k}_{x1} \underline{a}_{x2} + \underline{a}_{y1}{}^T \underline{k}_{y1} \underline{a}_{y1} \tag{E.1}$$

$$\underline{k}_{x1} = \begin{bmatrix} 1 \\ 0 \\ 2 \end{bmatrix} [5] \begin{bmatrix} 1 & 0 & 2 \end{bmatrix} + \begin{bmatrix} 0 \\ 1 \\ 0 \end{bmatrix} [0] \begin{bmatrix} 0 & 1 & 0 \end{bmatrix} = \begin{bmatrix} 5 & 0 & 10 \\ 0 & 0 & 0 \\ 10 & 0 & 20 \end{bmatrix} \tag{E.2}$$

Equation E.2 implies that 5 unit force is required to give a unit displacement to the first frame in x-direction (element [1,1] of $\underline{k}_{x1}$). In addition, 10 unit force in torsion, which is equal to translational force multiplied by moment arm (5*2), is generated when the first frame is given a unit displacement in x-direction (element [3,1] of $\underline{k}_{x1}$). Finally, 20 unit force, which corresponds to the moment due to

translational force multiplied by moment arm (5*2*2), is necessary to give a unit rotation to the floor which is shown in element [3,3] of $\underline{k}_{x1}$. Similarly, 10 units of lateral force is generated in frame #1 (element [1,3] of $\underline{k}_{x1}$) when a unit rotation is given causing displacement of two units (2*1*5).

Similar detailed check can also be performed for the second frame (skewed) by using the following relation;

$$\underline{k}_2 = \underline{a}_{x2}{}^T \underline{k}_{x2} \underline{a}_{x2} + \underline{a}_{y2}{}^T \underline{k}_{y2} \underline{a}_{y2} \tag{E.3}$$

After substitutions in Equation E.3, contribution of the second frame to the global stiffness matrix becomes,

$$\underline{k}_2 = \begin{Bmatrix} 1 \\ 0 \\ 0.5 \end{Bmatrix} [5\cos\alpha] \{1 \quad 0 \quad 0.5\} + \begin{Bmatrix} 0 \\ 1 \\ 2 \end{Bmatrix} [5\sin\alpha] \{0 \quad 1 \quad 2\} \tag{E.4}$$

$$\underline{k}_2 = \begin{bmatrix} 5\cos\alpha & 0 & 2.5\cos\alpha \\ 0 & 0 & 0 \\ 2.5\cos\alpha & 0 & 1.25\cos\alpha \end{bmatrix} + \begin{bmatrix} 0 & 0 & 0 \\ 0 & 5\sin\alpha & 10\sin\alpha \\ 0 & 10\sin\alpha & 20\cos\alpha \end{bmatrix} \tag{E.5}$$

Note that the second frame has stiffness in both x and y directions as 5cosα and 5sinα respectively. In global stiffness matrix generation algorithm, element [3,1] of stiffness in x-direction includes the effect of x-translation on torsion and corresponds to $y_2 \underline{k}_{x2}$ (5cosα*0.5). Similarly, the effect of y-translation on torsion is given by element [3,2] of stiffness in y-direction and equals to $x_2 \underline{k}_{y2}$ (5sinα*2). Torsional stiffness shown by element [3,3] of stiffness in both directions is given as the sum of $y_2{}^2 \underline{k}_{x2}$ and $x_2{}^2 \underline{k}_{y2}$ (5cosα*0.5^2 + 5sinα*2*2) since the displacement generated in x and y directions are 0.5 and 2.0, respectively which causes a force when multiplied by the distance to the origin (0.5 and 2.0 respectively).